2020

Novel Pausing Behavior Of The Kinesin-3 Family Member KIF1A Is Regulated By Tau

Dominique V. Lessard
University of Vermont

NOVEL PAUSING BEHAVIOR OF THE KINESIN-3 FAMILY MEMBER KIF1A IS REGULATED BY TAU

A Dissertation Presented

by

Dominique V. Lessard

to

The Faculty of the Graduate College

of

The University of Vermont

In Partial Fulfillment of the Requirements
for the Degree of Doctor of Philosophy
Specializing in Cellular, Molecular, and Biomedical Sciences

May, 2020

Defense Date: March 9th, 2020
Dissertation Examination Committee:

Christopher L. Berger, Ph.D., Advisor
Diane M. Jaworski, Ph.D., Chairperson
Jason K. Stumpff, Ph.D.
Kathleen M. Trybus, Ph.D.
Christopher S. Francklyn, Ph.D.
Jeffrey L. Spees, Ph.D.
Cynthia J. Forehand, Ph.D., Dean of the Graduate College

ABSTRACT

The unique relationship between neuronal structure and function is paramount for the complexity of the human nervous system. This relationship allows neurons to receive, process, and transmit information through many inter- and intracellular mechanisms. Axonal transport is an essential intracellular mechanism for neuronal health and viability. This process involves the transport of cellular cargo in the anterograde and retrograde direction along the axon, relaying materials between the soma and axon terminals, respectively. The necessity of an expedited form of transport becomes clear when one considers the magnitude of distance cargo must travel; in some cases, the axon can be up to a meter in length. While axonal transport increases the efficiency of cargo delivery, it is imperative that this process be regulated both spatially and temporally.

The choreography of axonal transport is mediated by molecular motor proteins that carry neuronal cargo along microtubule tracks within the axon. Kinesin proteins, a class of molecular motors, transport cargo in the anterograde direction. KIF1A is a kinesin-3 family member that is responsible for the transport of certain critical intracellular cargo. However, the mechanisms for KIF1A regulation remain largely misunderstood. A known regulatory mechanism of kinesin motors is via the presence of microtubule associated proteins (MAPs) that bind to and crowd microtubule roadways. Specifically, the neuronal MAP Tau has been shown to differentially regulate kinesin families found in the neuron, such as kinesin-1 and kinesin-2. Furthermore, these regulatory capabilities are directly related to the behavioral binding state of Tau, of which it can bind statically or diffusively to the microtubule. While the potential regulatory relationship between KIF1A and Tau is unknown, both of these players exhibit pathological behavior in neurodegenerative diseases such as Alzheimer's disease and frontotemporal dementia. These perturbations in KIF1A transport, in tandem with Tau dysfunction, present compelling evidence of important relationship between these two proteins.

To investigate and define the relationship between KIF1A and Tau, a single-molecule in vitro reconstituted system approach was employed. In doing so, an unexpected finding occurred in the early stages of experimentation. It was revealed that KIF1A exhibits a unique pausing behavior between segments of processive movement on the microtubule surface. This behavior, which had been unreported and uncharacterized, contradicts the canonical behavior of other well studied kinesin proteins. KIF1A pausing was found to be mediated by the C-terminal tail (CTT) structure of tubulin, the building blocks of microtubules. Further exploration revealed that KIF1A pausing was reliant upon the level of polyglutamylation, a post-translational modification enriched on neuronal tubulin, of the CTTs. Lastly, it was determined that polyglutamylated CTTs allow for an electrostatic tethering mechanism with the K-loop, a motor domain surface loop of KIF1A, that allows the motor to pause. Like KIF1A, Tau also relies on the tubulin CTTs to exhibit its characteristic diffusive binding behavior. In considering this fact, KIF1A regulation via Tau's behavioral binding state was investigated. Ultimately, it was discovered that the diffusive binding state of Tau regulates KIF1A, not the static binding state. This regulation occurs when KIF1A tries to engage in a pause, but cannot due to diffusive Tau occupying the CTTs. This work provides a new mechanism of Tau-mediated kinesin motor regulation and the first direct link between KIF1A and Tau function, expanding our knowledge of the spatiotemporal regulation of axonal transport.

CITATATION

Material from this dissertation has been published in the following form:

Lessard, D.V., Zinder, O.J., Hotta T., Verhey K.J., Ohi R., Berger C.L.. (2019). Polyglutamylation of tubulin's C-terminal tail controls pausing and motility of kinesin-3 family member KIF1A. Journal of Biological Chemistry, 294(16), 6353-6363.

Material from this dissertation has been submitted for publication to Biophysical Journal on February 23rd, 2020 in the following form:

Lessard, D.V., Berger, C.L.. The Microtubule Associated Protein Tau Regulates KIF1A Pausing Behavior and Motility. Biophysical Journal.

DEDICATION

For the communities who raised me, the communities that support me, and the communities that push me to the best version of myself. I am proud of who I am because of all of you.

For Amber. Your unwavering support, dedication, and love throughout this process has kept me going. You continue to be my role model of what it means to work hard, be kind, and stay true to what matters. Thank you.

ACKNOWLEDGEMENTS

Thank you to my committee members Dr. Jason Stumpff, Dr. Kathleen Trybus, Dr. Christopher Francklyn, and Dr. Jeffrey Spees for your commitment and insight. A special thank you to my committee chair, Dr. Diane Jaworski, for your unwavering support in science and in life.

Thank you to all of the members of the Berger Lab members I have had the privilege to work with as a team: Lynn Chrin, Dr. Gregory Hoeprich, Dr. Jamie Stern, Miranda Redmond, Rehan Ali, Alisa Cario, Gabrielle Booth, Oraya Zinder, Morgan Dexter, and Finlay Pilcher. Thank you to the Stumpff lab for always sharing space, ideas, and holiday parties. To the Molecular Physiology and Biophysics department and the Cellular, Molecular, and Biomedical Sciences program: thank you for creating and fostering outstanding environments that have allowed me to grow significantly during my graduate studies.

Finally, thank you to my mentor, Dr. Christopher Berger. Your guidance has been imperative to my success at UVM and beyond. Your encouragement has allowed me to reach heights I never thought I'd reach.

TABLE OF CONTENTS

LIST OF TABLES

Table **Page**

LIST OF FIGURES

Table **Page**

LIST OF ABBREVIATIONS

AD ..... Alzheimer's disease
ADP ..... Adenosine diphosphate
AMPPNP ..... Adenylylimidodiphosphate
AT ..... Axonal transport
ATP ..... Adenosine triphosphate
BSA ..... Bovine serum albumin
CI ..... Confidence interval
CRL ..... Continuous run length
CTT ..... C-terminal tail
DCX ..... Doublecortin
EB ..... End binding
FBS ..... Fetal bovine serum
FTD ..... Frontotemporal dementia
GDP ..... Guanosine diphosphate
GDP•P_i ..... Guanosine diphosphate + inorganic phosphate
GMPCPP ..... Guanosine-5'-[(α,β)-methyleno]triphosphate
GTP ..... Guanosine triphosphate
MAP ..... Microtubule associated protein
MB ..... Motility buffer
MTBR ..... Microtubule binding repeats
ORL ..... Overall run length
PBS ..... Phosphate-buffered saline
PTM ..... Post-translational modification
RL ..... Run length
ROI ..... Region of interest
SUB ..... Subtilisin
TIRF ..... Total internal reflection fluorescence
+TIP ..... Plus-end tracking protein
-TIP ..... Minus-end tracking protein
TTL ..... Tubulin-tyrosine ligase
TTLL ..... Tubulin-tyrosine ligase-like

CHAPTER 1: INTRODUCTION

1.1 Structure and Function of the Neuron

In the late 19th century, Santiago Ramón y Cajal introduced the "Neurone doctrine" to the scientific community and established the neuron as the basic anatomical unit of the nervous system (Bock 2013; Andres-Barquin 2001). While our understanding of this cell type has been greatly increased since this foundational publication, one theme of Ramón y Cajal's initial observations still rings true: the unique structure and function of this cell type is equal parts alluring and perplexing. The characteristic asymmetries of the neuron result in a uniquely polarized cell structure, as is observed in all morphologically distinct neuron types. This polarity is essential for the compartmentalization of neuronal regions, each with their respective cellular functions (Figure 1-1) (Donato et al. 2019; Terenzio, Schiavo, and Fainzilber 2017).

On a network level, the role of the neuron is to receive and transport both chemical and electrical information from other cells. This process is achieved in part through the genesis of the synapse, defined by a point of communication between two neurons across which information is transferred (Shaw 1913; Ovsepian 2017). Specifically, this point of contact is commonly made by the dendrite of one neuron and the axon terminal of another neuron. The axon terminals, defined as a distinct morphological branching at the retrograde end of the axon, are the pre-synaptic site of regulated synaptic vesicle release (Figure 1-1) (Bullock 1959; Kalil and Dent 2014). It is at this location that the synaptic vesicles containing neurotransmitters, and a population of dense core vesicles containing neuropeptides, are docked and waiting for the cellular cues to release their contents into the synaptic cleft (Sudhof 1995; Kaeser and Regehr 2017; van den Pol 2012). The

dendrites, branching off of the neuronal cell body, serve as the area in which a post-synaptic cell receives pre-synaptic inputs (Figure 1-1) (Peichl and Wassle 1983; Horton et al. 2005). Visually characterized by their complex structural arbor, the volume occupied by the dendrites is directly related to the number of synapses the dendrites can sample (Peichl and Wassle 1983) and is carefully regulated to match the volume of pre-synaptic axon terminals to avoid under- or over-sampling. Synapse structure and function is heavily supported by glial cells called astrocytes, which form what is referred to as a tripartite synapse (Araque et al. 1999; Pfrieger and Barres 1996). Astrocytes carry out many roles in synapse maintenance such as metabolic buffering, neurotransmitter exchange, and fine-tuned modulation of synaptic transmission (Pfrieger and Barres 1996; Tsacopoulos and Magistretti 1996; Mennerick and Zorumski 1994; Pfrieger and Barres 1997).

The axon links the soma, the site of protein synthesis, with the axon terminals, the site of neurotransmitter release (Figure 1-1). This defining structural feature of neuronal polarity branches off of the neuronal soma, the region where the vast majority, but not all, of protein synthesis occurs in the neuron (Kim and Jung 2015). Axons can extend striking magnitudes of length with some extending over one meter (Twelvetrees, Hendricks, and Holzbaur 2012). To address the inherent challenges of conveying cellular information in a polarized cell type that covers a great distance, the axon has many unique structural and functional characteristics.

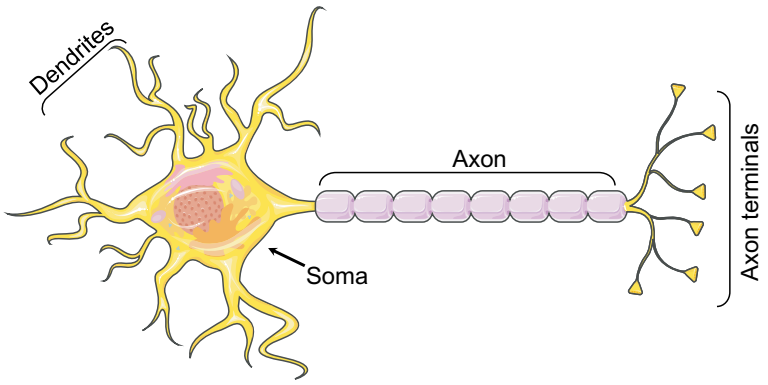

Figure 1-1. Schematic of basic neuronal morphology. Neurons have a uniquely polarized morphology. On one end is the soma, containing the nucleus and many types of organelles. Branching off of the soma are dendrites that receive input from pre-synaptic cells. Each neuron has one axon that projects off of the soma and can span great magnitudes of distance (up to a meter in length). On the opposing end of the neuron are the axon terminals that will form synapses with post-synaptic cells. The neuron in this image was acquired from Servier Medical Art (SMART) under a Creative Commons Attribution 3.0 Unported license- labels were added.

When looking at a cross section of the axon, one will find many layers of structural complexity. At the innermost point is the axoplasm, or the cytoplasm specific to the axon, that is ensheathed in a plasma membrane (Figure 1-2). One important characteristic of the axoplasm is its limited amount ribosomes and lack of endoplasmic reticulum, resulting in a limited amount of protein synthesis; this means that the majority of proteins expected to reach the axon terminals must be synthesized in the soma and then be transported down the length of the axon. While not a site of major protein synthesis, the axoplasm is rich in many cytoskeletal proteins such as actin, microtubules, and neurofilaments (Figure 1-2), by which filamentous polymerization promotes a long and slender axonal morphology (Price et al. 1988; Schnapp and Reese 1982). Surrounding the plasma membrane of large diameter neurons is an insulating layer of myelin. This neuron-specific membrane is often defined by its high lipid content and enrichment of proteins such as myelin proteolipid

protein and myelin basic protein (Quarles 1999). Myelin is formed by encapsulating glial cells, either oligodendrocytes (in the central nervous system) or Schwann cells (in the peripheral nervous system) (Quarles 1999; Simons and Nave 2015) (Figure 1-2), and is distributed in segments along the axon separated by unmyelinated segments known as the nodes of Ranvier (Ghosh, Sherman, and Brophy 2018; Huxley and Stampfli 1949).

One way that signals are able to efficiently travel down the length of the axon is through the generation of an action potential. Action potentials are an important communication tool within neurons, as they mainly result in the release of inhibitory or excitatory neurotransmitters. Action potentials, resulting in fast transduction of electrical signal, leads to rapid depolarization and repolarization of the neuronal membrane voltage, resulting from the influx and efflux of ions into and out of the neuron (Eccles 1966). The propagation of an action potential down the length of the axon is highly dependent on the segmented myelin sheathing through a process known as saltatory conduction, characterized by the action potential "leaping" between nodes of Ranvier due to the increased conduction velocity of electrical signals in myelinated axon segments (Huxley and Stampfli 1949).

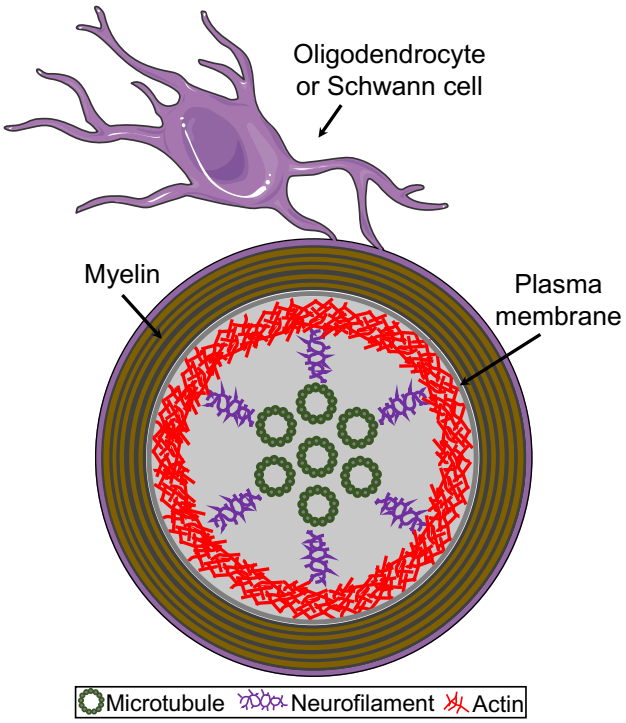

Figure 1-2. Cross section of an axon. In the center of an axon, there are many types of cytoskeletal proteins, such as microtubules, neurofilaments, and actin. These proteins play an important structural role in axon morphology and are surrounded by the axonal plasma membrane. The axon is encapsulated in many insulating layers of myelin that are generated from glial cells (either oligodendrocytes or Schwann cells). The cell in this image was acquired from Servier Medical Art (SMART) under a Creative Commons Attribution 3.0 Unported license.

While action potentials are one source of transport needed for neuronal communication, other forms of transport are necessary for intra- and inter-neuronal propagation of information. As discussed above, synaptic vesicles must be docked at the axon terminals in order to be released following an action potential. However, the contents of synaptic vesicles are synthesized and packaged at the proximal end of the neuron in the

soma. How is this neuronal cargo able to be transported intracellularly down the length of the axon in an efficient manner?

1.2 Axonal Transport

Intracellular transport of cellular components along axons is essential for neuronal survival and viability. Often analogized to a roadway full of cargo carrying trucks, this trafficking of cellular cargo between the soma and the axon terminals is known as axonal transport. Much like a busy roadway, there is an extensive amount of coordination and precision that must occur for efficient cargo transport within the axoplasmic environment. There are many challenges regarding the spatial regulation needed for axonal transport, such as a crowded roadway and obstacles. These spatial challenges heavily influence the narrow window of temporal regulation needed to ensure cargo is delivered to the right location at the right time. Below, a broad review of axonal transport characteristics will be discussed, all of which facilitate the spatiotemporal delivery of neuronal cargo.

The fundamental unit of the axonal transport "roadway" is the microtubule, a cytoskeletal polymer that contributes to the axon's long and protruding morphology (Banks, Mayor, and Tomlinson 1971; Yogev et al. 2016). On the surface of axonal microtubules are molecular motor proteins, specifically cytoplasmic dynein and members of the kinesin superfamily of proteins (Schnapp and Reese 1989; Vale et al. 1985; Dahlstrom, Pfister, and Brady 1991). The processive nature of these proteins allow them to function as cargo carrying "trucks", by attaching to and translocating cellular cargo along microtubules.

Tunable directionality of cargo transport is essential to avoid unbalanced protein accumulation at the proximal or distal ends of the neuron. Anterograde transport is the movement of cargo away from the soma towards the axon terminals (Figure 1-3). This sector of cargo transport is driven by specific kinesin motors, carrying family specific subsets of newly synthesized proteins (Hirokawa et al. 1991), required to uphold synaptic function. Conversely, retrograde cargo transport from the axon terminals to the soma is required to remove and recycle protein components. Unlike anterograde transport, retrograde transport is conducted by only one molecular motor, dynein (Figure 1-3) (Hirokawa et al. 1990). Because of this, dynein motors achieve cargo binding specificity through a variety of different motor-cargo adaptor proteins (Reck-Peterson et al. 2018; Carter, Diamant, and Urnavicius 2016). While reconstituted motility experiments revealed the monodirectional movement of kinesin and dynein mediated transport, extruded squid axoplasm motility experiments first revealed bidirectional movement of cargo (Figure 1-3). The introduction of bidirectional transport as a concept has significantly shifted the motility field's paradigms of how cargo directionality is regulated. Most notably it has brought forth the idea that kinesin and dynein motors work together in teams, thought to be regulated by a "tug-of-war" mechanism (Hendricks et al. 2010; Muller, Klumpp, and Lipowsky 2008; Belyy et al. 2016). To date, mitochondria and late endosomes/lysosomes are the most characterized cargo to undergo bidirectional axonal transport (Cai, Davis, and Sheng 2011; Zinsmaier, Babic, and Russo 2009; Hollenbeck and Saxton 2005; Hendricks et al. 2010; Maday, Wallace, and Holzbaur 2012).

Along with directionality of transport, axonal cargo can be transported at two different speeds: either "fast" axonal transport or "slow" axonal transport. These two types

of axonal transport were first discovered by "pulse-chase" experiments, wherein radiolabeled proteins were "pulse" injected into neuronal somas, followed by a "chase" injection of unlabeled protein; the transport of the radiolabeled protein was then monitored and analyzed over time (Cancalon and Beidler 1975; Gross and Beidler 1975). From these experiments, the rate of fast axonal transport was discovered (most often cited as ~100 mm/day) (Figure 1-3) (Shah and Cleveland 2002; Roy 2014; Vallee and Bloom 1991). A large percentage of fast anterograde cargo are lipid bound components, attached to kinesin motors, that need to reach the axon terminals with haste to promote synaptic function, such as dense core vesicles and synaptic vesicle precursors moving up to 1 μm/sec (Shah and Cleveland 2002). In fast retrograde axonal transport, the same logic applies; cargo needed to rapidly relay signaling information to the soma are transported by dynein complexes, including late endosomes and autophagosomes (Maday et al. 2014).

The rate of slow axonal transport is significantly slower than fast axonal transport, with reports ranging from 1-10 mm/day (Figure 1-3) (Vallee and Bloom 1991; McEwen and Grafstein 1968). Unlike the membrane bound cargo of fast axonal transport, slow axonal transport cargo is comprised of cytoskeletal polymers and soluble proteins. The cytoskeletal proteins of slow axonal transport can be broken up into two categories: slow axonal transport component A (neurofilaments and tubulin; up to 10 mm/day) and slow axonal transport component B (actin; up to 1 mm/day) (Roy 2014; Dillman, Dabney, and Pfister 1996; Black and Lasek 1980). The discovery of slow axonal transport was initially contentious, largely due to the technical limitations of microscopic resolution in the 1980's and 1990's. However, as spatial resolution in live cell imaging has advanced, the "Stop-and-Go" model has become the widely accepted mechanism of slow axonal transport. This

model, like fast axonal transport, relies on kinesin and dynein to transport cargo. However, in the "stop-and-go" model, these molecular motors spend a much larger fraction of time in a paused/stalled state on the microtubule, followed by shorter periods of processive movement, which results in a shorter distance travelled over time (Brown, Wang, and Jung 2005).

Over the past twenty years, the relationship between microtubules and the molecular motors responsible for axonal transport has been highly characterized at the molecular and single-molecule level. In considering these findings, the following sections of this chapter will dive deeper into our understanding of microtubules and the kinesin superfamily of motors, highlighting the molecular intricacies of these two components.

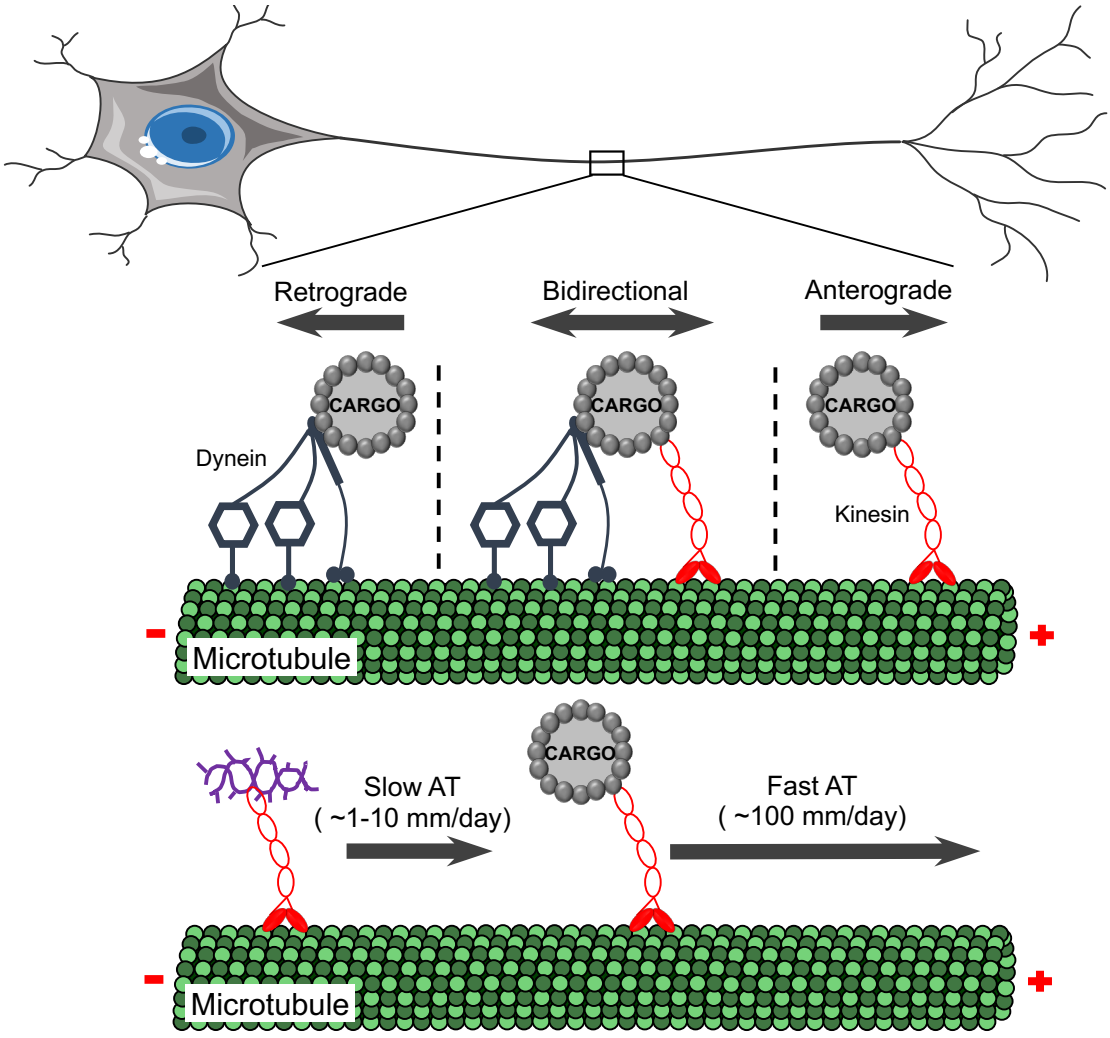

Figure 1-3. Characteristics of axonal cargo transport. *(top)* Axonal transport (AT) is conducted along microtubules and initiated by molecular motors. Cytoplasmic dynein is responsible for bringing cargo back to the neuronal soma via retrograde transport. Many kinesin protein families are responsible for bringing cargo to the axon terminals via anterograde transport. Cargo can also undergo bidirectional transport resulting from a "tug-of-war" between dynein and kinesin motors. *(bottom)* AT is grouped into two main rates of transport 1) slow AT, travelling at speeds of ~ 1-10 mm/day and 2) fast AT, travelling at speeds of ~ 100 mm/day. The neuron in this image (color modified) was acquired from Servier Medical Art (SMART) under a Creative Commons Attribution 3.0 Unported license.

1.3 Microtubules

While a simple microtubule "roadway" metaphor is a useful image, it greatly oversimplifies many microtubule characteristics. In reality, the microtubule is a sophisticated and intricate "roadway" with many unique facets. In this section, many of the characteristics of microtubules will be discussed, starting with the basic subunits and scaling up in complexity.

1.3.1 Constructing a microtubule

The microtubule is defined as a cytoskeletal polymer comprised of αβ-tubulin heterodimer subunits (Kirkpatrick et al. 1970). In the human genome there are eight α-tubulin and 9 β-tubulin genes, resulting in a variety of different tubulin isotypes (Minoura 2017). While many of these isotypes are expressed in neurons, β-tubulin isotype III is exclusively a neuronal isotype (Sullivan and Cleveland 1986). For initial heterodimer formation, both the α and β subunits must bind to a GTP nucleotide. However, the catalytic fate of GTP differs between the α and β subunits. GTP bound to the α subunit is in a non-exchangeable state, or unable to undergo catalysis, and remains in the GTP state while sandwiched between the α and β subunits (Figure 1-4A). GTP bound to the β subunit however is bound to an exchangeable site (Figure 1-4A), and is able to transition to the GDP•P_i and GDP state (Spiegelman, Penningroth, and Kirschner 1977; MacNeal and Purich 1978). Both the α and β subunits have an intrinsically disordered C-terminal tail (CTT) that will project off of the microtubule surface, once polymerization has occurred

(Nogales, Wolf, and Downing 1998). These CTTs are a vital regulatory structure subject to many modifications that influence molecular motor function in axonal transport.

For tubulin dimers to polymerize into higher order microtubule structures, there are many environmental criteria that must be controlled. First, tubulin dimers must be in the presence of GTP. Second, the tubulin dimer and GTP mixture must be at a temperature in which polymerization can occur, most commonly referenced as ~37ºC or "body temperature". Lastly, the local population of tubulin dimers must be above the critical concentration, or the equilibrium concentration of tubulin dimers that results in no net growth or net shrinkage (Lodish H 2000). Of note, the specific critical concentration of tubulin can be modulated by other environmental factors that can promote or hinder polymerization. With all of these stipulations achieved, the tubulin dimers must undergo a nucleation step to initiate polymerization. In cellular systems, this is often facilitated by microtubule-organizing centers and in *in vitro* reconstituted systems this process happens spontaneously, albeit under very high tubulin concentrations (Voter and Erickson 1984).

Once nucleated, tubulin dimers rapidly elongate in a "head-to-tail" arrangement and form linear protofilaments (Figure 1-4B). Then, individual protofilaments associate laterally into sheets and assemble to form the hollow and cylindrical microtubule structure (Figure 1-4C-D). Microtubule structures can occur in a variety of different protofilament arrangements, such as singlet, doublet, and triplet microtubules (Chaaban and Brouhard 2017). The rest of this section will focus on the singlet microtubule. The number of protofilaments per singlet microtubule can vary from 9-16, but 13 protofilaments is the most common arrangement (Chaaban and Brouhard 2017). As all protofilaments in a microtubule have the same orientation, polymerization also generates a "+" end (β subunit

capped) and a "-" end (α subunit capped) to establish a filamentous polarity (Figure 1-4). These two ends vary in rate of tubulin dimer assembly, with polymerization occurring most rapidly at the + end (Walker et al. 1988). Of note, the polarity of microtubules is important for regulating molecular motor based cargo transport.

Individual microtubules are highly dynamic structures and are often referred to as being "dynamically unstable" (Mitchison and Kirschner 1984). In a growing microtubule, tubulin dimers are preferentially added to the + end, leading to the tip of the microtubule being in a GTP-rich state; this local enrichment of GTP into the microtubule greatly increases the stability of the microtubule at the tip. After a tubulin dimer is incorporated into a microtubule, the GTP-molecules occupying the β-tubulin binding site undergo hydrolysis to the GDP•P_i state and, eventually, the GDP state (Desai and Mitchison 1997). As the microtubule transitions into the GDP state, a number of conformational changes occur that result in significant loss in microtubule stability, including the loss of the "GTP +-end cap". Once this cap is lost, the microtubule rapidly depolymerizes, or shrinks, in a process known as microtubule "catastrophe". In some instances, a microtubule can undergo a "rescue" event in which there is a switch between shrinkage and growth (Cassimeris, Pryer, and Salmon 1988). The inherent dynamic instability of microtubules is greatly beneficial to many cellular processes in which rapid turnover of microtubules aids in cellular function. The dynamics of microtubules can also be modulated in many ways in a cellular environment, including through the presence of microtubule associated proteins (MAPs).

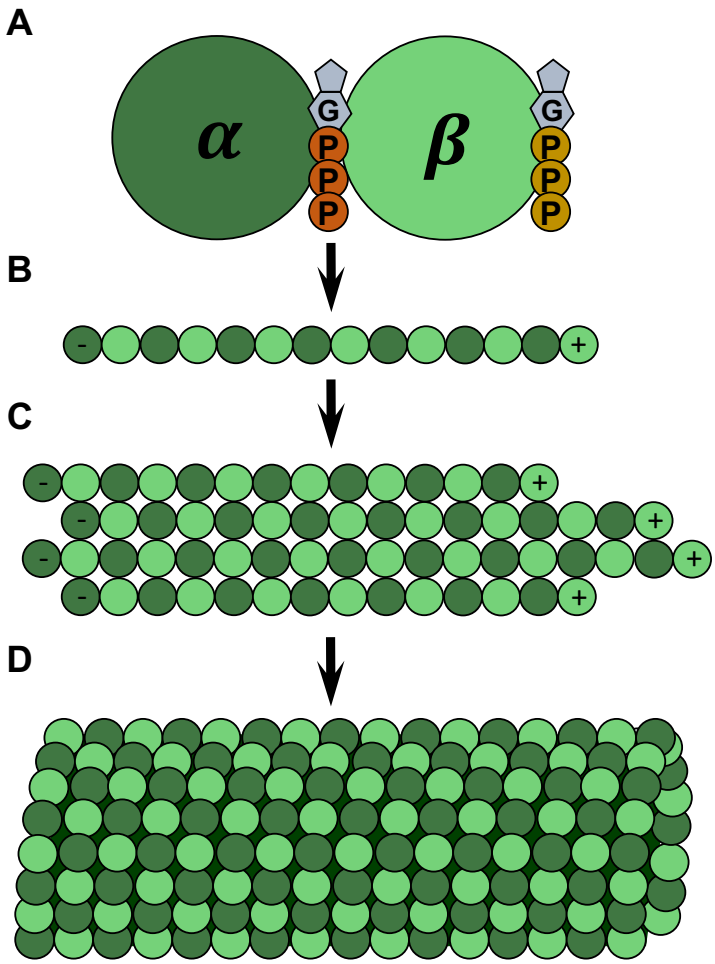

Figure 1-4. Hierarchy of microtubule structure. A) The smallest functional unit of the microtubule is the αβ-tubulin heterodimer. Both α- and β-tubulin bind to GTP. However, the GTP bound to α-tubulin is non-hydrolysable (orange), whereas the GTP bound to β-tubulin can undergo hydrolysis (yellow). **B)** αβ-tubulin heterodimers assemble in a "head-to-tail" arrangement to form a linear protofilament. **C)** Protofilaments form lateral contacts with other protofilaments to form a protofilament sheet. **D)** Protofilament sheets assemble to create the hollow and cylindrical microtubule structure.

1.3.2 Post-translational modifications of microtubules

Microtubule architecture is modified, in part, by chemical alterations to the microtubule structure known as post-translational modifications (PTMs). The CTTs are the most commonly modified location on the microtubule, although other regions of the microtubule are subject to PTMs as well, such as the microtubule lumen (inside of the microtubule cylinder). In the axonal cytoskeleton, these PTMs play an important role in the regulation of axonal transport by influencing the flow of cargo trafficking as well as recruiting necessary protein complexes. To elucidate how specific PTMs are involved in axonal transport, this section will focus on tubulin PTMs that are enriched in the axon: detyrosination/tyrosination, acetylation, and glutamylation.

Tyrosination/detyrosination occurs on the CTTs of α-tubulin and has three different levels of modification. First, a detyrosinated CTT can have a tyrosine added via a tubulin-tyrosine ligase (TTL), yielding a *tyrosinated state*. Second, a tyrosine on the CTT can be removed via a carboxypeptidase, yielding a *detyrosinated state* (Janke 2014; Janke and Kneussel 2010). After detyrosination, an α-tubulin penultimate glutamate residue is exposed (Mary et al. 1996). If this glutamate is removed, this generates the *Δ2-tubulin state* (Yu, Garnham, and Roll-Mecak 2015). Unlike tyrosination and detyrosination, the production of Δ2-tubulin is an irreversible modification causing the α-subunit to be removed from the cycle of tyrosination (Paturle-Lafanechere et al. 1994). The tyrosination state of α-tubulin CTTs serves an important role in the stability of neuronal microtubules. For example, detyrosination/Δ2-tubulin modifications are found on very stable microtubules in the axon, whereas tyrosination modifications are enriched in areas with

dynamic microtubules, such as the growth cone (Marcos et al. 2009; Paturle-Lafanechere et al. 1994). While it was initially thought that the physical addition/removal of tyrosine residues directly regulated microtubule stability, it is now believed that this PTM serves as a message to the greater cellular environment to recruit factors that modulate stability.

Acetylation is a PTM that does not occur on the tubulin CTTs. Instead, this modification occurs at the lysine 40 (K40) position in the microtubule lumen of the α-tubulin subunit (L'Hernault and Rosenbaum 1985). Due to the non-canonical location, the role of this PTM was initially puzzling. To add a layer of complication, this PTM is only found when tubulin is a part of a microtubule lattice, leading to the belief that that the enzymes responsible for acetylation/deacetylation must enter the microtubule lumen. Like the tyrosine modifications discussed above, acetylation of K40 is often found on stable populations of microtubules in the axon. This pattern supports the current hypothesis that K40 PTM of α-tubulin increases the flexibility of microtubules, making them less susceptible to perturbation by mechanical stressors that may lead to depolymerization, increasing their temporal stability/longevity (Janke and Montagnac 2017).

Glutamylation is the most abundant PTM in the neuron, and is heavily enriched in the axon. Addition of glutamate residues occurs on both α and β subunits via tubulin tyrosine like-ligase (TTLL) enzymes (Janke et al. 2005), with TTLL7 being the most abundant in neurons (Ikegami et al. 2006; Mukai et al. 2009). This process is commonly referred to as “polyglutamylation”, as chains of many glutamate residues can be added to the preexisting glutamates in the CTT sequence at multiple locations. Due to the acidic nature of glutamic acid, polyglutamylation introduces a local negative charge on the CTTs. This charge shift is important in regulating the initial electrostatic interactions between the

microtubule and MAPs/motor proteins and will be discussed further in chapter 2. Furthermore, tunable levels of polyglutamylation are required for neuronal function, as hyper- or hypo- polyglutamylation have been linked to disruptions in axonal cargo trafficking (Magiera, Bodakuntla, et al. 2018; Ikegami et al. 2007).

1.3.3 Microtubule associated proteins

Another layer of complexity contributing to the regulation of axonal transport is the presence of MAPs on axonal microtubules. Defined as proteins that interact with microtubules, MAPs engage in a variety of different roles such as microtubule stabilization, regulation of microtubule dynamics, recruitment of other proteins, and direct regulation of cargo transport.

Many different MAPs contribute to the overall structure of the axon, starting at the protofilament level and advancing to larger microtubule networks. Doublecortin (DCX), a MAP that is critical for axonal outgrowth during development, directly regulates the protofilament number of microtubules (Fourniol et al. 2010; Tint et al. 2009). DCX does this by cooperatively binding between adjacent protofilaments, reinforcing longitudinal and lateral bonds. In doing so, DCX forces the microtubule into a 13 protofilament arrangement and increases microtubule stability (Fourniol et al. 2010). The equilibrium of microtubule stability and instability is also mediated, in part, by MAPs. For example, the MAP1 and MAP2 family of proteins have been shown to increase microtubule stability not only by increasing rescue events at the individual level, but also crosslinking microtubule networks to each other and to the surrounding actin network (Mohan and John 2015). In contrast, many severing proteins purposefully destabilize microtubules by cutting them

into small pieces. This process, largely facilitated by katanin and spastin, aids in local microtubule reorganization throughout the axon (Lasser, Tiber, and Lowery 2018; Bodakuntla et al. 2019).

Certain factions of MAPs have precise regions of localization on axonal microtubules, with the most heavily researched being the microtubule plus-end tracking proteins (+TIP). Specifically, the end binding (EB) MAPs are of great importance in maintaining axonal structure. From a morphological standpoint, EB proteins play an important role in neuronal development and axon extension (van de Willige, Hoogenraad, and Akhmanova 2016). Arguably their most important role, EB proteins serve as scaffolding to mediate protein-protein interactions; these interactions range from other +TIP proteins to kinesin motor families (Gumy et al. 2013; Chen, Rolls, and Hancock 2014; Bearce, Erdogan, and Lowery 2015).

While the presence of MAPs on axonal microtubules creates many avenues for regulation, the most direct effect of MAPs on axonal transport occurs through the regulation of cargo carrying motors. The MAP2 family member Tau, with polarizing roles in axonal health and axonal degeneration, is vital to this process.

1.3.4 Tau

Tau is the most prevalent MAP in the axon and plays many roles in the healthy and diseased state. As stated above, Tau is a member of the MAP2 family of proteins, with Tau and MAP2 being the only family members expressed in neurons. The localization of MAP2 versus Tau in the neuron is quite stark: MAP2 is predominantly localized to the dendrites while Tau is predominantly localized to the axon (Dehmelt and Halpain 2005).

Perplexingly, knockout experiments of either Tau or MAP2 revealed that neither MAP is essential by itself, suggesting an important functional redundancy between these two proteins in the brain (Harada et al. 2002; Harada et al. 1994).

In humans, there are six different isoforms of Tau that arise from the alternative splicing of the *MAPT* gene. *MAPT* has 13 different exons with exons 2, 3, and 10 being subject to alternative splicing (Goedert and Jakes 1990). While Tau is highly dynamic and lacks a native structure, the protein can be segregated into two functional regions: the C-terminal binding domain and the N-terminal projection domain. The C-terminal binding domain directly interfaces with the microtubule surface through either three or four microtubule binding repeats (MTBR) (Dehmelt and Halpain 2005). Due to Tau's lack of tertiary structure and minimal secondary structure, the orientation of these bindings sites on the microtubule has been technically difficult to resolve. However, recent advancements have shown that the MTBRs likely bind along the microtubule protofilament ridge (Kellogg et al. 2018). The C-terminal projection domain is comprised of the proline-rich region and zero, one, or two acidic inserts.

In this dissertation, the nomenclature of a Tau isoform is defined by the extent of alternative splicing that has occurred. Tau isoforms can fall into a 4R (four MTBR) or 3R (3MTBR due to the splicing of exon 10) category. After this distinction, isoforms are categorized as "short" (no acid inserts; exons 2 and 3 spliced), "medium" (one acidic insert; exon 3 spliced), or long (two acidic inserts). This nomenclature yields the isoform names of 3RS, 3RM, 3RL, 4RS, 4RM, and 4RL (Figure 1-5A). The expression ratio of Tau isoforms is variable throughout development. When adulthood is reached, the 3R- and 4R-isoforms are expressed in a 1:1 ratio (Boutajangout et al. 2004).

Tau's highly dynamic structure facilitates the presence of two dominating behavioral states on the microtubule surface: the static binding state and the diffusive binding state (Figure 1-5B). Of note, the diffusive binding state of Tau is reliant upon an electrostatic interaction with the CTTs of tubulin (Hinrichs et al. 2012). While identifying Tau's structure on the microtubule surface is extremely technically difficult, it is assumed that these two binding states are structurally distinct; ongoing efforts in our lab seek to understand these structural differences.

Each isoform of Tau has its own equilibrium between time spent in the diffusive state and time spent in the static state, at a population-level. Using single molecule imaging techniques, our lab has characterized the diffusive and static binding behavior of multiple Tau isoforms on various microtubule lattices. In these investigations, both kymograph analysis (McVicker et al. 2014) and single-molecule particle tracking of Tau behavior (Stern et al. 2017) revealed that 3R-Tau isoforms favor the static binding state while 4R-isoforms favor the diffusive binding state on paclitaxel-stabilized microtubules. Specifically, we can state that the 3R-isoform equilibrium is 75% static and 25% diffusive, while the 4R-isoform equilibrium is 40% static and 60% diffusive. Additionally, both of 3RS- and 4RL-Tau favor the diffusive binding state on GMPCPP-stabilized microtubules, highlighting the influence of the microtubule lattice on Tau binding behavior (McVicker et al. 2014) (Figure 1-5C; unpublished data).

While Tau performs many functions, the function most relevant to this dissertation is Tau's ability to regulate the motility of kinesin motors involved in axonal transport. This was first demonstrated using an *in vitro* reconstituted system, detailing that kinesin-1 motility was reduced by Tau on the microtubule (Dixit et al. 2008; Vershinin et al. 2007). Furthermore,

these studies demonstrated that 3RS-Tau is more inhibitory than 4RL-Tau. This introduced the concept that certain kinesin motors are more heavily inhibited by one behavioral state of Tau versus the other. The relationship between kinesin regulation and the isoform-specific behavioral equilibrium of Tau has been a continuing point of investigation in our lab and is a key concept that will be explored throughout this dissertation.

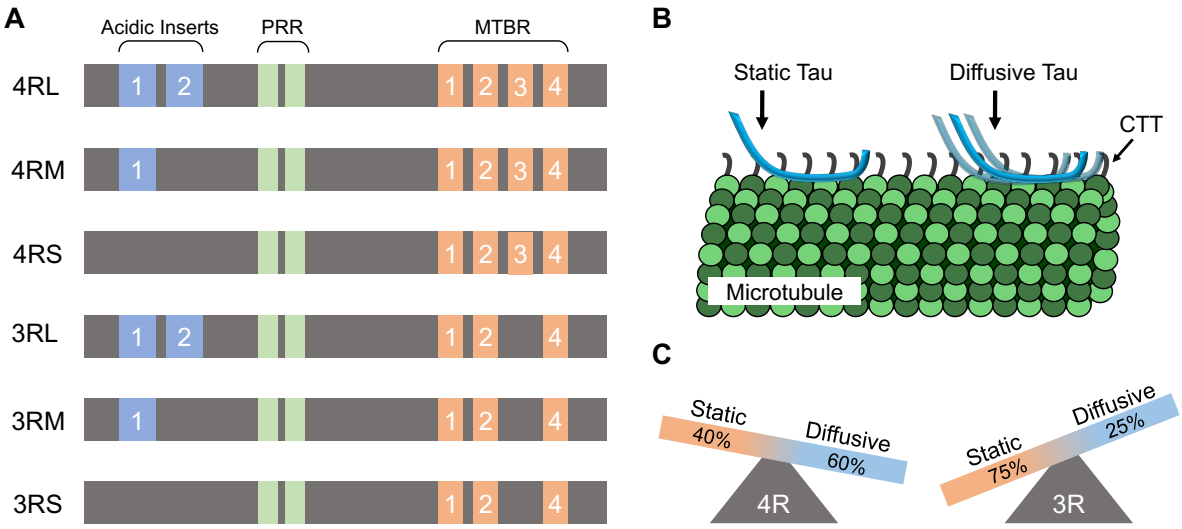

Figure 1-5. Structural and behavioral characteristics of Tau isoforms. A) There are six isoforms of human Tau, varying by length due to the alternative splicing of acidic inserts and microtubule binding repeats (MTBR). All isoforms contain a proline-rich region (PRR). **B)** Tau can bind to the microtubule in a static binding state or a diffusive binding state (reliant upon CTTs). **C)** Each Tau isoform has a characteristic equilibrium of time spend in the diffusive versus static binding state. As a rule of thumb, 3R-Tau isoforms favor the static state while 4R-Tau isoforms favor the diffusive state.

1.4 Kinesin Motors

Kinesin motors are the drivers of anterograde transport along axonal microtubules. Like all molecular motors, kinesin motors are enzymes that convert the chemical energy from ATP hydrolysis to mechanical energy (Vale, Reese, and Sheetz 1985; Brady 1985).

ATP hydrolysis occurs in the kinesin motor domain, found most commonly at the N-terminal end of the protein, and is a part of the protein that is engaged with the microtubule. Connecting the motor domain and the stalk, or "body", of a kinesin is a short, flexible chain of amino acids known as the neck linker. At the C-terminal end of most kinesin proteins, there is a tail/cargo binding domain that allows kinesins to bind directly to cargo or to adaptor proteins (Figure 1-6). The tight mechanochemical coupling of ATP hydrolysis allows kinesin motors to be processive by engaging with and taking 8 nanometer steps along microtubules towards the microtubule + end (Brady 1985; Kojima et al. 1997). In order to become processive, most monomeric kinesins need to dimerize to form either a homo- or heterodimeric protein complex.

The kinesin superfamily of proteins is comprised of 45 known mammalian kinesin genes, each expressing a protein with unique functional properties (Miki et al. 2001). To aid in organization, the kinesin super family is compartmentalized into 15 smaller subfamilies where kinesin motors are grouped together by common structural and functional characteristics (Hirokawa and Tanaka 2015). Of these families, three are known to play major roles in axonal transport: kinesin-1, kinesin-2, and kinesin-3.

1.4.1 Kinesin motors involved in axonal transport

In the mid 1980s, the first member of the kinesin superfamily, a kinesin-1 motor, was discovered. This foundational motor has been extensively researched in the 30+ years since its discovery and serves as an important historical comparator as other kinesin families are identified. This protein was originally isolated from the axoplasms of giant squid axons, and was found in a tetrameric protein complex (Brady 1985). It was further

determined that this complex was comprised of two kinesin-1 motors, forming a homodimer, and two kinesin light chain adaptors that connected the tail of kinesin-1 motors to cargo. In humans, three kinesin-1 motors are expressed: KIF5A, KIF5B, and KIF5C (Miki et al. 2001). All three kinesin-1 motors are expressed in neurons, however kinesin-1 proteins are expressed in many other cells/tissues within the body (Miki et al. 2001; Kanai et al. 2000). Kinesin-1 motors transport a variety of cargo along the axon, most notably mitochondria (Tanaka et al. 1998) and amyloid precursor protein (Kamal et al. 2000).

While much of the kinesin-1 literature has focused on how kinesin-1 motors are activated, many studies have also focused on how these motors are regulated. Findings from these studies have revealed two common themes of regulation amongst kinesin motors: 1) self-regulation through autoinhibition and 2) regulation from obstacles on the microtubule surface. Regarding self-regulation, kinesin-1 motors have been shown to adopt an autoinhibited state via an interaction between the motor domain and tail (Dietrich et al. 2008). This "folded" conformational state results in an inactive motor, and is a common theme amongst other kinesin motors. The microtubule obstacle regulation of kinesin-1 that is most relevant to this dissertation is the regulation of kinesin-1 motility by Tau (Dixit et al. 2008; Vershinin et al. 2007). Specifically, kinesin-1 motors are regulated by the static binding state of Tau while processing on the microtubule.

The kinesin-2 family of motors is comprised of four members: KIF3A, KIF3B, KIF3C, and KIF17. While KIF17 exists in a homodimeric state, KIF3 proteins form a heterotrimeric complex with a KAP3 accessory subunit as KIF3A/3B/KAP3 or KIF3A/3C/KAP3 (Berezuk and Schroer 2004). The kinesin-2 family has multiple functions throughout the human body, including intraflagellar transport (Scholey 2012)

and transport within neurons (Wong-Riley and Besharse 2012). While mainly a transporter of dendritic cargo, kinesin-2 motors are also known to transport cargo along the axon, such as fodrin (Takeda et al. 2000) and choline acetyltransferase (in *Drosophila*) (Ray et al. 1999). Like kinesin-1, kinesin-2 motors are also regulated by a folded autoinhibited state (Hammond, Blasius, et al. 2010). However, unlike kinesin-1, kinesin-2 motors are able to navigate around Tau obstacles and are insensitive to Tau's presence on the microtubule surface. Previous work in our lab has revealed that the "nimbleness" of kinesin-2 is directly related to its longer neck linker length (kinesin-1, 14 amino acids; kinesin-2, 17 amino acids) allowing it to switch microtubule protofilaments and side-step around obstacles (Hoeprich et al. 2014; Hoeprich et al. 2017).

The human kinesin-3 family of proteins is made up of 9 known members: KIF1A, KIF1Bα, KIF1Bβ, KIF1C, KIF13A, KIF13B, KIF14, KIF16A, and KIF16B (Siddiqui and Straube 2017). In the past 10 years, the kinesin-3 family has undergone a renaissance of investigation. This family of motors was first identified in the mid 1990s and was thought to exist purely in a monomeric state (Okada et al. 1995). Many hypotheses emerged regarding the function of this single-headed motor, ranging from being a diffusing monomer (Okada and Hirokawa 1999) to behaving like a Brownian ratchet with asymmetrical, saw-tooth like motion (Oriola and Casademunt 2013). Ten years ago, studies began to support the idea that kinesin-3 motors (most focused on KIF1A) are subject to two-phases of autoinhibition. First, there is an interaction between the FHA and CC2 (Figure 1-6) domains, preventing the motor from binding to the microtubule and, second, an interaction between the NC and CC1 domain (Figure 1-6) that regulates processivity (Soppina et al. 2014; Hammond et al. 2009). It was further determined that this

autoinhibition could be released when kinesin-3 monomers were bound to cargo; once the monomer switches to an active state, it can then dimerize with nearby monomers and become processive (Soppina et al. 2014).

When the activated state of kinesin-3 motors was uncovered it became clear that, not only is this a family of processive motors, but they also exhibit unique "superprocessive" qualities. Superprocessivity is defined by a motor that walks magnitudes of distance farther, at magnitudes of speed faster, than conventional kinesin motors. This is now an accepted intrinsic characteristic of all kinesin-3 motors (Soppina et al. 2014). The superprocessive nature of kinesin-3 motors is essential for their role in axonal transport. Since the discovery of their processive motility, kinesin-3 motors have been highlighted as one of the key players in long-distance, fast anterograde transport. Neuronal kinesin-3 motors are known to transport many types of cargo that must go from the soma to the axon terminals, such as synaptic vesicle precursors (Okada et al. 1995), dense core vesicles (Lo et al. 2011), and transient receptor potential cation channel subfamily V member 1 (Xing et al. 2012). The characterization of kinesin-3 family members is an ongoing process with much of the current research aiming to identify kinesin-3 regulatory mechanisms. The work in this dissertation will focus on the regulatory mechanisms of one kinesin-3 family member in particular, KIF1A.

1.4.2 Kinesin-3 family member, KIF1A

Since its discovery in 1995 (Okada et al. 1995), KIF1A has become the most characterized kinesin-3 member and is regarded as an essential protein for a healthy human nervous system. This necessity was first illustrated using a KIF1A knockout mouse model.

Complete KIF1A knockout pups present with motor/sensory defects and a severe failure to thrive, with most pups dying within 24 hours after birth (Yonekawa et al. 1998). Additionally, isolated primary neuron cultures and postmortem neuropathological analysis showed a significant decrease in both synaptic vesicle transport and synaptic terminal density (Yonekawa et al. 1998; Niwa et al. 2016). This finding, supported by preexisting literature, illuminated one of KIF1A's critical roles in the neuron: transporting synaptic vesicle precursors to promote normal levels of synaptogenesis. Since this foundational study, many other KIF1A cargo have been discovered such as dense core vesicles (Lo et al. 2011), the neurotrophic factor receptor TrkA (Tanaka et al. 2016), and AMPA receptors (Shin et al. 2003), to name a few.

Much attention has been payed to the unique structural elements of KIF1A (Figure 1-6), and how they relate to KIF1A function. All kinesin-3 motors have a family-specific surface loop 12 in the motor domain, known as the "K-loop", that interacts with the microtubule surface (Kikkawa, Okada, and Hirokawa 2000; Soppina and Verhey 2014). The K-loop is characterized by a multi-lysine insert in loop 12, and KIF1A's K-loop has the most insertions (six) of all the kinesin-3 motors (Soppina and Verhey 2014). The K-loop is important for KIF1A's characteristic high on rate on the microtubule as well as for partitioning KIF1A cargo to the axon (Karasmanis et al. 2018); work in this dissertation will go on to detail how this structure is also essential for KIF1A superprocessivity. From a catalytic perspective, the KIF1A K-loop is also known to work in tandem with surface loop 11 to facilitate the mechanochemical coupling of ATP hydrolysis (Nitta et al. 2004), which is discussed further in chapter two.

Perturbations in KIF1A function have now been linked to a variety of different neurodegenerative diseases. The most significant amount of disease-related literature is focused on mutations in the KIF1A gene. These diseases, such as hereditary spastic paraplegia, all share common characteristics of brain atrophy, spasticity, optic nerve atrophy, and motor dysfunction (Lee et al. 2015; Klebe et al. 2012; Ohba et al. 2015; Tomaselli et al. 2017). Current efforts to understand the effects of these mutations have shown that KIF1A can either be hypo- or hyperactivated, yielding a hypo- or hyperaccumulation of synaptic vesicles (Chiba et al. 2019). Recently, an emerging group of studies have focused on a scenario in which there are no perturbations in KIF1A at the genomic level, yet KIF1A motors exist in a diseased neuronal environment. The remainder of this chapter will focus on what is known about KIF1A function in a Tauopathy disease state, and how Tau dysfunction may impact KIF1A cargo transport.

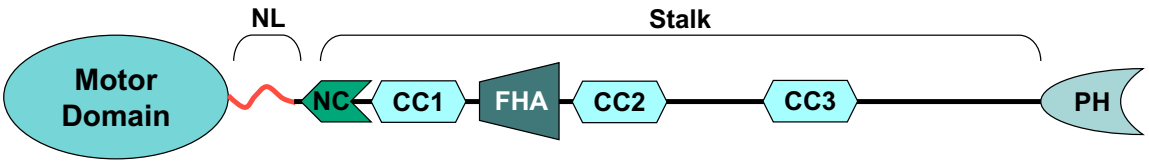

Figure 1-6. Linearized diagram of KIF1A monomer. NL: neck linker, NC: neck coil domain, CC: coiled-coil domain, FHA: forkhead-associated domain, PH: plekstrin homology domain.

1.5 Tau and KIF1A in Tauopathies: Scope and Purpose

Neurodegeneration, characterized in part by altered axonal transport, is one of the most common causes of dementia (Gale, Acar, and Daffner 2018). In healthy neurons,

anterograde axonal cargo transport is mediated by kinesin molecular motors and regulated by the MAP, Tau (Vershinin et al. 2007; Dixit et al. 2008; Hoeprich et al. 2014; McVicker, Chrin, and Berger 2011). However, in neurodegenerative tauopathies like Alzheimer's disease (AD) and frontotemporal dementia (FTD), axonal transport is dysregulated by pathological alterations of Tau expression, post-translation modification, and subsequent alterations in Tau binding behavior (Lacovich et al. 2017; Kanaan et al. 2011; Mandelkow et al. 2003). Specifically, pathological alterations in Tau isoform expression, resulting from mutations that promote exon 10 inclusion into the *MAPT* transcript encoding for Tau protein, are observed in both AD and FTD (Chen et al. 2010; D'Souza and Schellenberg 2005; Kopeikina, Hyman, and Spires-Jones 2012; Schoch et al. 2016; Spillantini and Goedert 2001; Hutton et al. 1998; Hong et al. 1998). This increase in 4R-Tau isoform expression tips the balance of Tau's binding behavior towards the diffusive state and has been directly linked to altered axonal cargo transport, a process mediated by molecular motors such as KIF1A (Lacovich et al. 2017; Majid et al. 2014; Ittner et al. 2008). Our recently published work extends this concept revealing that phospho-regulation of Tau modulates the inhibition of kinesin-1 motility, due to an increase in the diffusive binding behavior of Tau (Stern et al. 2017). While MT bound Tau was first presented as a regulator of kinesin-mediated axonal transport (Dixit et al. 2008; Vershinin et al. 2007), our lab has shown that Tau differentially regulates kinesin motors involved in axonal transport. Specifically, while kinesin-1 is regulated by Tau, we have found that kinesin-2's ability to navigate around MT bound obstacles makes this motor insensitive to Tau (Hoeprich et al. 2014; Hoeprich et al. 2017). However, Tau's regulatory effect on other neuronal kinesins remains unexplored.

KIF1A, a kinesin-3 family member, is a neuronally expressed kinesin motor essential for fast, long-range cargo transport (Hammond et al. 2009; Lo et al. 2011; Soppina et al. 2014; Soppina and Verhey 2014; Gumy et al. 2017). However, irregular localization and aggregation of cargo known to be transported by KIF1A has been identified in the neurons of tauopathy patients (Kandalepas et al. 2013; Lassmann et al. 1992; Kopeikina et al. 2011), suggesting that pathological shifts in Tau isoform expression and behavioral binding state yields dysregulated KIF1A transport. Despite this possible connection of KIF1A to tauopathy presentation, Tau's regulatory effect on dimeric KIF1A cargo transport is unknown. This lack of understanding of the basic molecular mechanisms regulating KIF1A cargo transport, and how these mechanisms are related to Tau-mediated disease progression, presents a significant gap in our current knowledge and is a limiting step toward the development of new neurodegenerative therapeutic strategies.

However, one cannot comprehensively tackle a problem as large as KIF1A's role in Tauopathy progression, without first understanding the basics of KIF1A and Tau's relationship at a molecular level. Therefore, in this dissertation, we have employed a bottom-up approach to address this problem by using single-molecule imaging techniques. Through these techniques we were able to define the effect of Tau on individual KIF1A motors in an *in vitro* reconstituted system. This investigation is strongly supported by data demonstrating that:

1. Cargo transported by KIF1A is irregularly localized in the brains of FTD and AD patients (Hung and Coleman 2016; Siddiqui and Straube 2017; Goetzl et al. 2016; Kopeikina et al. 2011; Kandalepas et al. 2013; Lassmann et al. 1992),

2. Altered Tau isoform expression, favoring the diffusive binding state of Tau, is observed in tauopathies such as AD and FTD (Goetzl et al. 2016; Kar et al. 2005), and

3. Long-distance KIF1A motility is important for synaptogenesis and synaptic vesicle transport (Kern et al. 2013; Zhang et al. 2016; Okada et al. 1995; Hall and Hedgecock 1991; Voelzmann et al. 2016). These persuasive data support the central hypothesis of this dissertation that Tau regulates the characteristic behavior and motility of KIF1A.

In chapter 2, we pursued an early observation that KIF1A engages in unique and unreported pausing behavior between segments of processive motion on the microtubule surface. When prompted with a finding such as this, we focused on the question: by what mechanism is KIF1A pausing? Considering past literature supporting KIF1A's reliance on tubulin's C-terminal tails, we hypothesized that KIF1A pausing was mediated through a K-loop/CTT interaction. To test this hypothesis, we assessed KIF1A motility and pausing behavior across: 1) multiple microtubule lattices, 2) varying degrees of CTT alteration, and 3) two different K-loop sequences created using site-directed mutagenesis. The culmination of these experiments dissected and uncovered a mechanism of KIF1A pausing that is indeed centered around a K-loop/CTT interaction. Specifically, we were able to determine that KIF1A pausing is directly linked to levels of CTT poluglutamylation, a PTM of CTTs in neurons.

Identifying KIF1A's pausing mechanism was vital for shaping the hypothesis and experimental design for chapter 3. In this chapter we defined Tau as a KIF1A regulator by directly testing the inhibitory capability of Tau isoforms on KIF1A pausing and subsequent motility. Taking into account the reliance of Tau on CTTs to engage in diffusive binding behavior, we hypothesized that the diffusive binding state of Tau inhibits KIF1A pausing

through competition for the CTT structure. Through quantifying KIF1A pausing and motility across 1) different Tau isoforms, 2) at multiple Tau concentrations on the microtubule and, 3) on microtubules with and without CTTs, we were able to show that the diffusive binding state, not the static binding state, of Tau regulates KIF1A pausing, resulting in a subsequent reduction in KIF1A motility. This study introduced a new mechanism of Tau-mediated regulation of kinesin motors.

Lastly, chapter 4 is a discussion of how these findings at the single-molecule level contribute to the field of Tauopathy research as a whole. Additionally, potential future avenues for investigation will be discussed, mainly focused on systems with higher orders of physiological complexity.

CHAPTER 2: POLYGLUTAMYLATION OF TUBULIN'S C-TERMINAL TAIL CONTROLS PAUSING AND MOTILITY OF KINESIN-3 FAMILY MEMBER KIF1A

Dominique V. Lessard[1], Oraya J. Zinder[1], Takashi Hotta[2], Kristen J. Verhey[2], Ryoma Ohi[2], Christopher L. Berger[1]*

From the [1] Department of Molecular Physiology & Biophysics, University of Vermont, Burlington, VT 05405 and the[2] Department of Cell and Developmental Biology, University of Michigan Medical School, Ann Arbor, MI 48109

Published in *Journal of Biological Chemistry*, January 2019.

Running Title: *Novel regulation of KIF1A motility*

*To whom correspondence should be addressed:
Christopher L. Berger, Ph.D.
Department of Molecular Physiology & Biophysics
University of Vermont
Burlington, Vermont 05405
Telephone: (802) 656-5707
Email: cberger@uvm.edu

Keywords: molecular motor, single-molecule biophysics, kinesin, posttranslational modification (PTM), microtubule, KIF1A, polyglutamylation, cytoskeleton, neuron, K-loop

ABSTRACT

The kinesin-3 family member KIF1A plays a critical role in site-specific neuronal cargo delivery during axonal transport. KIF1A cargo is mislocalized in many neurodegenerative diseases, indicating that KIF1A's highly efficient, superprocessive motility along axonal microtubules needs to be tightly regulated. One potential regulatory mechanism may be through post-translational modifications (PTMs) of axonal microtubules. These PTMs often occur on the C-terminal tails of the microtubule tracks, act as molecular "traffic signals" helping to direct kinesin motor cargo delivery, and include C-terminal tail polyglutamylation important for KIF1A cargo transport. KIF1A initially interacts with microtubule C-terminal tails through its K-loop, a positively charged surface loop of the KIF1A motor domain. However, the role of the K-loop in KIF1A motility and response to perturbations in C-terminal tail polyglutamylation is underexplored. Using single-molecule imaging, we present evidence that KIF1A pauses on different microtubule lattice structures, linking multiple processive segments together and contributing to KIF1A's characteristic superprocessive run length. Furthermore, modifications of the KIF1A K-loop or tubulin C-terminal tail polyglutamylation reduced KIF1A pausing and overall run length. These results suggest a new mechanism to regulate KIF1A motility via pauses mediated by K-loop/polyglutamylated C-terminal tail interactions, providing further insight into KIF1A's role in axonal transport.

INTRODUCTION

Axonal transport is a critical process for neuronal viability and function involving the highly-choreographed, long-distance trafficking of cargo. This process is facilitated in part by members of the kinesin superfamily of motors that utilize the mechanochemical coupling of ATP-hydrolysis (Schnitzer and Block 1997) to carry motor-specific cargo in the anterograde direction along axonal microtubules.

The neuron-specific kinesin-3 family member KIF1A (Okada et al. 1995) is a key mediator of axonal transport, delivering neuronal cargo, such as dense core vesicles (Lo et al. 2011) and synaptic vesicle proteins (Okada et al. 1995), in a spatiotemporally regulated manner along axonal microtubules (Hirokawa, Niwa, and Tanaka 2010; Vale and Milligan 2000). Upon cargo-mediated dimerization and release of steric autoinhibition, KIF1A motors are reported to exhibit "superprocessive" motility behavior, traveling comparatively long distances on microtubules when compared to conventional kinesin (Hammond et al. 2009; Soppina et al. 2014). The discovery of this superprocessive behavior supports KIF1A as an important player in long distance axonal transport, providing further insight into KIF1A's role in many neuronal processes such as synaptogenesis (Kondo, Takei, and Hirokawa 2012) and neurogenesis (Tsai et al. 2010). The importance of tightly regulated KIF1A cargo delivery is highlighted in neurodegenerative diseases where mislocalization and accumulation of KIF1A cargo is observed (Hung and Coleman 2016; Siddiqui and Straube 2017; Goetzl et al. 2016). However, our understanding of this disease-state presentation is limited by the gap in knowledge of the mechanisms that regulate KIF1A motility.

Beyond serving as tracks for kinesin motors, microtubules can direct subcellular trafficking by providing directional cues for motor specificity on select microtubule populations. These "traffic signs" are frequently introduced via microtubule post-translational modifications (PTMs), often on the C-terminal tails of microtubules (Verhey and Gaertig 2007; Magiera, Singh, et al. 2018). While there are many recent discoveries of how microtubule PTMs regulate different kinesin families (Sirajuddin, Rice, and Vale 2014; Hammond, Huang, et al. 2010; Ghosh-Roy et al. 2012), how this concept can be extended to kinesin-3 motors such as KIF1A is relatively unexplored. One potential PTM regulating KIF1A trafficking is the heavy polyglutamylation of both α- and β- tubulin subunits in neurons (Audebert et al. 1994) via the tubulin tyrosine ligase-like family of enzymes (Ikegami et al. 2006; Janke et al. 2005). KIF1A's dependence on optimal levels of polyglutamylation has been observed in the ROSA22 mouse model, characterized by a loss of neuronal α-tubulin polyglutamylation leading to altered KIF1A cargo trafficking and reduced KIF1A affinity for microtubules (Ikegami et al. 2007). These physiological repercussions of altered KIF1A function highlight the importance of further studying interactions between KIF1A and the polyglutamylation of C-terminal tails of tubulin at the molecular level.

Polyglutamylation may impact KIF1A motility via a lysine-rich surface loop (loop-12) that is characteristic of the kinesin-3 motor family (Soppina and Verhey 2014; Okada and Hirokawa 2000). Previous work has demonstrated that this "K-loop" is a critical component for optimal KIF1A function. From a catalytic perspective, it is thought that the K-loop is necessary for KIF1A's structural interaction with the microtubule during the ATP-hydrolysis cycle (Nitta et al. 2004). Furthermore, it is known that the K-loop interacts

electrostatically with the glutamic acid-rich C-terminal tail of tubulin (Kikkawa, Okada, and Hirokawa 2000; Okada and Hirokawa 1999), tethering the motor to the microtubule track (Soppina and Verhey 2014). This K-loop/C-terminal tail relationship, combined with the physiological detriment of reduced microtubule polyglutamylation, illustrates that specific interactions between the KIF1A K-loop and C-terminal tails of tubulin are essential for optimal KIF1A function. Therefore, we hypothesized that C-terminal tail polyglutamylation regulates KIF1A motility and behavior on microtubules mediated by interactions with the KIF1A K-loop structure. Using single-molecule total internal reflection fluorescence microscopy, we first tested our hypothesis by quantifying the motility and behavioral response of KIF1A on various microtubule lattices and then specifically perturbed the K-loop/C-terminal tail interaction. Our findings demonstrate that that KIF1A pauses on the microtubule lattice, and suggest that this behavior is caused by a polyglutamylation-sensitive K-loop/CTT interaction.

EXPERIMENTAL PROCEDURES

Tubulin isolation, microtubule preparation and labelling

Neuronal tubulin was isolated from bovine brains donated from Vermont Livestock Slaughter & Processing (Ferrisburgh, VT) using a high molarity PIPES buffer (1 M PIPES, pH 6.9 at room temperature, 10 mM $MgCl_2$, and 20 mM EGTA) as previously described (Castoldi and Popov 2003). Purified tubulin was clarified using ultracentrifugation for 20 minutes at 95,000 rpm at 4°C in an Optima TLX Ultracentrifuge (Beckman, Pasadena, CA). After clarification, tubulin concentration was calculated using the tubulin extinction coefficient of 115,000 cm^{-1} M^{-1} and read at 280nm in the spectrophotometer.

Tubulin was purified from HeLa Kyoto cells with TOG affinity column chromatography using gravity-flow setup (Widlund et al. 2012; Hotta et al. 2016). Cells were resuspended in BRB80 (80 mM PIPES, 1 mM EGTA, 1 mM $MgCl_2$ pH 6.8) supplemented with 1 mM DTT and protease inhibitors (cOmplete™, Mini, EDTA-free [Sigma-Aldrich, St. Louis, MO] and 0.2 mM PMSF) and sonicated. Cleared lysate was loaded onto a TOG column, in which ~ 15 mg of bacterially purified GST-TOG1/2 protein was conjugated with 1 ml of NHS-activated Sepharose 4 Fast Flow resin (GE Healthcare; Marlborough, MA). Wash, elution, desalting and concentration was carried out as described in Hotta et al, 2016 (Hotta et al. 2016). Glycerol was not added to the purified tubulin. Aliquoted tubulin was snap frozen in liquid nitrogen and stored at -80ºC.

Clarified tubulin was supplemented with 1mM GTP (Sigma-Aldrich) or guanosine-5′-[(α,β)-methyleno]triphosphate sodium salt (GMPCPP; Jena Bioscience, Jena, Germany). To label microtubules, unlabeled tubulin was mixed with rhodamine-labeled tubulin (Cytoskeleton, Denver, CO) at a ratio of 100:1. Microtubules were stabilized with

GMPCPP following previously reported methods (McVicker, Chrin, and Berger 2011) or polymerized at 37°C for 20 minutes and stabilized with 20 μM paclitaxel (taxol; Sigma-Aldrich) in DMSO. Microtubules were diluted to a working concentration of 1 μM in P12 Buffer (12mM PIPES, 1mM $MgCl_2$, 1 mM EGTA, pH 6.8 supplemented with 20 μM paclitaxel) (Soppina and Verhey 2014).

Plasmids, mutagenesis, and cell lysate motor expression

KIF1A(1-393)-LZ-3xmCitrine plasmid was a generous gift of Kristen Verhey (University of Michigan, Ann Arbor, MI) and the KIF1A(1-396)-GFP (Addgene plasmid # 45058) mammalian plasmid were a gift from Gary Banker (Oregon Health & Science University). TriAla-KIF1A-LZ-3xmCitrine was generated from the KIF1A(1-393)-LZ-3xmCitrine plasmid using the QuikChange II XL Site-Directed Mutagenesis Kit (Agilent Technologies, Santa Clara, CA). COS-7 monkey kidney fibroblasts (American Type Culture Collection, Mansses, VA) were cultured in DMEM-GlutaMAX™ with 10% fetal bovine serum (FBS) at 37°C with 5% CO_2. Cells were transfected with 1μg of either WT KIF1A-LZ-3xmCitrine, Tri-Ala KIF1A-LZ-3xmCitrine, or KIF1A-GFP mammalian plasmid using the Lipofectamine 2000 delivery system (Thermo Fisher Scientific, Waltham, MA) and incubated in Opti-MEM™ (Thermo Fisher Scientific) media with 4% FBS. The next day, cells were harvested, pelleted, and washed with DMEM GlutaMAX™. The pellet was vigorously resuspended in lysis buffer (25mM HEPES, 11mM K^+ Acetate, 5mM Na^+ Acetate, 5mM $MgCl_2$, 0.5mM EGTA, 1% Triton X-100, 1mM PMSF, 1mg/ml pepstatin, 10 μg/ml leupeptin, 5μg/ml aprotinin) and centrifuged at room temperature for 15 minutes at 14,000 rpm. Relative amounts of protein between preps and motor constructs

was determined using densitometry, and supernatant containing expressed motor protein was aliquoted and stored at -80°C until further use.

Subtilisin treatment

To remove C-terminal tails, 5 μM paclitaxel stabilized microtubules were treated with 0.05 μM Subtilisin A (Sigma Aldrich), resuspended in P12 Buffer, for 45 minutes at 25°C. The reaction was stopped by the addition of 5 mM phenylmethanesulfonyl fluoride. Subtilisin treatment was confirmed by Coomassie staining of SDS-PAGE denaturing gel. Tubulin concentration was determined as previously described**.**

In vitro single-molecule TIRF

Flow chambers used in *in vitro* TIRF experiments were constructed as previously described (Stern et al. 2017). Flow chambers were incubated with monoclonal anti-β III (neuronal) antibodies at 33 μg/ml for 5 minutes, then washed twice with 0.5 mg/ml bovine serum albumin (BSA; Sigma Aldrich) and incubated for 2 minutes. 1 μM of microtubules (any experimental condition) were administered and incubated for 8 minutes. Non-adherent microtubules were removed with a P12 wash supplemented with 20 μM paclitaxel. Kinesin motors in Motility Buffer consistent with past literature (MB; 12 mM PIPES, 1 mM $MgCl_2$, 1 mM EGTA, supplemented with 20 μM paclitaxel, 10 mM DTT, 10 mg/ml BSA, 2 mM ATP and an oxygen scavenger system [5.8 mg/ml glucose, 0.045 mg/ml catalase, and 0.067 mg/ml glucose oxidase; Sigma Aldrich]) (Soppina and Verhey 2014), or a High Salt Motility Buffer (same as Motility Buffer, only change being PIPES concentration raised to 80 mM), supplemented with 2 mM ATP, were added to the flow cell just before image acquisition. For landing rate assays, *in vitro* KIF1A motility assays

were prepared as described above, with the only change being that MB was supplemented with 2 mM ADP. Control *Drosophila melanogaster* biotin-tagged kinesin-1 motors were labeled with streptavidin-conjugated Qdot 655 (Life Technologies, Carlsbad, CA) at a 1:4 motor:Qdot ratio as previously described (Stern et al. 2017; Hoeprich et al. 2017).

Total internal reflection fluorescence (TIRF) microscopy was performed at room temperature using an inverted Eclipse Ti-E microscope (Nikon, Melville, NY) with a 100x Apo TIRF objective lens (1.49 N.A.) and dual iXon Ultra Electron Multiplying CCD cameras, running NIS Elements version 4.51.01. Rhodamine-labeled microtubules were excited with a 561 and a 590/50 filter. KIF1A-LZ-3xmCitrine (WT or Tri-Ala) motors were excited with a 488 laser and a 525/50 filter. Qdot 655 conjugated kinesin-1 motors were excited with a 640 laser and 655 filter. All movies were recorded with an acquisition time of 200 msec for 500 frames (100 sec observation).

Photobleaching assay

As an additional control, a photobleaching assay was performed to confirm that KIF1A run lengths were not underestimated due to photobleaching of the C-terminal 3xmCitrine tag (Figure S2-6). Motors were adhered to microtubules in the presense of adenylylimidodiphosphate (AMPPNP; Sigma-Aldrich) and washed once to remove unattached motors. Using Image J, a region of interest (ROI) was drawn around each fluorescent spot and the average intensity of each pixel within the ROI was measured over time. Intensity was background corrected and a motor was considered photobleached when the ROI average intensity was 0.

Western blot analysis

Purified tubulin protein was separated by electrophoresis on Mini-PROTEAN® TGX™ gels (Bio-Rad, Hercules, CA) and transferred to a polyvinylidene fluoride membrane (Bio-Rad). Membranes were blocked in a 1:1 solution of phosphate-buffered saline (PBS; 155 mM NaCl, 3 mM Na_2HPO_4, and 1 mM KH_2PO_4, pH 7.4) and Odyssey® blocking reagent (Li-COR, Lincoln, NE). A mouse anti-polyglutamylated tubulin antibody (1:8,000; GT335, AdipoGen, San Diego, CA) or a mouse anti-alpha tubulin antibody (1:10,000; DM1A, Sigma-Aldrich) was administered to membrane, followed by a secondary DyLight 800 anti-mouse IgG antibody (1:10,000; Thermo Fisher Scientific). Secondary antibody fluorescence was detected using an Odyssey CLx (Li-COR).

Data analysis

Motility events were analyzed as previously reported (Hoeprich et al. 2014; Hoeprich et al. 2017)). In brief, overall run length motility data was measured using the ImageJ MTrackJ plug-in, for a frame-by-frame quantification of KIF1A motility. Pauses are defined as segments where the average velocity is less than 0.2 μm/s over three frames or more. Continuous events were identified at the boundaries of pausing events. Average overall/continuous speed were plotted as a histogram, with mean and SD are reported in Table 2-1. KIF1A pause duration events were fit to a single exponential decay, represented as cumulative frequency plots with confidence intervals (CI) of 95%. Pause duration is reported as the inverse of the decay rate, representing the lifetime of pause duration events.

To assess statistical significance between motor populations, we account for the fact that the characteristic run length of the motor is directly coupled to the length distribution of the experimental microtubule population and 2) that microtubule length

distributions will vary between experimental set ups and condition. Furthermore, we recognize the uncertainty in our experimental data reporting due to variations in sampling. To account for this, we use a bootstrap analysis, involving the extensive resampling of data sets, to generate histograms of characteristic run length and characteristic track length. After bootstrapping, these previously exponential distributions now fit a Gaussian distribution, allowing us to measure 99% confidence interval of our data sets. To assess statistical significance between data sets, we then use a permutation resampling algorithm (tested against a null hypothesis), as this is a distribution independent test without the assumptions of other nonparametric tests (Thompson, Hoeprich, and Berger 2013).

Kymographs of motor motility were created using the MultipleKymograph ImageJ plug-in, with a set line thickness of 3. To correct for microtubule track length effects on motor motility, overall/continuous run length data was resampled to generate cumulative frequency plots (99% CI), using previously reported methods (Thompson, Hoeprich, and Berger 2013). After data resampling, statistical significance between motor run length and speed data sets was determined using a paired t-test.

To determine the landing rate of KIF1A on various microtubule conditions, the total number of motor landing events on the microtubule was divided by the length of the microtubule and further divided by the duration of the movie (events/μm/minute). To be considered a landing rate event, a motor must remain on the microtubule for three consecutive frames under ADP or AMPPNP state condition

RESULTS

KIF1A exhibits pausing behavior and superprocessive motility on taxol-stabilized and GMPCPP microtubules assembled from brain tubulin.

Initial single molecule TIRF microscopy observations revealed that dimeric KIF1A motors possess the novel ability to pause during a run on taxol-stabilized microtubules (Figure 2-1A, Movie S2-1). While pausing, the dimeric motor appears to be spatially constrained as it does not exhibit the highly diffusive behavior of the KIF1A monomer (Okada and Hirokawa 1999). While other kinesin motors have been shown to exhibit transient pauses (Gramlich et al. 2017; Padzik et al. 2016), the high pause frequency (Table 2-1) and substantial number of pauses per distance (Figure 2-2F) of KIF1A has not been previously characterized, leading us to investigate this behavior further.

The discovery of this novel pausing behavior led us to redefine our nomenclature of KIF1A motility by dissecting KIF1A motility into three segments (Figure 2-1A). First, we define the *continuous run length* as segments where, within a single event, KIF1A is moving at a constant velocity. Next, continuous run lengths are connected by *pauses* that occur at the beginning of continuous runs, in between continuous runs, or after continuous runs. To characterize KIF1A pausing, we have quantified both the *pause frequency* (# of pauses/overall run) and *pauses per distance* (# of pauses/μm microtubule). While representative KIF1A kymographs include long pauses (Figure 2-1C, 2-2A, 2-2B), it is important to note that the majority of pausing events are less than 1.5 seconds and occur at stochastic locations on the microtubule (Figure 2-1C, Table 2-1). Lastly, we define the *overall run length* as the sum of continuous run lengths during a single motility event on

the microtubule. KIF1A pausing behavior (Figure 2-1B, 2-1C) is best revealed at motor concentrations lower than those utilized in previous work (Soppina and Verhey 2014) .

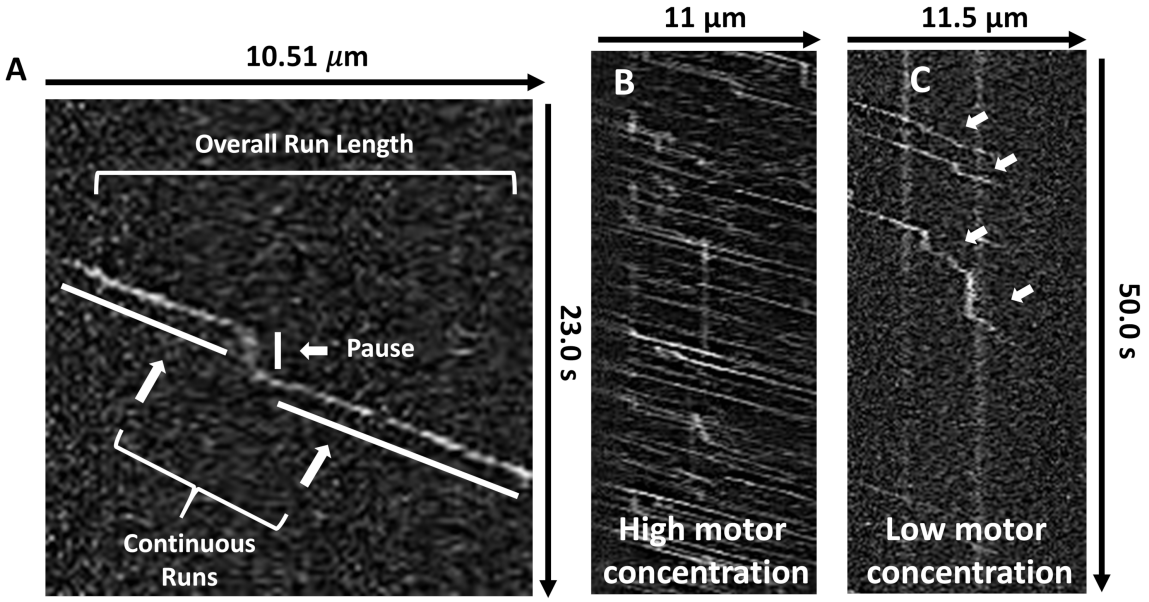

Figure 2-1. KIF1A pauses during runs along the microtubule. A) Representative kymograph with corresponding nomenclature used to describe novel KIF1A motility behavior. **B,C)** Representative kymographs demonstrating that at **B)** high motor concentrations, pausing becomes obscured by surrounding motor motility while at **C)** low motor concentrations, extensive pausing behavior (white arrows) is revealed at stochastic positions on the microtubule. This research was originally published in the Journal of Biological Chemistry. Lessard, DV, Zinder, OJ, Hotta, T, Verhey, KJ, Ohi, R, Berger, CL. Polyglutamylation of tubulin's C-terminal tail controls pausing and motility of kinesin-3 family member KIF1A. J. Biol. Chem. 2019; 29(16):6263-6363. © the American Society for Biochemistry and Molecular Biology

To confirm that this behavior was not dependent on the facilitated dimerization of our leucine zipper construct (KIF1A-LZ-3xmCitrine), we repeated our single molecule experiments with a non-leucine zipper construct (KIF1A-GFP). We confirmed that in the absence of the leucine zipper, KIF1A exhibits extensive pausing behavior and superprocessive motility (Figure S2-1). Additionally, we observed an increase in purely diffusive events with this construct (Figure S2-1A), likely resulting from KIF1A monomers (Soppina et al. 2014; Hammond et al. 2009). Our results demonstrate that the KIF1A-LZ-3xmCitrine construct is an appropriate model for dimeric KIF1A behavior. As our current investigations are focused on the processive, dimeric KIF1A motor, we performed all other experiments with the LZ construct.

We next investigated KIF1A's pausing on GMPCPP microtubules, which contain tubulin subunits in the GTP state rather than the GDP state and are known to have more protofilaments than taxol-stabilized microtubules (Ginsburg et al. 2017; Hyman et al. 1995; Zhang, LaFrance, and Nogales 2018). KIF1A pausing occurred on both microtubule lattices (Figure 2-2A, B) with similar frequencies of 0.95 pauses/overall run (Taxol [n=165]) versus 1.02 pauses/overall run (GMPCPP [n=171]) and pauses per distance of 0.14 pauses/μm (Taxol) versus 0.16 pauses/μm (GMPCPP) (Figure 2-2F, Table 2-1). However, there was a 46% decrease in pause duration from 1.23 sec (Taxol) to 0.66 sec (GMPCPP) (Figure 2-2D, 2-2E, Table 2-1). With respect to other motility characteristics, we observed no significant change in overall run length (6.24 ± 2.09 μm [n=165] and 6.01 ± 2.17 μm [n=171]) or continuous run length (2.95 ± 1.07 μm [n=282] and 2.81 ± 0.61μm [n=305]) along taxol-stabilized versus GMPCPP microtubules, respectively (Figure 2-2C, Table 2-1). We also observed no change in the overall speed (1.35 ± 0.41 μm/s and 1.27 ±

0.28 μm/s, respectively; Table 2-1, Figure S2-2) or continuous speed (2.01 ± 0.53 μm/s and 2.06 ± 0.54 μm/s, respectively; Table 2-1, Figure S2-3) along taxol-stabilized versus GMPCPP microtubules, respectively. However, there was a significant decrease in KIF1A's ability to land on GMPCPP microtubules in motility buffer with the presence of ADP with 4.86 ± 0.88 events/μm/min [n=958] compared to 7.93 ± 1.25 events/μm/min [n=1152] on taxol-microtubules (Figure 2-7, Table 2-1). Thus, while KIF1A displays a decrease in pause duration and a decreased landing rate on GMPCPP microtubules (Table 2-1), these results confirm that KIF1A's unique pausing behavior occurs on microtubules of varying protofilament and nucleotide composition.

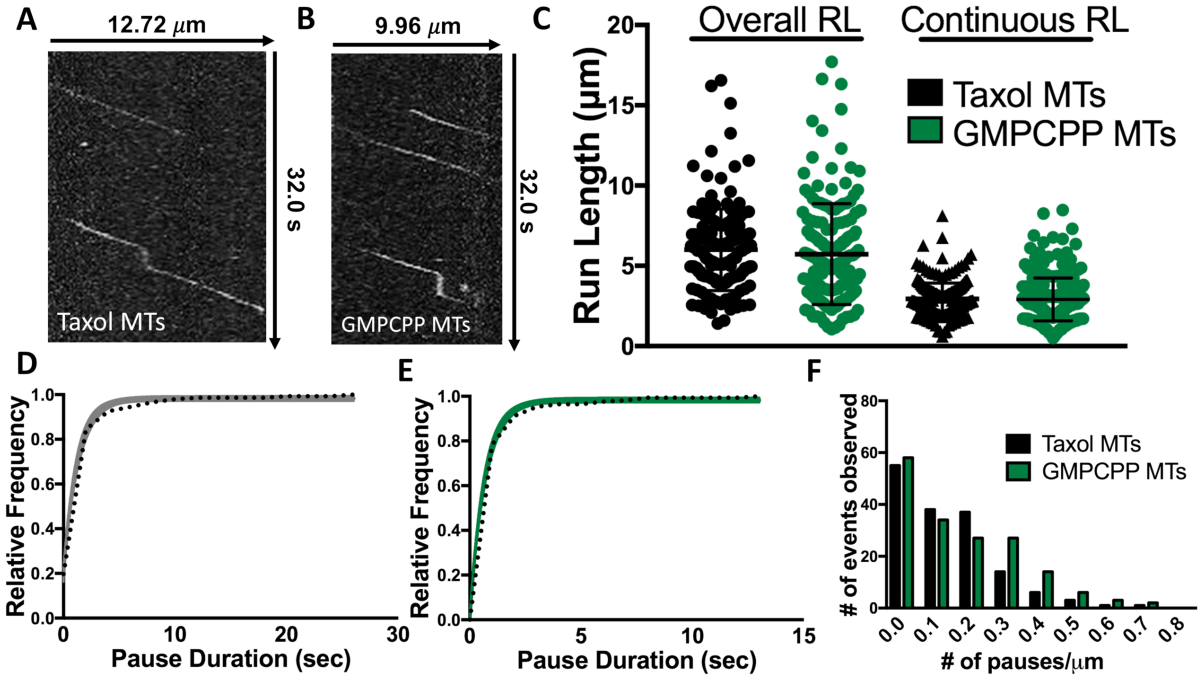

Figure 2-2. KIF1A pausing behavior occurs on taxol-stabilized and GMPCPP microtubules. A,B) Representative kymographs of KIF1A motility on **A)** taxol-stabilized or **B)** GMPCPP microtubules. **C)** Quantification demonstrates no significant differences in KIF1A overall run length (RL) (6.24 ± 2.09 μm [n=165] and 6.01 ± 2.17 μm [n=171], respectively) and continuous run length (2.95 ± 1.07 μm [n=282], and 2.81 ± 0.91μm [n=305], respectively). Run length values are reported as mean ± standard deviation and were calculated as previously reported (Thompson, Hoeprich, and Berger 2013). **D)** KIF1A pause duration is 1.23 sec (Confidence Interval [CI] 1.00 – 1.42 sec) on taxol-stabilized microtubules [n=147] and **E)** 0.66 sec (CI 0.59 – 0.73 sec) on GMPCPP microtubules [n=152]. **F)** KIF1A exhibits similar pauses per distance on taxol-stabilized (0.14 pauses/μm [n=165]) and GMPCPP (0.16 pauses/μm [n=171]) microtubules. Pause durations were fit to a single exponential decay and are represented as cumulative frequency distributions; the time constant of fit is reported in seconds with a 95% confidence interval. All other metrics are reported as Mean ± SD. * $p < 0.001$ Kinesin-1 was used as an experimental control across all conditions (Figure S2-2 through S2-5). Each condition is representative of at least four independent experiments. This research was originally published in the Journal of Biological Chemistry. Lessard, DV, Zinder, OJ, Hotta, T, Verhey, KJ, Ohi, R, Berger, CL. Polyglutamylation of tubulin's C-terminal tail controls pausing and motility of kinesin-3 family member KIF1A. J. Biol. Chem. 2019; 29(16):6263-6363. © the American Society for Biochemistry and Molecular Biology

Interaction with tubulin C-terminal tails mediates KIF1A pausing behavior, landing rate, and superprocessive motility.

To investigate a potential mechanism facilitating KIF1A pausing, we considered the known interaction of KIF1A's lysine-rich K-loop with tubulin's glutamate-rich C-terminal tail projections (Soppina and Verhey 2014; Okada and Hirokawa 2000). Previous work has shown that the positively-charged surface loop-12 (K-loop) of the KIF1A motor domain interacts with the microtubule C-terminal tails, helping to anchor KIF1A to the microtubule (Kikkawa, Okada, and Hirokawa 2000) and mediate KIF1A landing on the microtubule (Soppina and Verhey 2014). We thus asked if subtilisin-mediated proteolytic removal (Knipling, Hwang, and Wolff 1999) (Figure 2-3A) of the tubulin C-terminal tails could influence KIF1A motility and pausing behavior. On subtilisin-treated microtubules, we observed a 47% reduction of KIF1A overall run length (3.31 ± 1.34 μm [n=171]) when compared to untreated microtubules (Figure 2-3B, 2-3C, Table 2-1). Subtilisin treatment did not significantly change the continuous run length (2.91 ± 1.16 μm [n=205]) of KIF1A (Figure 2-3C, Table 2-1), however we did observe a 45% decrease in pause duration (1.23 sec to 0.68 sec), a 79% reduction in pause frequency (0.95 pauses/overall run to 0.18 pauses/overall run), and an 85% reduction in pauses per distance (0.14 pauses/μm to 0.02 pauses/μm) (Figure 2-3D, 2-3E, Table 2-1). Due to the decreased pausing events, KIF1A's overall speed increased on subtilisin-treated microtubules from 1.35 ± 0.41 μm/s (untreated) to 1.58 ± 0.38 μm/s (Table 2-1, Figure S2-2). However, continuous speed remained relatively unchanged between untreated and subtilisin-treated microtubules (2.01 ± 0.53 μm/s and 1.94 ± 0.50 μm/s, respectively) (Table 2-1, Figure S2-3).

It has been previously reported that the perturbation of KIF1A's interaction with the C-terminal tail reduces the motor's landing rate (Soppina and Verhey 2014). Measuring KIF1A landing rate in ADP-containing motility buffer confirms the necessity of this interaction, showing that subtilisin-treatment of microtubules reduces the landing rate of KIF1A by 65% (7.93 ± 1.25 events/μm/min to 2.80 ± 0.42 events/μm/min, Figure 2-7, Table 2-1). Taken together, these results expose KIF1A's reliance on the microtubule C-terminal tail to engage with the microtubule, initiate pausing behavior, and generate superprocessive overall run lengths.

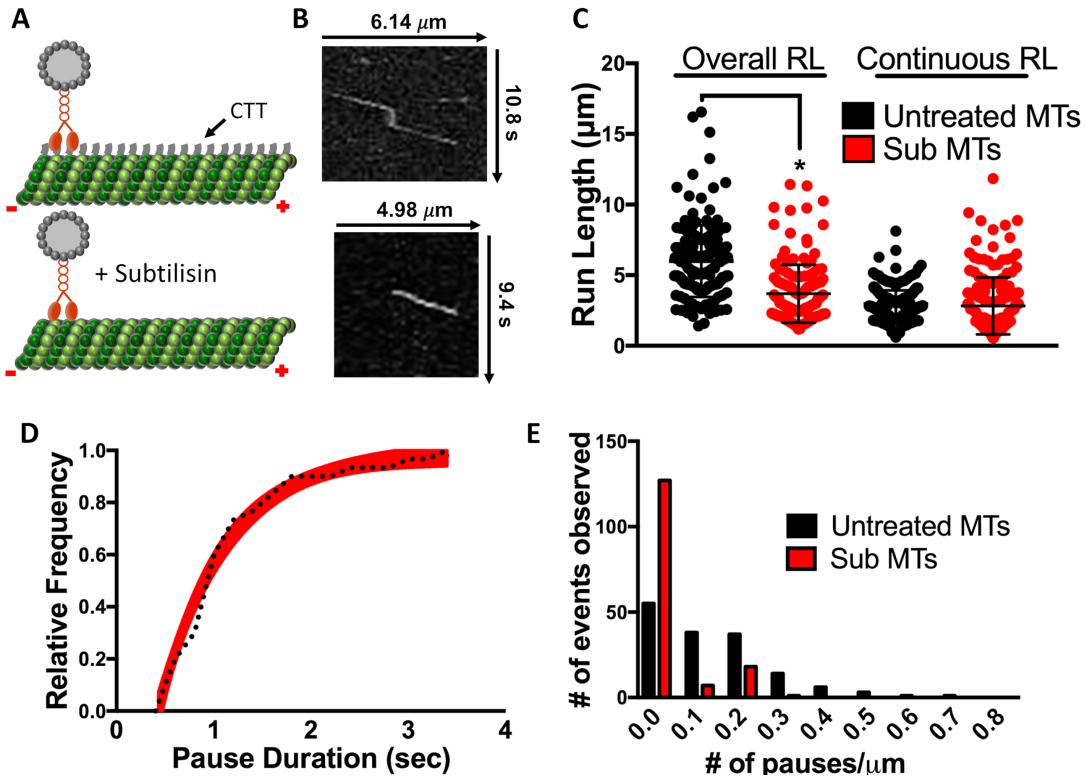

Figure 2-3. Removal of the tubulin C-terminal tail reduces KIF1A pausing. A) Cartoon depiction of tubulin C-terminal tail (CTT) cleavage upon addition of subtilisin. **B)** Representative kymographs of KIF1A motility on untreated microtubules (top) vs subtilisin (Sub) treated microtubules (bottom). **C)** The overall run length of KIF1A was reduced from 6.24 ± 2.09 µm to 3.31 ± 1.34 µm [n=171] upon subtilisin treatment of microtubules, while continuous run length was not significantly changed (2.95 ± 1.07 µm and 2.91 ± 1.16 µm [n= 205], respectively). **D)** KIF1A pause duration is 0.68 sec (CI 0.57 – 0.83 sec) on subtilisin-treated microtubules [n=34], compared to untreated microtubules (1.23 sec; Figure 2-2D). **E)** KIF1A pauses per distance was significantly decreased from 0.14 pauses/µm to 0.02 pauses/µm upon subtilisin-treatment of taxol-stabilized microtubules. Run length values and standard deviations were calculated as previously reported (Thompson, Hoeprich, and Berger 2013). Kinesin-1 was used as an experimental control across all conditions (Figure S2-2 through S2-5). Each condition is representative of at least four independent experiments. Pause durations were fit to a single exponential decay and are represented as cumulative frequency distributions; the time constant of fit is reported in seconds with a 95% confidence interval. All other metrics are reported as Mean ± SD. * $p < 0.001$ This research was originally published in the Journal of Biological Chemistry. Lessard, DV, Zinder, OJ, Hotta, T, Verhey, KJ, Ohi, R, Berger, CL. Polyglutamylation of tubulin's C-terminal tail controls pausing and motility of kinesin-3 family member KIF1A. J. Biol. Chem. 2019; 29(16):6263-6363. © the American Society for Biochemistry and Molecular Biology

Conserved lysine residues of the K-loop are key mediators in KIF1A pausing and motility.

Given the influence of the tubulin C-terminal tails on KIF1A pausing behavior, we further investigated the influence of the electrostatic interaction between the KIF1A K-loop and the microtubule C-terminal tails. First, we assessed the dependence of KIF1A pausing on the local electrostatic environment by increasing the salt concentration of our motility buffer from 12 mM to 80 mM PIPES. We observed a decrease in pause duration (1.23 sec to 0.78 sec, Figure 2-4C) with no significant changes in pause frequency (0.90 pauses/overall run), pauses per distance (0.14 pauses/μm) or any motility parameters (Figure 2-4A, 2-4B, S2-2, S2-3). Furthermore, in 80 mM PIPES we observed a decrease in KIF1A landing rate to 3.28 ± 0.61 events/μm/min [n=592] (Figure 2-7, Table 2-1).

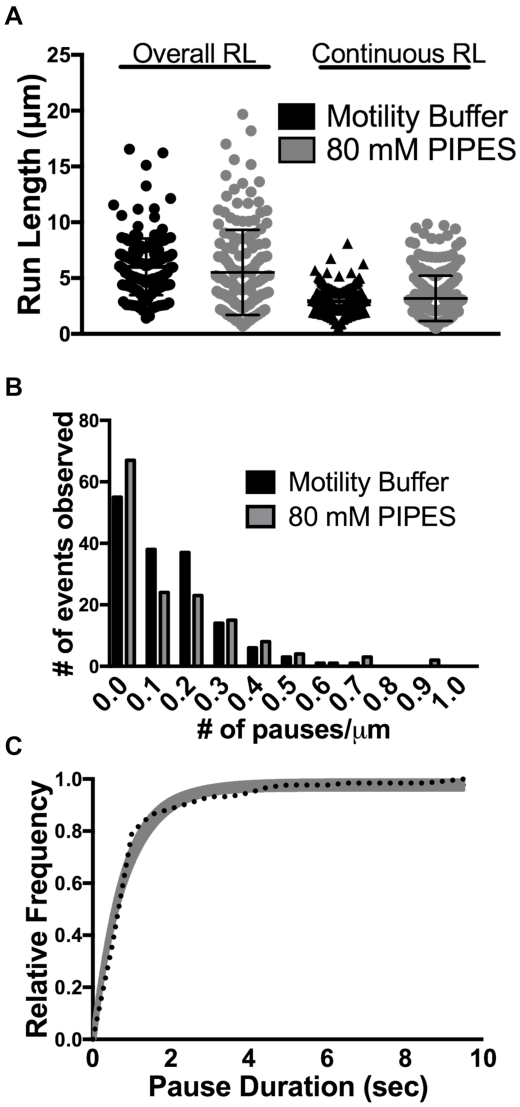

Figure 2-4. KIF1A behavior and motility in 80 mM PIPES Motility Buffer on taxol-stabilized microtubules. A) KIF1A exhibits a similar overall run length (5.98 ± 2.14 μm [n=164]) and a continuous run length (3.14 ± 0.98 μm [n=280]) in 80 mM PIPES as compared to standard motility buffer. **B)** KIF1A exhibits a similar number of pauses per distance in Motility Buffer (0.14 pauses/μm) and 80 mM PIPES (0.14 pauses/μm). **C)** In 80 mM PIPES, KIF1A pause duration is 0.78 sec (CI 0.66 – 0.91 sec) [n=132], compared to Motility Buffer (1.23 sec; Figure 2-2D). Pause durations were fit to a single exponential decay and are represented as cumulative frequency distributions; the time constant of fit is reported in seconds with a 95% confidence interval. All other metrics are reported as Mean ± SD. This research was originally published in the Journal of Biological Chemistry. Lessard, DV, Zinder, OJ, Hotta, T, Verhey, KJ, Ohi, R, Berger, CL. Polyglutamylation of tubulin's C-terminal tail controls pausing and motility of kinesin-3 family member KIF1A. J. Biol. Chem. 2019; 29(16):6263-6363. © the American Society for Biochemistry and Molecular Biology

Second, we investigated how positively-charged residues within the K-loop contribute to KIF1A pausing and motility. It has been previously reported that mutating all six lysines of the K-loop to alanine residues abolishes KIF1A motility and interaction with the microtubule (Soppina and Verhey 2014), highlighting the importance of the K-loop/microtubule interaction to the intrinsic motility properties of KIF1A. Therefore, we mutated the three lysines most conserved across the kinesin-3 family to maintain the ability of KIF1A motors to engage with the microtubule surface (Figure 2-5A). The KIF1A K-loop mutants (Tri-Ala KIF1A) displayed a marked reduction in both motility and pausing behavior (Figure 2-5B-E). Specifically, both the overall run length (2.41 ± 1.42 μm [n=173]) and continuous run length (2.00 ± 1.11 μm [n=207]) were significantly reduced by 61% and 32%, respectively, when compared to WT KIF1A on taxol-stabilized microtubules (Figure 2-5C, Table 2-1). Due to fewer pausing events, there was a 23% increase in overall speed (1.66 ± 0.45 μm/s) and a continuous speed of 1.72 ± 0.45 μm/s (Table 2-1, Figure S2-2, Figure S2-3). Tri-Ala KIF1A mutants also exhibited impaired pausing behavior quantified by a 62% reduction in pause duration (1.23 sec to 0.47 sec), a 75% decrease in pause frequency (0.95 pauses/overall run to 0.23 pauses/overall run, and a 64% decrease in pauses per distance (0.14 pauses/μm to 0.05 pauses/μm) (Figure 2-5D,E, Table 2-1). As expected from previous work (Soppina and Verhey 2014), the Tri-Ala KIF1A mutant also had a dramatic, 92% reduction in landing rate when compared to WT KIF1A on taxol-stabilized microtubules (0.64 ± 0.14 events/μm/min [n=527] for Tri-Ala and 7.93 ± 1.25 events/μm/min [n=1552] for WT) in motility buffer supplemented with ADP (Figure 2-7, Figure S2-7, Table 2-1) but no change in microtubule interaction in motility buffer supplemented with AMPPNP (1.47 ± 0.34 events/μm/min [n=574] for Tri-

Ala and 2.01 ± 0.49 events/μm/min [n=917] for WT (Figure S2-7). These results confirm that the KIF1A K-loop/microtubule C-terminal tail interaction plays a critical role not only in the landing rate as previously described (Soppina and Verhey 2014), but also for the pausing behavior of KIF1A.

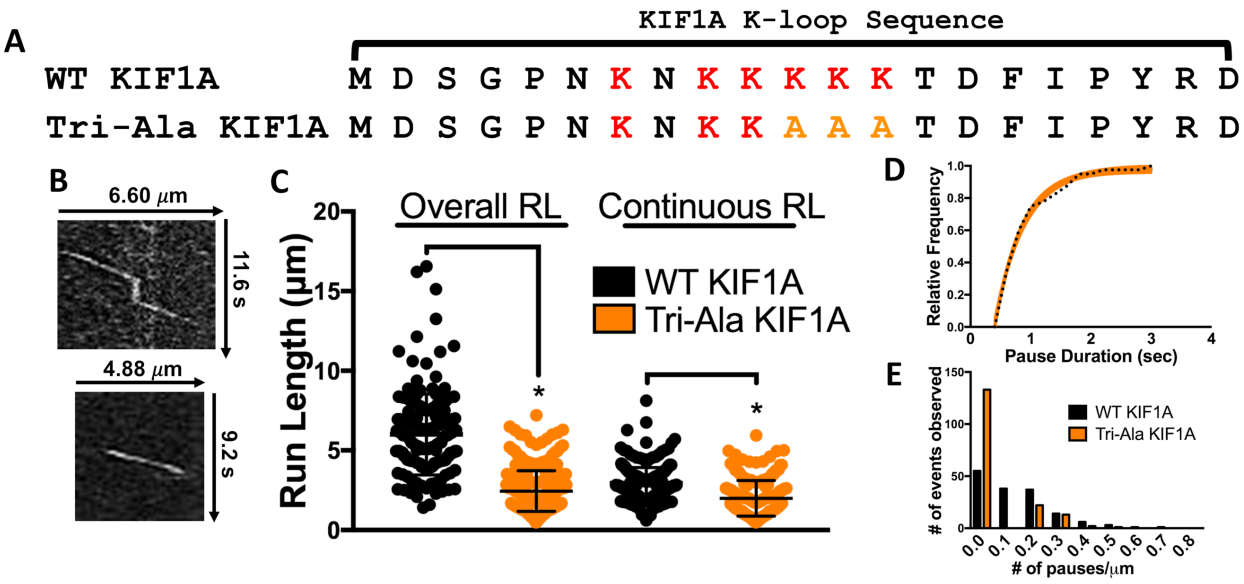

Figure 2-5. The KIF1A K-loop regulates pausing. A) Amino acid sequence alignment of the KIF1A loop 12 (K-loop) of WT KIF1A and the Tri-Ala KIF1A mutant. For the Tri-Ala mutant, the three most conserved lysines amongst the kinesin-3 family have been mutated to alanine residues (yellow text). **B)** Representative kymographs of WT KIF1A motility (top) vs Tri-Ala KIF1A motility (bottom). **C)** The Tri-Ala mutation of the KIF1A K-loop significantly reduced both overall (6.24 ± 2.09 µm to 2.41 ± 1.42 µm [n=173]) and continuous (2.95 ± 1.07 µm to 2.00 ± 1.11 µm [n=207]) run length. **D)** KIF1A pause duration is 0.47 sec (CI 0.41 – 0.53 sec) upon mutation of the K-loop [n=36], compared to WT KIF1A (1.23 sec; Figure 2-2D). **E)** Mutation of the K-loop significantly decreased number of pauses per distance from 0.14 pauses/µm (WT KIF1A) to 0.05 pauses/µm (Tri-Ala KIF1A). Run length values and standard deviations were calculated as previously reported (Thompson, Hoeprich, and Berger 2013). Kinesin-1 was used as an experimental control across all conditions (Figure S2-2 through S2-5). Each condition is representative of at least four independent experiments. Pause durations were fit to a single-exponential decay and are represented as cumulative frequency distributions; the time constant of fit is reported in seconds with a 95% confidence interval. All other metrics are reported as Mean ± SD. * $p < 0.001$ This research was originally published in the Journal of Biological Chemistry. Lessard, DV, Zinder, OJ, Hotta, T, Verhey, KJ, Ohi, R, Berger, CL. Polyglutamylation of tubulin's C-terminal tail controls pausing and motility of kinesin-3 family member KIF1A. J. Biol. Chem. 2019; 29(16):6263-6363. © the American Society for Biochemistry and Molecular Biology

Microtubule C-terminal tail polyglutamylation regulates KIF1A pausing behavior and motility.

We next aimed to identify a specific property of the tubulin C-terminal tail that could influence KIF1A pausing and motility. It has been previously established that reduced levels of α-tubulin polyglutamylation result in improper KIF1A localization and insufficient cargo delivery in hippocampal and superior cervical ganglia neurons of ROSA22 mice (Ikegami et al. 2007). As neuronal microtubules are subjected to extensive C-terminal tail polyglutamlation (Audebert et al. 1994), we hypothesized that this post-translational modification is important for regulation of KIF1A motility behavior including pausing. We thus assessed KIF1A's pausing and superprocessivity on tubulin purified from HeLa cells, which are known to contain markedly less polyglutamylation than neuronal tubulin (Figure 2-6A) due to low expression of the tubulin tyrosine-like ligase enzymes (Regnard et al. 1999; Lacroix and Janke 2011; Lacroix et al. 2010). It is important to note that this change in tubulin polyglutamylation alters the local charge of the microtubule surface as compared to neuronal tubulin. KIF1A overall run length was reduced by 34% on taxol-stabilized HeLa microtubules (4.12 ± 1.48 μm [n=164]) when compared to taxol-stabilized neuronal microtubules with no significant reduction in continuous run length (Figure 2-6C, Table 2-1). In regards to pausing behavior, we observed a 58% reduction in pause frequency (0.95 pauses/overall run to 0.40 pauses/overall run), a 50% reduction in pauses per distance (0.14 pauses/μm to 0.07 pauses/μm), and a 51% decrease in pause duration (1.23 sec to 0.59 sec) (Figure 2-6B, 2-6D-E, Table 2-1). Due to the reduction in pausing events, the overall speed of KIF1A on HeLa tubulin (1.70 ± 0.41 μm/s) increased by 26% when compared to KIF1A on neuronal microtubules, while continuous speed

decreased by only 7% (Table 2-1, Figure S2-2, Figure S2-3). We also observed a substantial, 94% reduction in KIF1A landing rate on HeLa microtubules when compared to neuronal microtubules (7.93 ± 1.25 events/μm/min [n=1552] versus 0.49 ± 0.13 events/μm/min [n=429]) (Figure 2-7, Table 2-1). Taken together, these results confirm that microtubule C-terminal tail polyglutamylation dictates KIF1A's ability to pause and thus mediates superprocessive behavior.

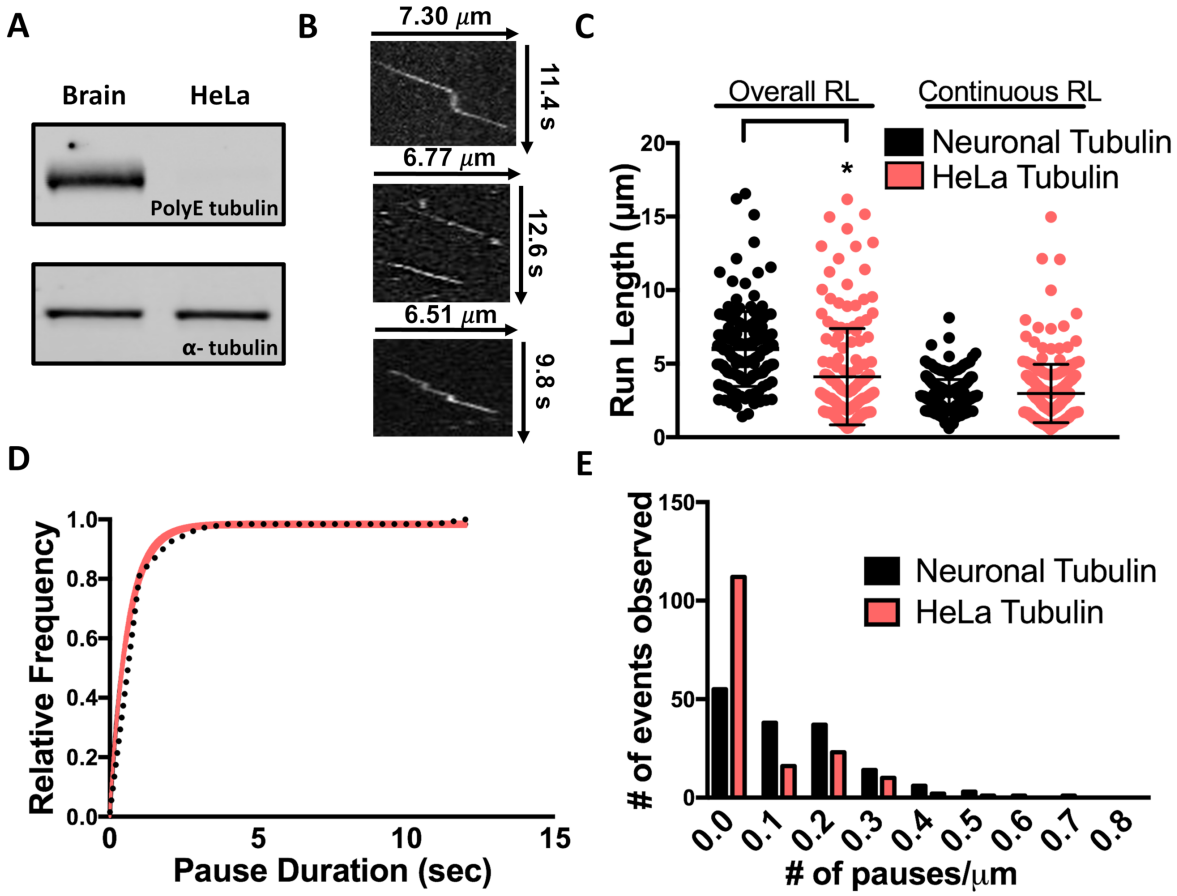

Figure 2-6. KIF1A pausing is regulated by the polyglutamyation state of the microtubule. A) Western blot revealing higher levels of polyglutamylation (polyE, top) on purified neuronal (brain) tubulin in comparison to purified HeLa tubulin, known to have little tubulin polyglutamylation (Regnard et al. 1999; Lacroix et al. 2010; Lacroix and Janke 2011). The total α-tubulin loading control is shown in the bottom blot. **B)** Representative kymographs of KIF1A motility on neuronal microtubules (top) vs HeLa microtubules (middle and bottom). **C)** The overall run length of KIF1A was reduced from 6.24 ± 2.09 μm to 4.12 ± 1.48 μm [n=164] on HeLa microtubules, while continuous run length was not significantly changed (2.95 ± 1.07 μm on HeLa microtubules vs 2.98 ± 0.96 μm [n=222] on brain microtubules). **D)** KIF1A pause duration is 0.59 sec (CI 0.54 – 0.64 sec) on HeLa microtubules [n=58], compared to neuronal microtubules (1.23 sec; Figure 2-2D). **E)** KIF1A pauses per distance was significantly decreased from 0.14 pauses/μm on brain microtubules to 0.07 pauses/μm on HeLa microtubules. Run length values and standard deviations were calculated as previously reported (Thompson, Hoeprich, and Berger 2013). Kinesin-1 was used as an experimental control across all conditions (Figure S2-2 through S2-5). Each condition is representative of at least four independent experiments. Pause durations were fit to a single-exponential decay and are represented as cumulative frequency distributions; the time constant of fit is reported in seconds with a 95% confidence interval. All other metrics are reported as Mean ± SD. * $p < 0.001$ This research was originally published in the Journal of Biological Chemistry. Lessard, DV, Zinder, OJ, Hotta, T, Verhey, KJ, Ohi, R, Berger, CL. Polyglutamylation of tubulin's C-

terminal tail controls pausing and motility of kinesin-3 family member KIF1A. J. Biol. Chem. 2019; 29(16):6263-6363. © the American Society for Biochemistry and Molecular Biology

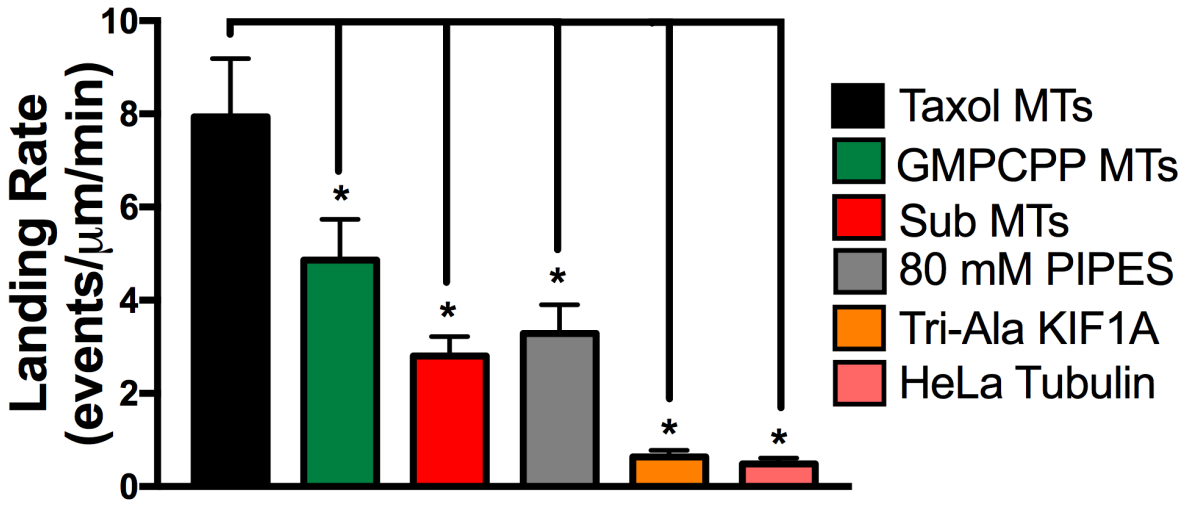

Figure 2-7. KIF1A landing is influenced by microtubule state and the K-loop/C-terminal tail interaction. Quantification of KIF1A landing rate in the ADP state on indicated microtubule (MT) subsets (Mean ± SD). On taxol-stabilized microtubules KIF1A had a landing rate of 7.93 ± 1.25 events/μm/min [n=1552]. On GMPCPP microtubules, KIF1A landing rate was significantly reduced to 4.86 ± 0.88 events/μm/min [n=958]. Removal of the tubulin C-terminal tails (Sub MTs) significantly reduced KIF1A landing rate to 2.80 ± 0.42 events/μm/min [n=717]. Increasing salt concentration (80 mM PIPES) of the motility buffer reduced the landing rate to 3.28 ± 0.61 events/μm/min [n=592]. Mutation of the KIF1A K-loop (Tri-Ala KIF1A) significantly reduced the landing rate to 0.64 ± 0.14 events/μm/min [n=527]. On HeLa microtubules with reduced polyglutamylation, the KIF1A landing rate was significantly reduced to 0.49 ± 0.13 events/μm/min [n=429]. Each condition is representative of at least four independent experiments. Mean ± SD reported. * $p < 0.001$ This research was originally published in the Journal of Biological Chemistry. Lessard, DV, Zinder, OJ, Hotta, T, Verhey, KJ, Ohi, R, Berger, CL. Polyglutamylation of tubulin's C-terminal tail controls pausing and motility of kinesin-3 family member KIF1A. J. Biol. Chem. 2019; 29(16):6263-6363. © the American Society for Biochemistry and Molecular Biology

Table 2-1. Summary of KIF1A motility and behavior on microtubules across all conditions. Pause durations were fit to a single-exponential decay and the time constant of the fit is reported in seconds. All other metrics are reported as Mean ± SD. * = $p<0.001$ relative to KIF1A on taxol-stabilized MTs. This research was originally published in the Journal of Biological Chemistry. Lessard, DV, Zinder, OJ, Hotta, T, Verhey, KJ, Ohi, R, Berger, CL. Polyglutamylation of tubulin's C-terminal tail controls pausing and motility of kinesin-3 family member KIF1A. J. Biol. Chem. 2019; 29(16):6263-6363. © the American Society for Biochemistry and Molecular Biology

	Overall Run Length (µm)	Overall Speed (µm/s)	Continuous Run Length (µm)	Continuous Speed (µm/s)	Pause Frequency (# pauses/overall run)	Pauses per Distance (# pauses/µm)	Pause Duration (sec)	Landing Rate (events/µm/min)
Taxol	6.24 ± 2.09	1.35 ± 0.41	2.95 ± 1.07	2.01 ± 0.53	0.95	0.14	1.23	7.93 ± 1.25
GMPCPP	6.01 ± 2.17	1.27 ± 0.28	2.81 ± 0.91	2.06 ± 0.54	1.02	0.16	0.66	4.86 ± 0.88*
Subtilisin	3.31 ± 1.34*	1.58 ± 0.38	2.91 ± 1.16	1.94 ± 0.50	0.18*	0.02*	0.68	2.80 ± 0.42*
80 mM PIPES	5.98 ± 2.14	1.34 ± 0.30	3.14 ± 0.98	1.99 ± 0.47	0.90	0.14	0.78	3.28 ± 0.61*
Tri-Ala	2.41 ± 1.42*	1.66 ± 0.45	2.00 ± 1.11*	1.72 ± 0.45	0.23*	0.05*	0.47	0.64 ± 0.14*
HeLa Tubulin	4.12 ± 1.48*	1.70 ± 0.41	2.98 ± 0.96	1.87 ± 0.40	0.40*	0.07*	0.59	0.49 ± 0.13*

DISCUSSION

The superprocessivity of the kinesin-3 family member KIF1A has been previously established (Soppina et al. 2014), supporting its known role in long-distance axonal transport (Lo et al. 2011; Hung and Coleman 2016). Here we present a novel molecular mechanism that influences KIF1A's superprocessive motion. First, we demonstrate that KIF1A engages in previously unreported pauses on the microtubule lattice. KIF1A walks a superprocessive distance (~3 μm on average) before initiating a pause, supporting the notion that although pausing is rare, it is related to the superprocessive nature of the motor itself. Pausing has several effects on the overall motility of dimeric KIF1A motors. Pauses enable KIF1A to string together multiple continuous runs to generate a longer overall run. Of note, even in the absence of pauses, KIF1A remains a superprocessive motor, with continuous run lengths of ~ 3 μm. KIF1A's overall speed is also increased in the absence of pauses, with no effect on continuous speed. This response is expected, considering that a reduction in pause frequency will reduce a slower population of motors undergoing pauses.

Furthermore, we show that pauses are mediated by interactions between the KIF1A K-loop and tubulin C-terminal tails. When the K-loop/C-terminal tail interaction is interrupted (e.g., subtilisin treatment, K-loop mutation), KIF1A shows a reduced pause frequency and duration on the microtubule lattice. Disruption of the K-loop/C-terminal tail interaction also results in a dramatic reduction in the landing rate of dimeric KIF1A motors, consistent with previous work (Soppina and Verhey 2014). The K-loop is also critical for monomeric KIF1A motors to diffuse along the surface of microtubules (Okada and Hirokawa 1999). In addition, cellular work has shown that loop-12 is important for

regulation of KIF1A dendritic cargo sorting (Eva P. Karasmanis 2018). As the K-loop is conserved across members of the kinesin-3 family, our newly-identified pausing mechanism is likely to be a conserved feature of this class of motor.

Finally, we demonstrate that polyglutamylation of the tubulin C-terminal tail is a post-translational modification that regulates KIF1A pausing behavior and subsequent motility. Along HeLa microtubules, which lack polyglutamylation, KIF1A displayed significantly reduced landing rate, pause frequency, and pause duration. Electrostatic interactions between the K-loop and C-terminal tail play an important role as increasing the salt concentration in our motility buffer resulted in a reduced landing rate and pause duration. That the increased salt concentration did not influence pause frequency suggests that the factors that influence pausing are not completely based on electrostatics. That tubulin C-terminal tail polyglutamylation influences KIF1A behavior at the single molecule level provides a mechanistic understanding of how polyglutamylation can regulate KIF1A cargo trafficking (Ikegami et al. 2007). The levels of tubulin C-terminal tail polyglutamylation are highly tuned during neural development (Audebert et al. 1994; Audebert et al. 1993) and could also influence KIF1A during synaptogenesis (Stavoe et al. 2016) and interkinetic nuclear migration (Dantas et al. 2016). Compartmentalizing neuronal tubulin polyglutamylation into localized hotspots (Janke, Rogowski, and van Dijk 2008) may contribute an advantageous level of regulation to fine-tune KIF1A function during these developmental processes.

With a molecular regulatory mechanism identified in regards to KIF1A pausing and motility, a question still remains: *how* is KIF1A able to pause in between processive segments (continuous runs)? Our proposed mechanism states that pausing is mediated in

part by a KIF1A/C-terminal tails interaction. A structural mechanism responsible for KIF1A pausing can be proposed based on past work examining the flexibility and structural confirmation of the K-loop during ATP hydrolysis (Nitta et al. 2004). This study demonstrated that when KIF1A is bound to AMPPNP, loop-12 is positioned up and away from the microtubule surface whereas when KIF1A is bound ADP, loop-12 adopts a "downward" position to interact with the C-terminal tails on the microtubule surface. From this, we propose that pauses are initiated by loop-12 interaction with the microtubule C-terminal tail when KIF1A is in the ADP state. Importantly, a pause would happen when both motor domains are in the same nucleotide state at the same time, making this a catalytically rare event and explaining why pausing occurs on the magnitude of every ~ 3 μm. We speculate that with both loop-12s in a downward position, KIF1A exhibits a spatially-constrained form of diffusion close to the resolution limit of our TIRF microscope as compared to the previously observed highly diffusive behavior of the KIF1A monomer (Okada and Hirokawa 1999).

The mechanistic importance of loop-12 positioning is further supported by our data comparing the landing rate of WT and Tri-Ala motors in the presence of ADP or AMPPNP in the motility buffer. Under ADP conditions, the landing rate of the K-loop mutant (Tri-Ala) is significantly reduced when compared to WT KIF1A (Figure S2-7), consistent with previous work (Soppina and Verhey 2014). However, under AMPPNP conditions, there is no significant difference in landing rates between WT and Tri-Ala KIF1A motors (Figure S2-7). These findings support our proposed structural mechanism of pausing in which the "downward" positioning of KIF1A loop-12 when bound to ADP enables loop-12 to interact with the microtubule C-terminal tails and facilitate pausing. Furthermore, the significant

reduction of Tri-Ala KIF1A pausing and continuous run length in motility assays (Figure 2-5C, 2-5E) highlight the importance of the K-loop for KIF1A motility. Further testing how KIF1A catalytic activity and structural states influence pausing is an enticing future direction beyond the scope of this current study.

Our results demonstrate that KIF1A responds not only to post-translational modification of the microtubule surface but also to the state of the microtubule. Specifically, we demonstrate that KIF1A has a reduced landing rate (Figure 2-7) and pause duration (Figure 2-2D, Table 2-1) on GMPCPP microtubules as compared to taxol-stabilized microtubules. This is potentially due to a nucleotide-specific difference in positioning of the C-terminal tails on the microtubule surface. Whether the motor is influenced by protofilament number and/or nucleotide state of the GMPCPP lattice will require further study. Recent compelling work has demonstrated that microtubule associated proteins (MAPs) and septins can also influence KIF1A motility and function (Monroy et al. 2018; Eva P. Karasmanis 2018; Gumy et al. 2017; Lipka et al. 2016). Pausing may allow KIF1A to navigate around MAPs and other obstacles on the microtubule. The necessity to regulate kinesin cargo transport through pausing is a pre-established concept on a cellular level, as many neuronal cargo have been observed to halt processive movement in order to navigate around obstacles in the crowded cellular environment (Trybus 2013; Maday et al. 2014; Hendricks et al. 2010; Castle et al. 2014). On the other hand, microtubule C-terminal tail polyglutamylation can regulate the microtubule affinity of MAPs such as MAP1A, MAP1B, MAP2, and Tau (Bonnet et al. 2001; Larcher et al. 1996). For example, Tau interacts with tubulin C-terminal tails in a unique diffusive behavior that is important for Tau function on a cellular and systemic level

(Hinrichs et al. 2012). Tau could thus compete with KIF1A for microtubule C-terminal tails and thereby regulate KIF1A pausing and motility. This concept is a compelling topic for further study.

Understanding the mechanisms responsible for KIF1A motility is critical when one considers the extensive range of axonal cargo that KIF1A transports along neuronal microtubules (Siddiqui and Straube 2017; Tsai et al. 2010; Lo et al. 2011; Niwa et al. 2016; Tanaka et al. 2016; Carabalona, Hu, and Vallee 2016; Lee et al. 2015; Niwa, Tanaka, and Hirokawa 2008; Lee et al. 2003; Yonekawa et al. 1998). Furthermore, until we advance our understanding of KIF1A regulation, we are limited in our ability to address the disease state manifestations of altered KIF1A function. The regulatory capabilities of Tau's binding behavior on KIF1A cargo transport are critical to understanding KIF1A's role in in diseases known for impaired axonal transport, such as frontotemporal dementia (FTD), where changes in Tau isoform expression have been correlated to disease progression (Iqbal et al. 2010). For example, pathological overexpression (Kopeikina, Hyman, and Spires-Jones 2012; Schoch et al. 2016; Goedert, Ghetti, and Spillantini 2000) of the more diffusive Tau isoforms (McVicker et al. 2014) and reduced transport of cargo known to be transported by KIF1A are observed in FTD (Goetzl et al. 2016; Siddiqui and Straube 2017; Rodriguez-Martin et al. 2016). As we speculate that the diffusive binding state of Tau may compete with KIF1A for the microtubule C-terminal tail, this is an enticing concept for further investigation on a molecular and cellular level. In summary, our discovery of a microtubule C-terminal tail polyglutamylation-mediated mechanism for regulation of KIF1A motility provides crucial insight as to how KIF1A cargo delivery is regulated during axonal transport and how this process may become altered in the disease state.

ACKNOWLEDGEMENTS

We thank David Warshaw and Guy Kennedy for training and use of the TIRF microscope at the University of Vermont. A special thank you to Vermont Livestock Slaughter & Processing (Ferrisburgh, VT) for supporting our work. We thank Gary Banker & Marvin Bentley for the gifted pBa.Kif1a 1-396.GFP (Addgene plasmid # 45058), William Hancock for the use of his kinesin-1 construct, and Adam Hendricks for support.

CONFLICT OF INTEREST

The authors declare that they have no conflicts of interest with the contents of this article.

FOOTNOTES

This work was supported by National Institute of General Medicine Sciences/National Institutes of Health funding to C.B. (Grant GM101066), K.J.V (GM070862), and R.O. (GM086610).

SUPPORTING INFORMATION

Title: Polyglutamylation of tubulin's C-terminal tail controls pausing and motility of kinesin-3 family member KIF1A

Authors: Dominique V. Lessard[1], Oraya J. Zinder[1], Takashi Hotta[2], Kristen J. Verhey[2], Ryoma Ohi[2], Christopher L. Berger[1]

[1] Department of Molecular Physiology & Biophysics, University of Vermont, Burlington, VT 05405
[2] Department of Cell and Developmental Biology, University of Michigan Medical School, Ann Arbor, MI 48109

Materials Included:
Supplemental Movie 2-1 (available through online publication)
Supplemental Movie 2-1 Legend
Supplemental Figures and Legends 2-1 through 2-7

SI FIGURES

Movie S2-1. Sample motility of KIF1A on taxol-stabilized microtubules. TIRF microscopy was used to observe the motility of KIF1A-LZ-3xmCitrine on rhodamine labeled, taxol-stabilized microtubules. 500 frames were recorded at 5 fps, shown here at 25 fps. Data was analyzed as described in the Methods section.

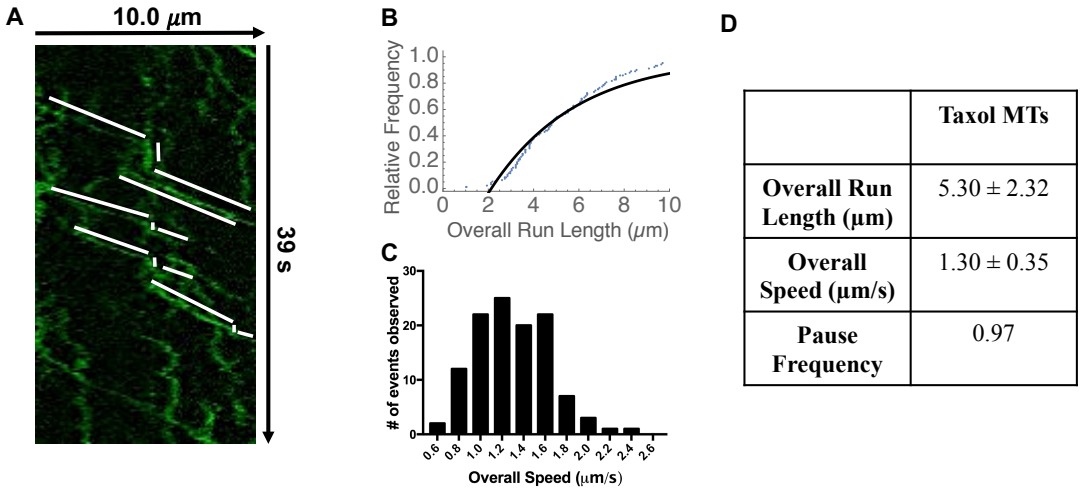

	Taxol MTs
Overall Run Length (μm)	5.30 ± 2.32
Overall Speed (μm/s)	1.30 ± 0.35
Pause Frequency	0.97

Figure S2-1. **The LZ does not influence KIF1A pausing behavior. A)** Representative kymograph of the non-leucine zipper KIF1A construct (KIF1A[1-396]-GFP) on taxol-stabilized microtubules. KIF1A-GFP undergoes extensive pausing behavior during a single overall run (outlined in white). There are also many purely diffusive events of KIF1A molecules not stabilized by the leucine zipper, presumably monomeric motors (Soppina et al. 2014). **B)** Quantification of overall run length displayed as cumulative frequency plot. **C)** Histogram of overall speed. **D)** Summary of KIF1A-GFP motility and behavior on taxol-stabilized microtubules. KIF1A-GFP exhibits an overall run length (ORL) of 5.30 ± 2.32 μm [n=123]), an overall speed of 1.30 ± 0.35 μm/s [n=123] and exhibits 0.17 pauses/μm. Run length values and standard deviations were calculated as previously reported (Thompson, Hoeprich, and Berger 2013). Each condition is representative of at least four independent experiments. Mean ± SD reported. This research was originally published in the Journal of Biological Chemistry. Lessard, DV, Zinder, OJ, Hotta, T, Verhey, KJ, Ohi, R, Berger, CL. Polyglutamylation of tubulin's C-terminal tail controls pausing and motility of kinesin-3 family member KIF1A. J. Biol. Chem. 2019; 29(16):6263-6363. © the American Society for Biochemistry and Molecular Biology

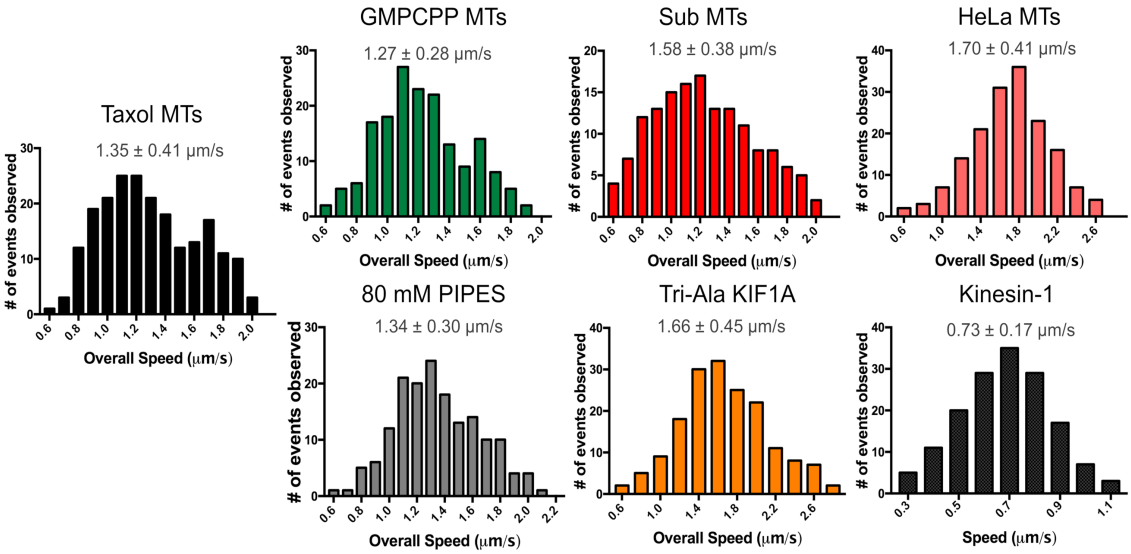

Figure S2-2. Histograms of overall speed across all conditions The Mean ± SD for each condition is presented above each graph. This research was originally published in the Journal of Biological Chemistry. Lessard, DV, Zinder, OJ, Hotta, T, Verhey, KJ, Ohi, R, Berger, CL. Polyglutamylation of tubulin's C-terminal tail controls pausing and motility of kinesin-3 family member KIF1A. J. Biol. Chem. 2019; 29(16):6263-6363. © the American Society for Biochemistry and Molecular Biology

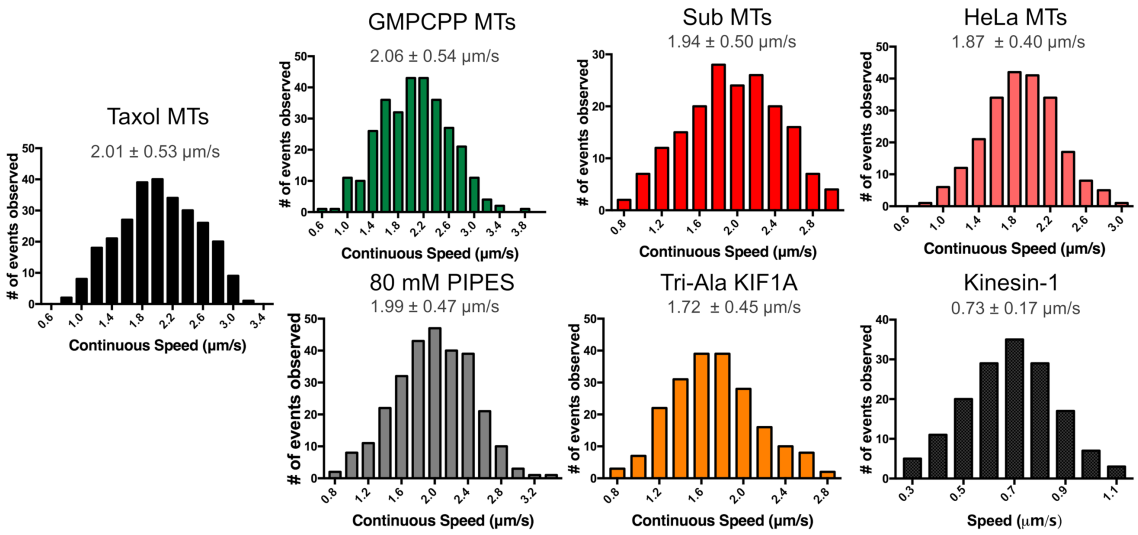

Figure S2-3. Histograms of continuous speed across all conditions The Mean ± SD for each condition is presented above each graph. This research was originally published in the Journal of Biological Chemistry. Lessard, DV, Zinder, OJ, Hotta, T, Verhey, KJ, Ohi, R, Berger, CL. Polyglutamylation of tubulin's C-terminal tail controls pausing and motility of kinesin-3 family member KIF1A. J. Biol. Chem. 2019; 29(16):6263-6363. © the American Society for Biochemistry and Molecular Biology

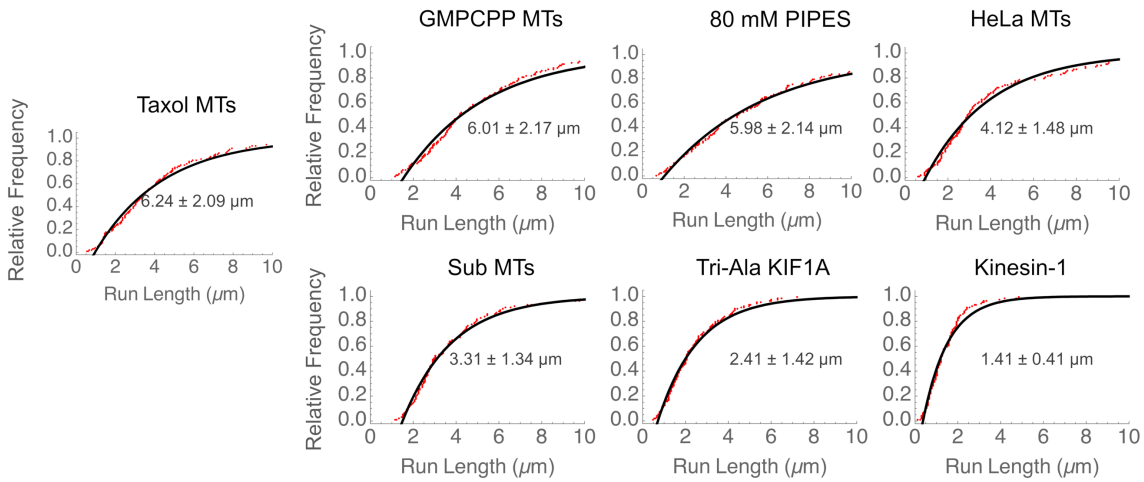

Figure S2-4. Cumulative frequency plots of overall run length across all conditions. Black dots represent the raw run length and red dots represent the observed cumulative frequency. Kinesin-1 was used as an experimental control; run length of kinesin-1 is reported. The mean overall run length was calculated as previously reported (Thompson, Hoeprich, and Berger 2013) and is shown within each graph (Mean ± SD). This research was originally published in the Journal of Biological Chemistry. Lessard, DV, Zinder, OJ, Hotta, T, Verhey, KJ, Ohi, R, Berger, CL. Polyglutamylation of tubulin's C-terminal tail controls pausing and motility of kinesin-3 family member KIF1A. J. Biol. Chem. 2019; 29(16):6263-6363. © the American Society for Biochemistry and Molecular Biology

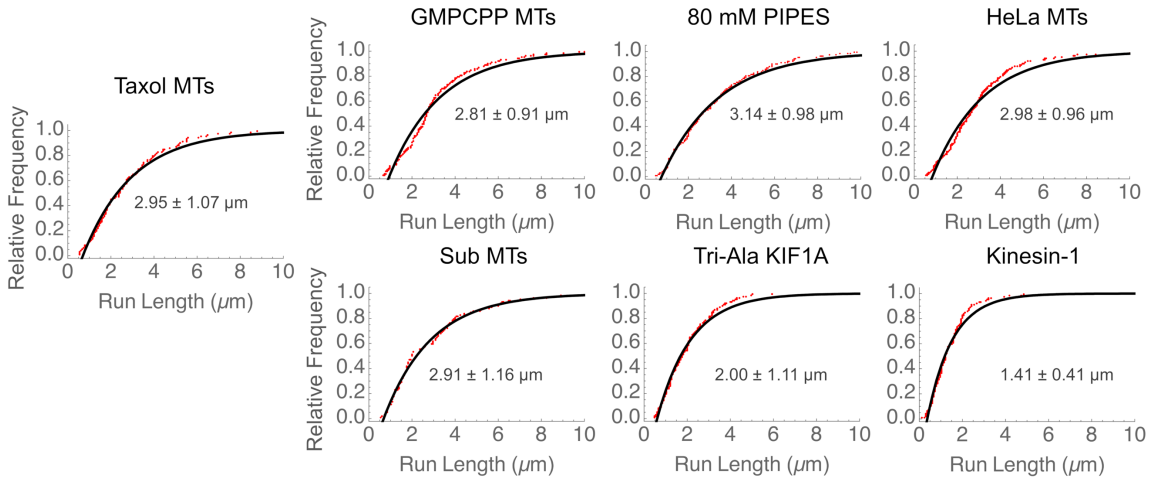

Figure S2-5. Cumulative frequency plots of continuous run length across all conditions. Black dots represent the raw run length and red dots represent the observed cumulative frequency. Kinesin-1 was used as an experimental control; run length of kinesin-1 is reported. A continuous run length was calculated as previously reported (Thompson, Hoeprich, and Berger 2013) and is shown within each graph (Mean ± SD). This research was originally published in the Journal of Biological Chemistry. Lessard, DV, Zinder, OJ, Hotta, T, Verhey, KJ, Ohi, R, Berger, CL. Polyglutamylation of tubulin's C-terminal tail controls pausing and motility of kinesin-3 family member KIF1A. J. Biol. Chem. 2019; 29(16):6263-6363. © the American Society for Biochemistry and Molecular Biology

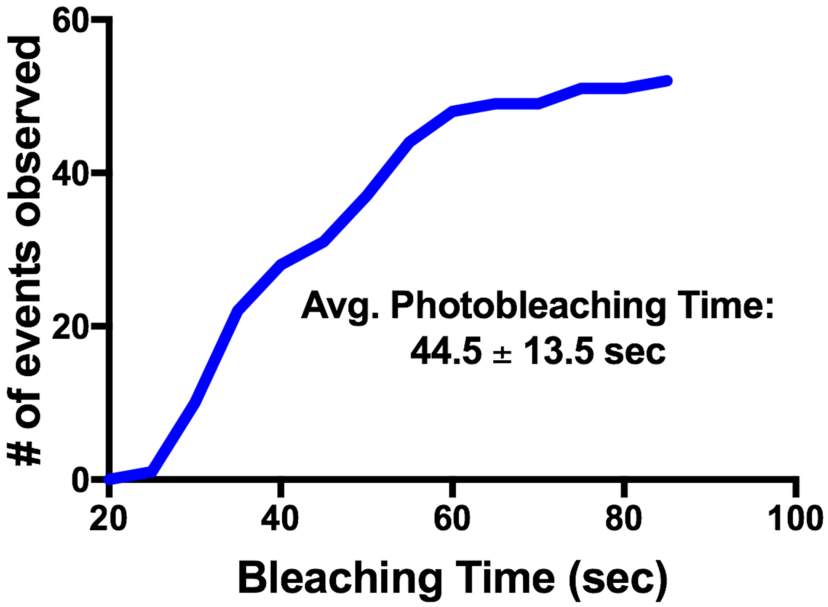

Figure S2-6. Photobleaching assay measuring average KIF1A-LZ-3xmCitrine bleaching time. KIF1A motors in an AMPPNP nucleotide state were imaged using TIRF microscopy. Fluorescence intensity over time of individual motors was measured and corrected for channel background noise. Mean ± SD reported. This research was originally published in the Journal of Biological Chemistry. Lessard, DV, Zinder, OJ, Hotta, T, Verhey, KJ, Ohi, R, Berger, CL. Polyglutamylation of tubulin's C-terminal tail controls pausing and motility of kinesin-3 family member KIF1A. J. Biol. Chem. 2019; 29(16):6263-6363. © the American Society for Biochemistry and Molecular Biology

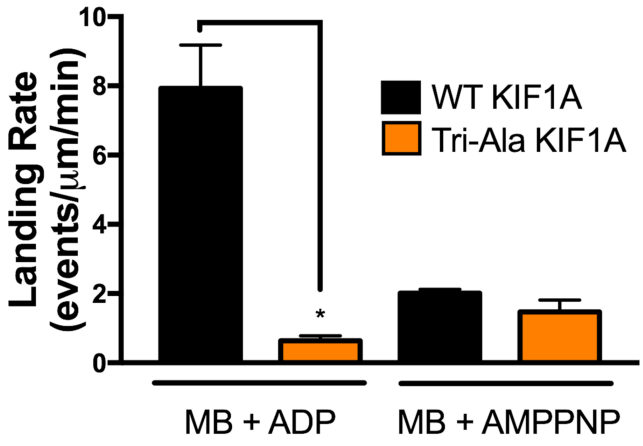

	MB + ADP	MB + AMPPNP
WT KIF1A	7.93 ± 1.25	2.01 ± 0.49
Tri-Ala KIF1A	0.64 ± 0.14*	1.47 ± 0.34*

Figure S2-7. Comparison of WT and Tri-Ala KIF1A landing rates in the ADP vs AMPPNP state. In motility buffer supplemented with ADP as the available nucleotide (MB + ADP), WT KIF1A had a landing rate of 7.93 ± 1.25 events/μm/min (n=1552) while Tri-Ala KIF1A had a landing rate of 0.64 ± 0.14 events/μm/min (n=527). In motility buffer supplemented with AMPPNP (MB + AMPPNP), WT KIF1A had a landing rate of 2.01 ± 0.49 events/μm/min (n=917) while Tri-Ala KIF1A had a landing rate of 1.47 ± 0.34 events/μm/min (n=574). Mean ± SD reported. * = $p<0.001$ relative to WT KIF1A under corresponding condition. This research was originally published in the Journal of Biological Chemistry. Lessard, DV, Zinder, OJ, Hotta, T, Verhey, KJ, Ohi, R, Berger, CL. Polyglutamylation of tubulin's C-terminal tail controls pausing and motility of kinesin-3 family member KIF1A. J. Biol. Chem. 2019; 29(16):6263-6363. © the American Society for Biochemistry and Molecular Biology

REFERENCES CITED

Audebert, S., E. Desbruyeres, C. Gruszczynski, A. Koulakoff, F. Gros, P. Denoulet, and B. Edde. 1993. 'Reversible polyglutamylation of alpha- and beta-tubulin and microtubule dynamics in mouse brain neurons', *Mol Biol Cell*, 4: 615-26.

Audebert, S., A. Koulakoff, Y. Berwald-Netter, F. Gros, P. Denoulet, and B. Edde. 1994. 'Developmental regulation of polyglutamylated alpha- and beta-tubulin in mouse brain neurons', *J Cell Sci*, 107 (Pt 8): 2313-22.

Bonnet, C., D. Boucher, S. Lazereg, B. Pedrotti, K. Islam, P. Denoulet, and J. C. Larcher. 2001. 'Differential binding regulation of microtubule-associated proteins MAP1A, MAP1B, and MAP2 by tubulin polyglutamylation', *J Biol Chem*, 276: 12839-48.

Carabalona, A., D. J. Hu, and R. B. Vallee. 2016. 'KIF1A inhibition immortalizes brain stem cells but blocks BDNF-mediated neuronal migration', *Nat Neurosci*, 19: 253-62.

Castle, M. J., E. Perlson, E. L. Holzbaur, and J. H. Wolfe. 2014. 'Long-distance axonal transport of AAV9 is driven by dynein and kinesin-2 and is trafficked in a highly motile Rab7-positive compartment', *Mol Ther*, 22: 554-66.

Castoldi, M., and A. V. Popov. 2003. 'Purification of brain tubulin through two cycles of polymerization-depolymerization in a high-molarity buffer', *Protein Expr Purif*, 32: 83-8.

Dantas, T. J., A. Carabalona, D. J. Hu, and R. B. Vallee. 2016. 'Emerging roles for motor proteins in progenitor cell behavior and neuronal migration during brain development', *Cytoskeleton (Hoboken)*, 73: 566-76.

Eva P. Karasmanis, Cat-Thi Phan, Dimitrios Angelis, Ilona A. Kesisova, Casper C. Hoogenraad, Richard J. McKenney, Elias T. Spiliotis. 2018. 'Polarity of Neuronal Membrane Traffic Requires Sorting of Kinesin Motor Cargo during Entry into Dendrites by a Microtubule-Associated Septin', *Developmental Cell*, 46: 204-18.

Ghosh-Roy, A., A. Goncharov, Y. Jin, and A. D. Chisholm. 2012. 'Kinesin-13 and tubulin posttranslational modifications regulate microtubule growth in axon regeneration', *Dev Cell*, 23: 716-28.

Ginsburg, A., A. Shemesh, A. Millgram, R. Dharan, Y. Levi-Kalisman, I. Ringel, and U. Raviv. 2017. 'Structure of Dynamic, Taxol-Stabilized, and GMPPCP-Stabilized Microtubule', *J Phys Chem B*, 121: 8427-36.

Goedert, M., B. Ghetti, and M. G. Spillantini. 2000. 'Tau gene mutations in frontotemporal dementia and parkinsonism linked to chromosome 17 (FTDP-17). Their relevance for understanding the neurogenerative process', *Ann N Y Acad Sci*, 920: 74-83.

Goetzl, E. J., D. Kapogiannis, J. B. Schwartz, I. V. Lobach, L. Goetzl, E. L. Abner, G. A. Jicha, A. M. Karydas, A. Boxer, and B. L. Miller. 2016. 'Decreased synaptic proteins in neuronal exosomes of frontotemporal dementia and Alzheimer's disease', *FASEB J*, 30: 4141-48.

Gramlich, M. W., L. Conway, W. H. Liang, J. A. Labastide, S. J. King, J. Xu, and J. L. Ross. 2017. 'Single Molecule Investigation of Kinesin-1 Motility Using Engineered Microtubule Defects', *Sci Rep*, 7: 44290.

Gumy, L. F., E. A. Katrukha, I. Grigoriev, D. Jaarsma, L. C. Kapitein, A. Akhmanova, and C. C. Hoogenraad. 2017. 'MAP2 Defines a Pre-axonal Filtering Zone to Regulate KIF1- versus KIF5-Dependent Cargo Transport in Sensory Neurons', *Neuron*, 94: 347-62 e7.

Hammond, J. W., D. Cai, T. L. Blasius, Z. Li, Y. Jiang, G. T. Jih, E. Meyhofer, and K. J. Verhey. 2009. 'Mammalian Kinesin-3 motors are dimeric in vivo and move by processive motility upon release of autoinhibition', *PLoS Biol*, 7: e72.

Hammond, J. W., C. F. Huang, S. Kaech, C. Jacobson, G. Banker, and K. J. Verhey. 2010. 'Posttranslational modifications of tubulin and the polarized transport of kinesin-1 in neurons', *Mol Biol Cell*, 21: 572-83.

Hendricks, A. G., E. Perlson, J. L. Ross, H. W. Schroeder, 3rd, M. Tokito, and E. L. Holzbaur. 2010. 'Motor coordination via a tug-of-war mechanism drives bidirectional vesicle transport', *Curr Biol*, 20: 697-702.

Hinrichs, M. H., A. Jalal, B. Brenner, E. Mandelkow, S. Kumar, and T. Scholz. 2012. 'Tau protein diffuses along the microtubule lattice', *J Biol Chem*, 287: 38559-68.

Hirokawa, N., S. Niwa, and Y. Tanaka. 2010. 'Molecular motors in neurons: transport mechanisms and roles in brain function, development, and disease', *Neuron*, 68: 610-38.

Hoeprich, G. J., K. J. Mickolajczyk, S. R. Nelson, W. O. Hancock, and C. L. Berger. 2017. 'The axonal transport motor kinesin-2 navigates microtubule obstacles via protofilament switching', *Traffic*, 18: 304-14.

Hoeprich, G. J., A. R. Thompson, D. P. McVicker, W. O. Hancock, and C. L. Berger. 2014. 'Kinesin's neck-linker determines its ability to navigate obstacles on the microtubule surface', *Biophys J*, 106: 1691-700.

Hotta, T., S. Fujita, S. Uchimura, M. Noguchi, T. Demura, E. Muto, and T. Hashimoto. 2016. 'Affinity Purification and Characterization of Functional Tubulin from Cell Suspension Cultures of Arabidopsis and Tobacco', *Plant Physiol*, 170: 1189-205.

Hung, C. O., and M. P. Coleman. 2016. 'KIF1A mediates axonal transport of BACE1 and identification of independently moving cargoes in living SCG neurons', *Traffic*, 17: 1155-67.

Hyman, A. A., D. Chretien, I. Arnal, and R. H. Wade. 1995. 'Structural changes accompanying GTP hydrolysis in microtubules: information from a slowly hydrolyzable analogue guanylyl-(alpha,beta)-methylene-diphosphonate', *J Cell Biol*, 128: 117-25.

Ikegami, K., R. L. Heier, M. Taruishi, H. Takagi, M. Mukai, S. Shimma, S. Taira, K. Hatanaka, N. Morone, I. Yao, P. K. Campbell, S. Yuasa, C. Janke, G. R. Macgregor, and M. Setou. 2007. 'Loss of alpha-tubulin polyglutamylation in ROSA22 mice is associated with abnormal targeting of KIF1A and modulated synaptic function', *Proc Natl Acad Sci U S A*, 104: 3213-8.

Ikegami, K., M. Mukai, J. Tsuchida, R. L. Heier, G. R. Macgregor, and M. Setou. 2006. 'TTLL7 is a mammalian beta-tubulin polyglutamylase required for growth of MAP2-positive neurites', *J Biol Chem*, 281: 30707-16.

Iqbal, K., F. Liu, C. X. Gong, and I. Grundke-Iqbal. 2010. 'Tau in Alzheimer disease and related tauopathies', *Curr Alzheimer Res*, 7: 656-64.

Janke, C., K. Rogowski, and J. van Dijk. 2008. 'Polyglutamylation: a fine-regulator of protein function? 'Protein Modifications: beyond the usual suspects' review series', *EMBO Rep*, 9: 636-41.
Janke, C., K. Rogowski, D. Wloga, C. Regnard, A. V. Kajava, J. M. Strub, N. Temurak, J. van Dijk, D. Boucher, A. van Dorsselaer, S. Suryavanshi, J. Gaertig, and B. Edde. 2005. 'Tubulin polyglutamylase enzymes are members of the TTL domain protein family', *Science*, 308: 1758-62.
Kikkawa, M., Y. Okada, and N. Hirokawa. 2000. '15 A resolution model of the monomeric kinesin motor, KIF1A', *Cell*, 100: 241-52.
Knipling, L., J. Hwang, and J. Wolff. 1999. 'Preparation and properties of pure tubulin S', *Cell Motil Cytoskeleton*, 43: 63-71.
Kondo, M., Y. Takei, and N. Hirokawa. 2012. 'Motor protein KIF1A is essential for hippocampal synaptogenesis and learning enhancement in an enriched environment', *Neuron*, 73: 743-57.
Kopeikina, K. J., B. T. Hyman, and T. L. Spires-Jones. 2012. 'Soluble forms of tau are toxic in Alzheimer's disease', *Transl Neurosci*, 3: 223-33.
Lacroix, B., and C. Janke. 2011. 'Generation of differentially polyglutamylated microtubules', *Methods Mol Biol*, 777: 57-69.
Lacroix, B., J. van Dijk, N. D. Gold, J. Guizetti, G. Aldrian-Herrada, K. Rogowski, D. W. Gerlich, and C. Janke. 2010. 'Tubulin polyglutamylation stimulates spastin-mediated microtubule severing', *J Cell Biol*, 189: 945-54.
Larcher, J. C., D. Boucher, S. Lazereg, F. Gros, and P. Denoulet. 1996. 'Interaction of kinesin motor domains with alpha- and beta-tubulin subunits at a tau-independent binding site. Regulation by polyglutamylation', *J Biol Chem*, 271: 22117-24.
Lee, J. R., H. Shin, J. Ko, J. Choi, H. Lee, and E. Kim. 2003. 'Characterization of the movement of the kinesin motor KIF1A in living cultured neurons', *J Biol Chem*, 278: 2624-9.
Lee, J. R., M. Srour, D. Kim, F. F. Hamdan, S. H. Lim, C. Brunel-Guitton, J. C. Decarie, E. Rossignol, G. A. Mitchell, A. Schreiber, R. Moran, K. Van Haren, R. Richardson, J. Nicolai, K. M. Oberndorff, J. D. Wagner, K. M. Boycott, E. Rahikkala, N. Junna, H. Tyynismaa, I. Cuppen, N. E. Verbeek, C. T. Stumpel, M. A. Willemsen, S. A. de Munnik, G. A. Rouleau, E. Kim, E. J. Kamsteeg, T. Kleefstra, and J. L. Michaud. 2015. 'De novo mutations in the motor domain of KIF1A cause cognitive impairment, spastic paraparesis, axonal neuropathy, and cerebellar atrophy', *Hum Mutat*, 36: 69-78.
Lipka, J., L. C. Kapitein, J. Jaworski, and C. C. Hoogenraad. 2016. 'Microtubule-binding protein doublecortin-like kinase 1 (DCLK1) guides kinesin-3-mediated cargo transport to dendrites', *EMBO J*, 35: 302-18.
Lo, K. Y., A. Kuzmin, S. M. Unger, J. D. Petersen, and M. A. Silverman. 2011. 'KIF1A is the primary anterograde motor protein required for the axonal transport of dense-core vesicles in cultured hippocampal neurons', *Neurosci Lett*, 491: 168-73.
Maday, S., A. E. Twelvetrees, A. J. Moughamian, and E. L. Holzbaur. 2014. 'Axonal transport: cargo-specific mechanisms of motility and regulation', *Neuron*, 84: 292-309.

Magiera, M. M., P. Singh, S. Gadadhar, and C. Janke. 2018. 'Tubulin Posttranslational Modifications and Emerging Links to Human Disease', *Cell*, 173: 1323-27.
McVicker, D. P., L. R. Chrin, and C. L. Berger. 2011. 'The nucleotide-binding state of microtubules modulates kinesin processivity and the ability of Tau to inhibit kinesin-mediated transport', *J Biol Chem*, 286: 42873-80.
McVicker, D. P., G. J. Hoeprich, A. R. Thompson, and C. L. Berger. 2014. 'Tau interconverts between diffusive and stable populations on the microtubule surface in an isoform and lattice specific manner', *Cytoskeleton (Hoboken)*, 71: 184-94.
Monroy, B. Y., D. L. Sawyer, B. E. Ackermann, M. M. Borden, T. C. Tan, and K. M. Ori-McKenney. 2018. 'Competition between microtubule-associated proteins directs motor transport', *Nat Commun*, 9: 1487.
Nitta, R., M. Kikkawa, Y. Okada, and N. Hirokawa. 2004. 'KIF1A alternately uses two loops to bind microtubules', *Science*, 305: 678-83.
Niwa, S., D. M. Lipton, M. Morikawa, C. Zhao, N. Hirokawa, H. Lu, and K. Shen. 2016. 'Autoinhibition of a Neuronal Kinesin UNC-104/KIF1A Regulates the Size and Density of Synapses', *Cell Rep*, 16: 2129-41.
Niwa, S., Y. Tanaka, and N. Hirokawa. 2008. 'KIF1Bbeta- and KIF1A-mediated axonal transport of presynaptic regulator Rab3 occurs in a GTP-dependent manner through DENN/MADD', *Nat Cell Biol*, 10: 1269-79.
Okada, Y., and N. Hirokawa. 1999. 'A processive single-headed motor: kinesin superfamily protein KIF1A', *Science*, 283: 1152-7.
Okada, Y., and N. Hirokawa. 2000. 'Mechanism of the single-headed processivity: diffusional anchoring between the K-loop of kinesin and the C terminus of tubulin', *Proc Natl Acad Sci U S A*, 97: 640-5.
Okada, Y., H. Yamazaki, Y. Sekine-Aizawa, and N. Hirokawa. 1995. 'The neuron-specific kinesin superfamily protein KIF1A is a unique monomeric motor for anterograde axonal transport of synaptic vesicle precursors', *Cell*, 81: 769-80.
Padzik, A., P. Deshpande, P. Hollos, M. Franker, E. H. Rannikko, D. Cai, P. Prus, M. Magard, N. Westerlund, K. J. Verhey, P. James, C. C. Hoogenraad, and E. T. Coffey. 2016. 'KIF5C S176 Phosphorylation Regulates Microtubule Binding and Transport Efficiency in Mammalian Neurons', *Front Cell Neurosci*, 10: 57.
Regnard, C., E. Desbruyeres, P. Denoulet, and B. Edde. 1999. 'Tubulin polyglutamylase: isozymic variants and regulation during the cell cycle in HeLa cells', *J Cell Sci*, 112 (Pt 23): 4281-9.
Rodriguez-Martin, T., A. M. Pooler, D. H. Lau, G. M. Morotz, K. J. De Vos, J. Gilley, M. P. Coleman, and D. P. Hanger. 2016. 'Reduced number of axonal mitochondria and tau hypophosphorylation in mouse P301L tau knockin neurons', *Neurobiol Dis*, 85: 1-10.
Schnitzer, M. J., and S. M. Block. 1997. 'Kinesin hydrolyses one ATP per 8-nm step', *Nature*, 388: 386-90.
Schoch, K. M., S. L. DeVos, R. L. Miller, S. J. Chun, M. Norrbom, D. F. Wozniak, H. N. Dawson, C. F. Bennett, F. Rigo, and T. M. Miller. 2016. 'Increased 4R-Tau Induces Pathological Changes in a Human-Tau Mouse Model', *Neuron*, 90: 941-7.
Siddiqui, N., and A. Straube. 2017. 'Intracellular Cargo Transport by Kinesin-3 Motors', *Biochemistry (Mosc)*, 82: 803-15.

Sirajuddin, M., L. M. Rice, and R. D. Vale. 2014. 'Regulation of microtubule motors by tubulin isotypes and post-translational modifications', *Nat Cell Biol*, 16: 335-44.
Soppina, V., S. R. Norris, A. S. Dizaji, M. Kortus, S. Veatch, M. Peckham, and K. J. Verhey. 2014. 'Dimerization of mammalian kinesin-3 motors results in superprocessive motion', *Proc Natl Acad Sci U S A*, 111: 5562-7.
Soppina, V., and K. J. Verhey. 2014. 'The family-specific K-loop influences the microtubule on-rate but not the superprocessivity of kinesin-3 motors', *Mol Biol Cell*, 25: 2161-70.
Stavoe, A. K., S. E. Hill, D. H. Hall, and D. A. Colon-Ramos. 2016. 'KIF1A/UNC-104 Transports ATG-9 to Regulate Neurodevelopment and Autophagy at Synapses', *Dev Cell*, 38: 171-85.
Stern, J. L., D. V. Lessard, G. J. Hoeprich, G. A. Morfini, and C. L. Berger. 2017. 'Phosphoregulation of Tau modulates inhibition of kinesin-1 motility', *Mol Biol Cell*, 28: 1079-87.
Tanaka, Y., S. Niwa, M. Dong, A. Farkhondeh, L. Wang, R. Zhou, and N. Hirokawa. 2016. 'The Molecular Motor KIF1A Transports the TrkA Neurotrophin Receptor and Is Essential for Sensory Neuron Survival and Function', *Neuron*, 90: 1215-29.
Thompson, A. R., G. J. Hoeprich, and C. L. Berger. 2013. 'Single-molecule motility: statistical analysis and the effects of track length on quantification of processive motion', *Biophys J*, 104: 2651-61.
Trybus, K. M. 2013. 'Intracellular transport: the causes for pauses', *Curr Biol*, 23: R623-5.
Tsai, J. W., W. N. Lian, S. Kemal, A. R. Kriegstein, and R. B. Vallee. 2010. 'Kinesin 3 and cytoplasmic dynein mediate interkinetic nuclear migration in neural stem cells', *Nat Neurosci*, 13: 1463-71.
Vale, R. D., and R. A. Milligan. 2000. 'The way things move: looking under the hood of molecular motor proteins', *Science*, 288: 88-95.
Verhey, K. J., and J. Gaertig. 2007. 'The tubulin code', *Cell Cycle*, 6: 2152-60.
Widlund, P. O., M. Podolski, S. Reber, J. Alper, M. Storch, A. A. Hyman, J. Howard, and D. N. Drechsel. 2012. 'One-step purification of assembly-competent tubulin from diverse eukaryotic sources', *Mol Biol Cell*, 23: 4393-401.
Yonekawa, Y., A. Harada, Y. Okada, T. Funakoshi, Y. Kanai, Y. Takei, S. Terada, T. Noda, and N. Hirokawa. 1998. 'Defect in synaptic vesicle precursor transport and neuronal cell death in KIF1A motor protein-deficient mice', *J Cell Biol*, 141: 431-41.
Zhang, R., B. LaFrance, and E. Nogales. 2018. 'Separating the effects of nucleotide and EB binding on microtubule structure', *Proc Natl Acad Sci U S A*, 115: E6191-E200.

CHAPTER 3: THE MICROTUBULE ASSOCIATED PROTEIN TAU REGULATES KIF1A PAUSING BEHAVIOR AND MOTILITY

Dominique V. Lessard[1] and Christopher L. Berger[1]*

From the [1] Department of Molecular Physiology & Biophysics, University of Vermont, Burlington, VT 05405

Submitted to *Biophysical Journal*.

Running Title: *Tau regulates KIF1A behavior and motility*

*To whom correspondence should be addressed:
Christopher L. Berger, Ph.D.
Department of Molecular Physiology & Biophysics
University of Vermont
Burlington, Vermont 05405
Telephone: (802) 656-5707
Email: cberger@uvm.edu

Keywords: KIF1A, Tau, C-terminal tail, kinesin, microtubule, axonal transport, neurodegenerative disease, microtubule associated protein (MAP)

ABSTRACT

Many neurodegenerative diseases result from dysfunction of axonal transport, a highly regulated cellular process responsible for site-specific neuronal cargo delivery. The kinesin-3 family member KIF1A is a key mediator of this process by facilitating long-distance cargo delivery in a spatiotemporally regulated manner. While misregulation of KIF1A cargo delivery is observed in many neurodegenerative diseases, the regulatory mechanisms responsible for KIF1A cargo transport are largely unexplored. Our lab has recently characterized a mechanism for a unique pausing behavior of KIF1A in between processive segments on the microtubule. This behavior, mediated through an interaction between the KIF1A K-loop and the polyglutamylated C-terminal tails of tubulin, helps us further understand how KIF1A conducts long-range cargo transport. However, how this pausing behavior is influenced by other regulatory factors on the microtubule is an unexplored concept. The microtubule associated protein Tau is one potential regulator, as altered Tau function is a pathological marker in many neurodegenerative diseases. However, while Tau's effect on kinesin-1 and -2 has been extensively characterized, Tau's role in regulating KIF1A transport is greatly unexplored at the behavioral level. Using single-molecule imaging, we have identified Tau-mediated regulation of KIF1A pausing behavior and motility. Specifically, we have elucidated the competitive interaction between Tau and KIF1A for the C-terminal tails of tubulin. This competition introduces a new mechanism of Tau-mediated kinesin regulation by inhibiting KIF1A's ability to use pauses to connect multiple processive segments into a longer run length. Moreover, we have correlated this regulatory mechanism to Tau's behavioral dynamics, further elucidating the function of Tau's diffusive and static behavioral state on the microtubule surface. In

summary, we introduce a new mechanism of Tau-mediated motility regulation, providing insight on how disruptions in axonal transport can lead to disease state pathology.

SIGNIFICANCE

KIF1A mediated cargo transport is essential in many cellular processes such as axonal transport and neuronal development. Defects in KIF1A transport have been implicated in neurodegenerative diseases including Alzheimer's disease and frontotemporal dementia. However, the mechanism of KIF1A's pathological misregulation remains elusive, highlighting the importance of identifying regulators of KIF1A function. The microtubule associated protein Tau is an attractive potential regulator of KIF1A motility as Tau dysfunction is a hallmark of these neurodegenerative diseases. Here, we demonstrate a direct connection between Tau and KIF1A motility, revealing a unique form of Tau-mediated regulation of axonal transport. Our results provide a molecular foundation for understanding the role of motor protein misregulation in neurodegenerative disease progression.

INTRODUCTION

Impaired cellular cargo trafficking is a hallmark of many neurodegenerative diseases, such as Alzheimer's disease (AD) and frontotemporal dementia (FTD) (Bodea et al. 2016; Ballatore, Lee, and Trojanowski 2007; Kneynsberg et al. 2017; Zempel and Mandelkow 2014). This disease-state pathology implicates a deficiency in axonal transport, a critical process for neuronal viability and function, involving the spatiotemporal trafficking of cellular cargo along the length of the axon. A key mediator of this process is the kinesin-3 family member KIF1A, known to transport cargo that must travel great magnitudes of distance down the axon, such as dense core vesicles (Lo et al. 2011) and synaptic vesicle proteins (Chiba et al. 2019; Okada et al. 1995). Recent discoveries uncovering the motor specific behavior of KIF1A, such as its "superprocessive" motility, or ability to travel comparatively farther distances than other kinesin motors, (Soppina et al. 2014; Soppina and Verhey 2014) and characteristic pausing in-between processive segments of motility (Lessard et al. 2019), have provided significant insight as to how this motor is able to transport cargo such extreme magnitudes of distance in comparison to other kinesin motors. Moreover, KIF1A's motor specific behavior and motility must be tightly regulated to achieve efficient spatiotemporal cargo delivery within the neuron. The systemic importance of proper KIF1A regulation is demonstrated in neurodegenerative diseases presenting with KIF1A cargo mislocalization, such as AD and FTD (Hung and Coleman 2016; Siddiqui and Straube 2017; Goetzl et al. 2016). However, the mechanisms contributing towards pathological KIF1A cargo delivery are greatly unexplored, stemming from our lack of knowledge of mechanisms that regulate KIF1A motility.

The complex landscape of axonal microtubules may provide a regulatory mechanism for the spatiotemporal delivery of KIF1A cargo, via the presence of microtubule associated proteins (MAPs) that bind to the microtubule surface. Specifically, the neuronal MAP Tau is an attractive potential regulator of KIF1A, as Tau has been shown to differentially regulate the motility of specific kinesin families. Initial observations of the highly characterized kinesin-1 family of motors revealed that, upon encountering microtubule bound Tau, kinesin-1 motors prematurely dissociate from the microtubule surface (Dixit et al. 2008; Vershinin et al. 2007). Our lab has further explored Tau's regulation of kinesin-1 motility, discovering that a pathologically relevant phosphomimetic mutation of Tau leads to an intermediary level of kinesin-1 motility inhibition, as well as showing that Tau's regulation of kinesin-1 depends on the nucleotide binding state of microtubules (Stern et al. 2017; McVicker, Chrin, and Berger 2011). Contrastingly, our lab has also shown that unlike kinesin-1, kinesin-2 motility is insensitive to Tau (Hoeprich et al. 2014; Hoeprich et al. 2017). Despite the complex array of Tau's regulatory mechanisms on other kinesin family members, no studies have yet explored the effects of Tau on dimeric KIF1A motility parameters. It is imperative that the relationship between KIF1A and Tau be thoroughly characterized at a molecular level to build the cellular framework needed to understand Tau's effect on KIF1A cargo transport in a neurodegenerative setting. Pathologically, irregular Tau function in AD and FTD further emphasizes the importance of defining this relationship (Zempel and Mandelkow 2014; Kneynsberg et al. 2017; Iqbal et al. 2010; Avila et al. 2004; Boutajangout and Wisniewski 2014), insinuating that Tau's loss-of-function could sacrifice a critical regulatory mechanism of KIF1A cargo delivery.

However, the lack of research on this topic highlights a gap in knowledge, halting our understanding of neurodegenerative disease progression.

Intriguingly, both KIF1A and Tau demonstrate unique behavioral interactions with the microtubule surface. Tau binds to the microtubule surface both statically and diffusively in an equilibrium that is isoform specific (Hinrichs et al. 2012; McVicker et al. 2014). It has been further shown that Tau relies on the tubulin C-terminal tails (CTTs) to facilitate specifically diffusive binding behavior (Hinrichs et al. 2012). Based on this interaction, the isoform-dependent equilibrium of Tau's static and diffusive binding is an important parameter to consider when assessing Tau's regulation of kinesin motors. For example, our lab has shown that the run length of kinesin-1 motors are more severely inhibited by the static binding state of Tau, not the diffusive binding state of Tau (Stern et al. 2017; Hoeprich et al. 2014; Hoeprich et al. 2017). Yet, how Tau's isoform-specific binding equilibrium may regulate KIF1A is a concept entirely unexplored.

Much like Tau, the CTTs of tubulin are an essential structure for KIF1A function. The KIF1A/CTT interaction is largely mediated by an electrostatic "tethering" between KIF1A's K-loop, a positively charged surface loop in the motor domain, and post-translational addition of negatively charged glutamic acid residues to the CTTs, a signature of neuronal tubulin (Lessard et al. 2019). This K-loop/CTT interaction is known to be important for many KIF1A characteristics such as landing rate and facilitating diffusive events along the microtubule surface in the weakly-bound ADP state (Soppina and Verhey 2014; Hirokawa, Nitta, and Okada 2009). In addition to these findings, our lab has recently described the characteristic pausing behavior of KIF1A, revealing that KIF1A relies on the CTTs to engage in pauses in-between segments of processive movement on the

microtubule (Lessard et al. 2019). Considering that both KIF1A and diffusively bound Tau interact with the microtubule C-terminal tails, we hypothesized that diffusive Tau has the potential to act as regulator of KIF1A motility by competitively interacting with the CTT during KIF1A pausing (Figure 3-1). Using single-molecule total internal reflection fluorescence microscopy (TIRF), we tested our hypothesis by quantifying the motility and behavioral response of KIF1A on Tau decorated microtubules. Our findings uncovered a new mechanism of Tau-mediated kinesin motor regulation. From this, we present the discovery of diffusive Tau's regulation of KIF1A motility during KIF1A pausing.

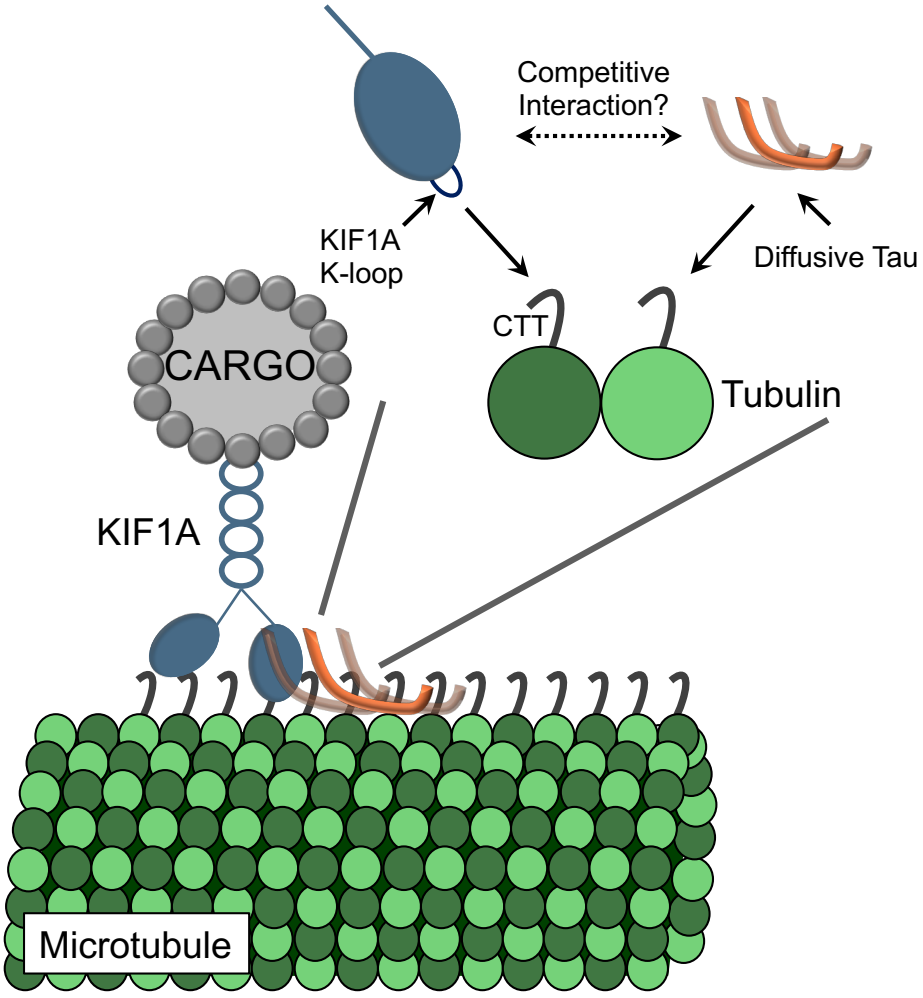

Figure 3-1. Graphical representation of experimental hypothesis. Previous literature has detailed that both KIF1A and Tau interact with the C-terminal tails (CTT) of tubulin subunits. The interaction between KIF1A's "K-loop" and the polyglutamylated CTTs has been shown to facilitate KIF1A's recently characterized pausing behavior (Lessard et al. 2019). Each Tau isoform has a characteristic behavioral equilibrium between a static and a diffusing binding state. The diffusive binding state of Tau is achieved through an interaction with the CTTs (Hinrichs et al. 2012). As both proteins rely on interactions with the CTTs to exhibit protein-specific behavior, we hypothesis that KIF1A and the diffusive binding state of Tau compete for CTT interaction.

MATERIALS AND METHODS

Microtubule preparation and labelling

Tubulin was isolated from bovine brains donated from Vermont Livestock Slaughter & Processing (Ferrisburgh, VT) as previous described (Lessard et al. 2019). Isolated tubulin was clarified using an Optima TLX Ultracentrifuge (Beckman, Pasadena, CA) at 95,000 rpm for 20 minutes at 4ºC. Clarified tubulin was read at 280nm in a spectrophotomer and the extinction coefficient of 115,000 cm^{-1} M^{-1} was used to determine concentration. Clarified tubulin was supplemented with 1 mM GTP (Sigma-Aldrich, St. Luois, MO) and labelled, stabilized, and diluted as previously described (Lessard et al. 2019). For microtubule C-terminal tail removal, microtubules were treated with Subtilisin A (Sigma Aldrich) as previously described (Lessard et al. 2019). For experiments containing Tau, tubulin polymerization was performed as described above, in the absence of labeled tubulin. Polymerized microtubules were incubated with 200 nM, 100 nM or 50 nM Alexa 647 labeled Tau (1:5, 1:10 or 1:20 Tau to tubulin ratio) for an additional 20 minutes at 37°C. Tau and microtubules mixture was centrifuged at room temperature for 30 minutes at 15,000 rpm. The pellet was then resuspended in Motility Buffer (MB).

Protein expression and labelling

Wild-type (WT) 3RS- and 4RL-Tau constructs were expressed in BL21 CodonPlus(DE3)-RP Escherichia coli cells (Stratagene, La Jolla, CA) and purified as previously described (McVicker, Chrin, and Berger 2011; McVicker et al. 2014). Purified protein was dialyzed in 1x BRB80, and concentration was determined using the Bicinchoninic Acid (BCA) Protein Assay (Pierce, Rockford, IL) using WT 3RS-Tau as a standard. To label Tau, protein was incubated with a 10-fold molar excess of dithiothreitol

(DTT) at room temperature for 2 hours. DTT was then removed using a 2 ml 7K MWCO Zeba spin desalting column (Pierce, Rockford, IL). Protein was then incubated with fivefold molar excess of Alexa 647 C5 Maleimide (Invitrogen Molecular Probes, Carlsbad, CA) overnight at room temperature. Excess fluor was removed using the previously mentioned Zeba desalting columns. To determine the labeling efficiency, Alexa Fluor 647 concentration was determined using an extinction coefficient of 270,000 cm^{-1} M^{-1} at 495 nm using a 640 Spectrophotometer. Labeled protein concentration was determined using a BCA assay. KIF1A(1-393)-LZ-3xmCitrine motors (a generous gift of Dr. Kristen Verhey, University of Michigan, Ann Arbor, MI) were expressed in COS-7 monkey kidney fibroblasts (American Type Culture Collection, Mansses, VA) as previously described (Lessard et al. 2019).

In vitro single-molecule TIRF

Flow chambers used in *in vitro* TIRF experiments were constructed as previously described (Stern et al. 2017). Flow chambers were incubated with monoclonal anti-β III (neuronal) antibodies at 33 μg/ml for 5 minutes, then washed twice with 0.5 mg/ml bovine serum albumin (BSA; Sigma Aldrich) and incubated for 2 minutes. 1 μM of microtubules (all experimental conditions) were administered and incubated for 8 minutes. Non-adherent microtubules were removed with a MB wash supplemented with 20 μM paclitaxel. Kinesin motors in MB (12 mM PIPES, 1 mM $MgCl_2$, 1 mM EGTA, supplemented with 20 μM paclitaxel, 10 mM DTT, 1 mM $MgCl_2$, 10 mg/ml BSA, 2 mM ATP and an oxygen scavenger system [5.8 mg/ml glucose, 0.045 mg/ml catalase, and 0.067 mg/ml glucose oxidase; Sigma Aldrich]), supplemented with 2 mM ATP, were added to the flow cell just before image acquisition. For landing rate assays, *in vitro* KIF1A motility assays were

prepared as described above, with the only change being that MB was supplemented with 2 mM ADP. Control *Drosophila melanogaster* biotin-tagged kinesin-1 motors were labeled with streptavidin-conjugated Qdot 655 (Life Technologies, Carlsbad, CA) at a 1:4 motor:Qdot ratio as previously described (Stern et al. 2017; Hoeprich et al. 2017).

In vitro fluorescence based Tau binding assay

To assess the affinity of Tau for subtilisin treated microtubules, we performed a TIRF binding assay, as previously described (Stern et al. 2017). In brief, unlabeled subtilisin-treated microtubules were diluted to a working concentration of 1.5 μM, adhered to flow chambers as previously described, and washed with MB to remove non-adherent microtubules. Next, 10 nM of Alexa 647 labeled Tau was flowed in and imaged at 10 frames/s for 20 frames. This process was repeated with increasing concentrations of Alexa 647 labeled Tau and conducted on the previously described TIRF set up.

Data Analysis

In vitro motility assays

Motility events were analyzed as previously reported (Hoeprich et al. 2014; Hoeprich et al. 2017). In brief, overall run length motility data was measured using the ImageJ (v. 2.0.0, National Institute of Health, Bethesda, MD) MTrackJ plug-in, for a frame-by-frame quantification of KIF1A motility. Pauses are defined as segments in where the average velocity is less than 0.2 μm/s over three frames or more. Processive events were identified at the boundaries of pausing events (Lessard et al. 2019). Kymographs of motor motility were created using the MultipleKymograph ImageJ plugin, with a set line thickness of 3. To correct for microtubule track length effects on motor motility, overall/processive run length data was resampled to generate cumulative frequency plots

(99% CI), using previously reported methods as described in Chapter 2 (Thompson, Hoeprich, and Berger 2013). To determine the landing rate of KIF1A on various microtubule conditions, the total number of motor landing events on the microtubule was divided by the length of the microtubule and further divided by the duration of the movie (events/μm/minute).

Tau Binding Assay

TIRF Tau binding assays were analyzed as previously described (Stern et al. 2017). In summary, using the MultiMeasure tool in FIJI, the average intensity of Tau per unit length of microtubule (Avg I) was measured for each frame. Average intensity was normalized to B_{max} for each respective concentration, then plotted against [Tau] to generate a binding curve and fit to one-site-specific binding with Hill slope. From this fit, a Hill coefficient (h) and K_D were determined and used to calculate the fraction of bound Tau at a given tubulin concentration.

RESULTS

3RS-Tau regulates KIF1A overall run length, but not continuous run length.

Using TIRF microscopy, we first assessed the regulatory effect of 3RS-Tau, a well characterized isoform in terms of kinesin motility regulation that favors the static binding state (Figure 3-2A), on single-molecule KIF1A motility. KIF1A's motility was first investigated on paclitaxel-stabilized microtubules in the presence of Alexa 647 labeled wild-type (WT) 3RS-Tau at three concentrations (50 nM, 100 nM, or 200 nM 3RS-Tau ; 1 μM microtubules). In the absence of Tau, KIF1A's overall run length was 6.84 ± 2.07 μm (Figure 3-2A, Table 3-1) and overall speed was 1.37 ± 0.42 μm/s (Figure S3-1, Table 3-1), supporting past reports of this motor's superprocessivity and consistent with our previous work characterizing KIF1A's pausing behavior (Lessard et al. 2019; Soppina et al. 2014). In the presence of 3RS- Tau KIF1A's overall run length significantly decreased in a dosage dependent manner (50 nM 3RS-Tau; 4.65 ± 1.83 μm, 100 nM 3RS-Tau; 3.84 ± 1.50 μm, 200 nM 3RS-Tau; 3.31 ± 1.06 μm) (Figure 3-2C, Figure S3-3, Table 3-1), while overall speed increased with the addition of Tau (50 nM 3RS-Tau; 1.38 ± 0.34 μm/s, 100 nM 3RS-Tau; 1.40 ± 0.37 μm/s, 200 nM 3RS-Tau; 1.59 ± 0.39 μm/s) (Figure S3-1, Table 3-1). These results provide direct evidence of 3RS-Tau's ability to regulate KIF1A motility by both decreasing the overall run length while simultaneously increasing overall speed.

To further investigate the process by which *overall* run length is reduced by 3RS-Tau, we next assessed changes in KIF1A's *continuous* run length, a main component of the overall run length measurement (Lessard et al. 2019). In contrast to the trends observed with overall run length, there was no significant reduction of KIF1A's continuous run length between our control microtubules (no Tau), or at any concentration of 3RS-Tau (No

Tau; 2.82 ± 0.73 μm, 50 nM 3RS-Tau; 2.84 ± 0.76 μm, 100 nM 3RS-Tau; 2.70 ± 0.57 μm, 200 nM 3RS-Tau; 2.82 ± 0.73 μm) (Figure 3-2D, Figure S3-4, Table 3-1). Following suit, there was also no change in continuous speed at any 3RS-Tau concentration (50 nM 3RS-Tau; 2.09 ± 0.59 μm/s, 100 nM 3RS-Tau; 1.95 ± 0.52 μm/s, 200 nM 3RS-Tau; 2.10 ± 0.58 μm/s) when compared to our control (Figure S3-2, Table 3-1). From these experiments we can conclude that, while 3RS-Tau regulates KIF1A's overall run length and speed, it does not do so by regulating KIF1A's continuous run length or speed.

4RL-Tau is more regulatory than 3RS-Tau on KIF1A motility.

To compare the KIF1A regulation via two Tau isoforms with contrasting binding equilibriums, we next turned to Alexa 647 labeled WT 4RL-Tau, an isoform that favors the diffusive binding state (Figure 3-2A-B). Similar to 3RS-Tau, we observed a dosage dependent decrease of KIF1A overall run length (50 nM 4RL-Tau; 3.89 ± 1.36 μm, 100 nM 4RL-Tau; 3.09 ± 1.09 μm, 200 nM 4RL-Tau; 2.54 ± 0.94 μm) (Figure 3-2C, Figure S3-3, Table 3-1) and a dosage dependent increase in overall speed (50 nM 4RL-Tau; 1.48 ± 0.45 μm/s, 100 nM 4RL-Tau; 1.54 ± 0.48 μm/s, 200 nM 4RL-Tau; 1.61 ± 0.35 μm/s) in the presence of 4RL-Tau. However, when KIF1A's overall run length was compared between 3RS- and 4RL- Tau, KIF1A's overall run length was significantly shorter on 4RL-Tau coated microtubules at every Tau concentration (Figure 3-2C, Figure S3-3, Table 3-1). The culmination of these results revealed to us that 4RL-Tau is statistically more inhibitory than 3RS-Tau on KIF1A overall run length across a dosage of Tau concentrations.

To further investigate how 4RL-Tau is more regulatory on KIF1A overall run

length, we compared the effects of 3RS- vs 4RL-Tau on KIF1A continuous run length. Like 3RS-Tau, there was no significant difference between KIF1A continuous run length at any concentration of 4RL-Tau (50 nM 4RL-Tau; 2.69 ± 0.78 μm, 100 nM 4RL-Tau; 2.62 ± 0.83 μm, 200 nM 4RL-Tau; 2.52 ± 0.81μm) (Figure 3-2D, Figure S3-4, Table 3-1); however, all 4RL-Tau concentrations significantly reduced KIF1A continuous run length when compared to control microtubules. Unlike 3RS-Tau, we observed a dosage dependent decrease in continuous speed (50 nM 4RL-Tau; 1.96 ± 0.52 μm/s, 100 nM 4RL-Tau; 1.80 ± 0.56 μm/s, 200 nM 4RL-Tau; 1.73 ± 0.40 μm/s) when compared to our control (Figure S3-2, Table 3-1). Additionally, at our highest Tau concentration (200 nM), KIF1A continuous run length is significantly shorter on 4RL-Tau coated microtubules than 3RS-Tau coated microtubules (Figure 3-2D, Figure S3-4, Table 3-1). Taken together, these results show that 4RL-Tau does not shorten KIF1A continuous run length between any of our experimental concentrations of 4RL-Tau. However, the changes in continuous speed as well as significant differences in continuous run length when compared to our control or 3RS-Tau at our highest experimental concentration support the idea that 4RL-Tau is more regulatory than 3RS-Tau on KIF1A motility.

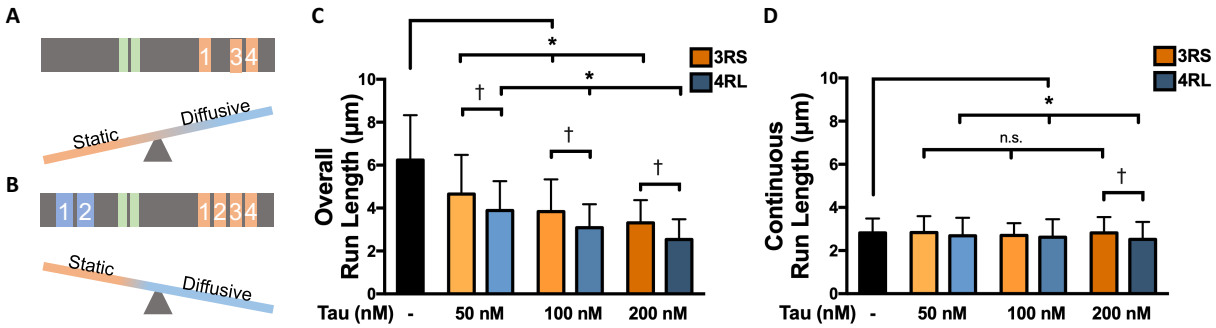

Figure 3-2. 4RL-Tau more strongly reduces KIF1A run length than 3RS-Tau. A) Cartoon depicting structural and behavioral characteristics of 3RS-Tau. Top: Linearized 3RS-Tau protein structure, featuring a proline rich region (green) and three microtubule binding repeats (orange). Bottom: The behavioral equilibrium of 3RS-Tau favors the static binding state. **B)** Cartoon depicting structural and behavioral characteristics of 4RL-Tau. Top: Linearized 4RL-Tau protein structure, featuring two acidic inserts (blue) a proline rich region (green) and four microtubule binding repeats (orange). Bottom: The behavioral equilibrium of 4RL-Tau favors the diffusive binding state. **C)** The overall run length (ORL) of KIF1A was reduced upon the addition of either 3RS- or 4RL-Tau in a dosage dependent manner. When 3RS- and 4RL-Tau are compared at specific concentrations, it is revealed that 4RL is more inhibitory than 3RS-Tau. (3RS ORL: 50 nM N=130, 100 nM N=147, 200 nM N=212; 4RL ORL: 50 nM N=170, 100 nM N=144, 200 nM N=155) **D)** Continuous run length was not significantly reduced between 3RS- and 4RL-Tau at 50 nM and 100 nM concentrations, but was significantly reduced at the highest Tau concentration (200 nM). (3RS CRL: 50 nM N=206, 100 nM N= 198, 200 nM N=243; 4RL CRL: 50 nM N=249, 100 nM N=171, 200 nM N=167)Run length values are reported as mean ± standard deviation and were calculated as previously reported (Thompson, Hoeprich, and Berger 2013). *,† $p < 0.05$

KIF1A pausing behavior is regulated by 3RS- and 4RL- Tau in a dosage dependent manner, and is more strongly regulated by 4RL-Tau than 3RS-Tau.

As referenced earlier, KIF1A's overall run length is defined as the summation of continuous run lengths and pausing events during a single motility event on the microtubule (Lessard et al. 2019). With the effect of 3RS- and 4RL-Tau on KIF1A overall and continuous run length established, we next investigated Tau's effect on KIF1A's characteristic pausing behavior. KIF1A's pausing behavior, and other quantifiable behaviors such as landing rate, are made possible through an interaction between the CTTs

of tubulin and the KIF1A K-loop (Lessard et al. 2019; Soppina and Verhey 2014). Moreover, Tau also relies on the CTTs to engage in diffusive binding behavior (Hinrichs et al. 2012). The potential competition between KIF1A and Tau for the tubulin CTTs, combined with the observed regulatory effect of 3RS- and 4RL-Tau on KIF1A's overall run length, but not continuous run length, lead us to investigate KIF1A pausing as the point of Tau-mediated regulation.

Upon addition of either 3RS- or 4RL-Tau, KIF1A pause frequency (# of pauses/overall run length) was drastically reduced (Figure 3-3A-B). Similar to what we observed regarding the influence of Tau on KIF1A's overall run length, we observed a dosage dependent decrease on KIF1A pause frequency on both 3RS- (50 nM 3RS-Tau; 0.59 ± 0.06 pauses/ORL, 100 nM 3RS-Tau; 0.35 ± 0.07 pauses/ORL, 200 nM 3RS-Tau; 0.15 ± 0.03 pauses/ORL) and 4RL-Tau (50 nM 4RL -Tau; 0.47 ± 0.05 pauses/ORL, 100 nM 4RL -Tau; 0.19 ± 0.03 pauses/ORL, 200 nM 4RL -Tau; 0.08 ± 0.02 pauses/ORL) coated microtubules when compared to control microtubules (0.97 ± 0.07 pauses/ORL) (Figure 3-3C, Figure S3-5, Table 3-1). A reduction in KIF1A pause duration was observed in two instances: 1) with 4RL- Tau at 100 nM concentration between 3RS- Tau (3RS; 2.03 ± 1.96 s, 4RL; 1.92 ± 2.51 s) and 2) between 4RL-Tau at 100 nM concentration and our control microtubules (2.27 ± 3.04 s) (Figure 3-3D). However, it is important to consider that the extensive variability between conditions due to small sample sizes (less measureable pauses as Tau concentration increases) and large standard deviations is likely to skew this result.

In comparing kymographs of KIF1A motility we also observed a visually appreciable reduction in motor landing events on Tau-coated microtubules when compared

to control microtubules, consistent with past literature (Monroy et al. 2018). This, combined with KIF1A's previous established reliance of the tubulin CTT for landing (Soppina and Verhey 2014), lead us to explore potential differences in KIF1A landing rate in the absence and presence of 3RS- and 4RL-Tau. At our highest Tau concentration (200 nM), we observed a significant reduction in KIF1A landing rate on microtubules coated in either 3RS- (2.50 ± 0.40 events/μm/min) or 4RL-Tau (0.68 ± 0.06 events/μm/min) when compared to our control microtubules (6.35 ± 1.37 events/μm/min) (Figure 3-6).

If KIF1A's pausing is the point of Tau-mediated regulation, then how might this relate to the characteristic binding equilibrium of each Tau isoform? Considering that Tau must also engage with the tubulin CTTs to bind diffusively, and that 4RL-Tau favors the diffusive binding state, we further hypothesized that 4RL-Tau would be more inhibitory to KIF1A pausing than 3RS-Tau. This was confirmed when KIF1A's pause frequency was compared between 3RS- and 4RL- Tau, revealing that KIF1A's pause frequency was significantly reduced on 4RL-Tau coated microtubules at every Tau concentration (Figure 3-3C, Figure S3-5, Table 3-1). The culmination of these results support our idea that KIF1A pauses are heavily subjected to Tau-mediated regulation. Furthermore, these findings insinuate that the diffusive binding state, not the static binding state, of Tau is regulating KIF1A pausing and subsequent motility.

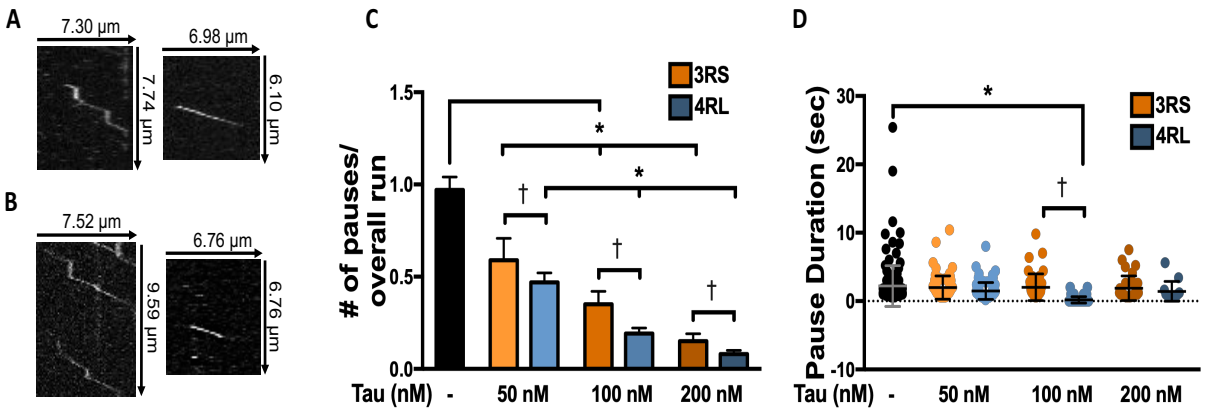

Figure 3-3. 4RL-Tau more strongly inhibits KIF1A pausing behavior when compared to 3RS-Tau. A) Representative kymographs of KIF1A behavior on microtubules with no Tau (left) and 3RS-Tau (200 nM; right). **B)** Representative kymographs of KIF1A behavior on microtubules with no Tau (left) and 4RL-Tau (200 nM; right). **C**) KIF1A pause frequency (# ofpauses/ overall run) decreases in a dosage-dependent manner upon addition of 3RS- and 4RL-Tau. At individual concentrations of Tau (50 nM, 100 nM, or 200 nM), 4RL-Tau significantly reduces the pause frequency of KIF1A when compared to 3RS-Tau. **D)** KIF1A pause duration did not significantly change upon addition of 3RS- or 4RL-Tau (with the exception of 100 nM 4RL-Tau). (3RS pauses: 50 nM N=64, 100 nM N=36, 200 nM N=20; 4RL pauses: 50 nM N=62, 100 nM N=24, 200 nM N=12) *,† $p < 0.05$

A purely static Tau obstacle, 3RS-Tau on subtilisin-treated microtubules, does not further impede KIF1A motility.

In order to ascribe diffusive Tau as the regulatory binding state on KIF1A pausing and subsequent motility, we needed to rule out static Tau as a potential regulatory binding state. Previously conducted studies have revealed that removal of CTTs removes the diffusive behavior of Tau, and shifts the microtubule bound population to a static binding state (Figure 3-4A) (Hinrichs et al. 2012). As our previous studies have characterized KIF1A's motility and pausing behavior on subtilisin-treated microtubules (Lessard et al. 2019), we next assessed the motility and pausing of KIF1A on 3RS-Tau coated, subtilisin-treated microtubules (purely static Tau obstacles) to compare these findings to the motility

and pausing of KIF1A on 3RS-Tau coated, untreated microtubules (a mix of diffusive and static obstacles).

First, to account for differences in 3RS-Tau binding affinity for the microtubule surface after microtubule CTT removal (Figure 3-4A-B), we performed a TIRF binding assay conducted as previously reported (Stern et al. 2017). Upon removal of CTTs, 3RS-Tau's K_D decreased from 116 ± 40 nM to 70 ± 7 nM (Figure 3-4C). Additionally, we saw an increase in Hill coefficient from 1.8 to 4.1 (Figure 3-4C), suggesting that the removal of CTTs results in an increase of 3RS-Tau's cooperativity on paxlitaxel-stabilized microtubules. With this knowledge, we calculated the fraction of bound 3RS-Tau on subtilisin-treated microtubules at our highest experimental concentration of 200 nM. We then adjusted the concentration of 3RS-Tau added to ensure that the same fraction of 3RS-Tau is bound to subtilisin microtubules as our untreated microtubules, making shifts in 3RS-Tau's behavioral state the only changing variable.

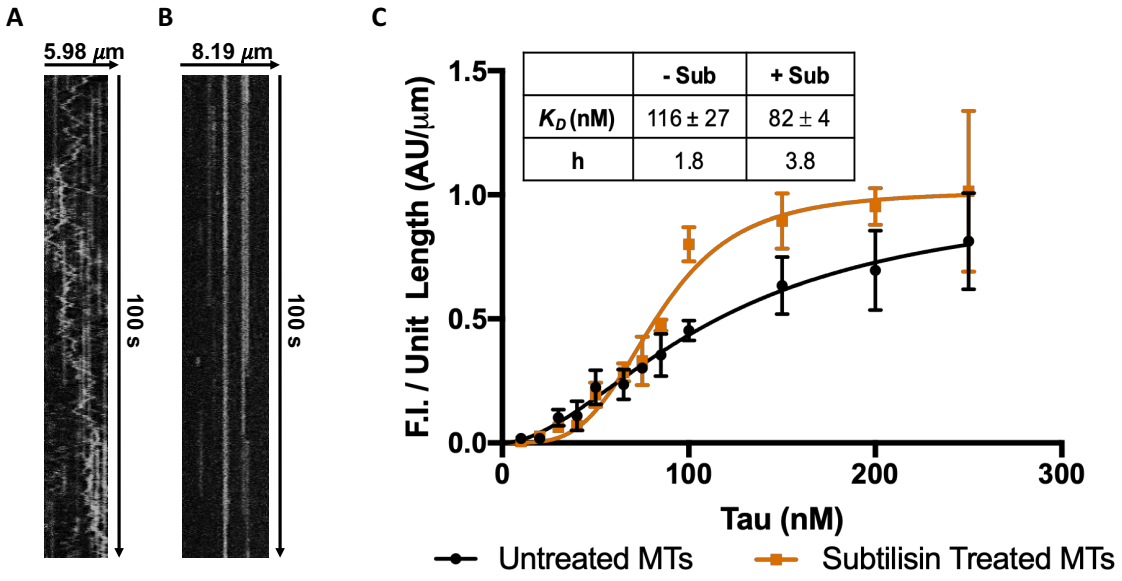

Figure 3-4. TIRF binding assays for Tau on untreated and subtilisin-treated microtubules (MTs). A) Representative kymograph of 3RS-Tau on untreated microtubules demonstrating the static (straight lines) and diffusive (jagged lines) behavioral states of Tau. **B)** Representative kymograph of 3RS-Tau on subtilisin-treated microtubules demonstrating that C-terminal tail removal shifts Tau to the static state. **C)** Upon subtilisin treatment of MTs, Tau's affinity and cooperativity increased. 3-5 experiments per concentration, totaling N=50 microtubules at each concentration.

With the addition of 3RS-Tau to subtilisin treated microtubules (Figure 3-5A), we saw no significant change in KIF1A's overall run length (3.26 ± 1.22 μm), overall speed (1.22 ± 0.23 μm/s), continuous run length (3.12 ± 1.12 μm), continuous speed (2.10 ± 0.47 μm/s), pause duration (1.34 ± 0.91 s), or pause frequency (0.17 pauses/overall run), when compared to KIF1A on subtilisin-treated microtubules without 3RS-Tau (Figure 3-5B-D, Figure S3-1 through S3-4, Table 3-1). Intriguingly, the addition of 3RS-Tau to subtilisin-treated microtubules significantly reduced the landing rate (1.92 ± 0.40 events/μm/min) of KIF1A in comparison to subtilisin-treated microtubules without Tau (Figure 3-6, Table 3-

1), indicating that 3RS-Tau can regulate KIF1A landing rate independently of the CTT structure. Taken together, our results imply that the diffusive state of Tau relies on an interaction with the CTTs to regulate KIF1A motility and behavior on the microtubule, and that the statically bound state of Tau does not regulate KIF1A motility or pausing.

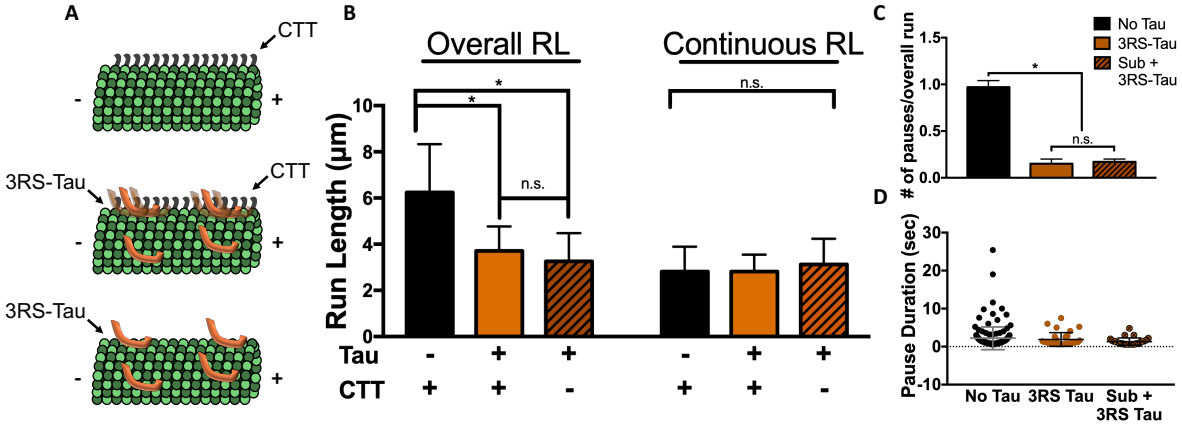

Figure 3-5. Addition of 3RS-Tau to subtilisin treated microtubules does not further inhibit KIF1A motility or pausing. A) Cartoon depiction of experimental conditions including microtubules without Tau and with C-terminal tails (CTT; top), microtubules with 3RS-Tau added (200 nM) and with CTTs (middle), or microtubules with with 3RS-Tau added (200 nM) and no CTTs (bottom). **B)** KIF1A overall run length was significantly reduced upon the addition of 3RS-Tau, or the addition of Tau on subtilisin (Sub)-treated microtubules, when compared to control microtubules (untreated, no Tau). KIF1A continuous run length was not significantly changed upon the addition of Tau, or the addition of Tau on subtilisin-treated microtubules, when compared to control microtubules (untreated, no Tau; Sub + 3RS-Tau: ORL N=162, CRL N=189). **C)** KIF1A pause frequency (# of pauses/overall run) decreased on subtilisin-treated + 3RS-Tau microtubules (200 nM 3RS-Tau) when compared to control (no Tau, no subtilisin treatment) but not when compared to untreated microtubules with 3RS-Tau (200 nM 3RS-Tau). **D)** KIF1A pause duration on control microtubules, 3RS-Tau coated microtubules (200 nM 3RS-Tau) and subtilisin-treated + 3RS-Tau microtubules (200 nM 3RS-Tau). Sub + 3RS-Tau pauses: N=26. Characteristic run length values and standard deviations were calculated as previously reported (Thompson, Hoeprich, and Berger 2013).* $p < 0.05$

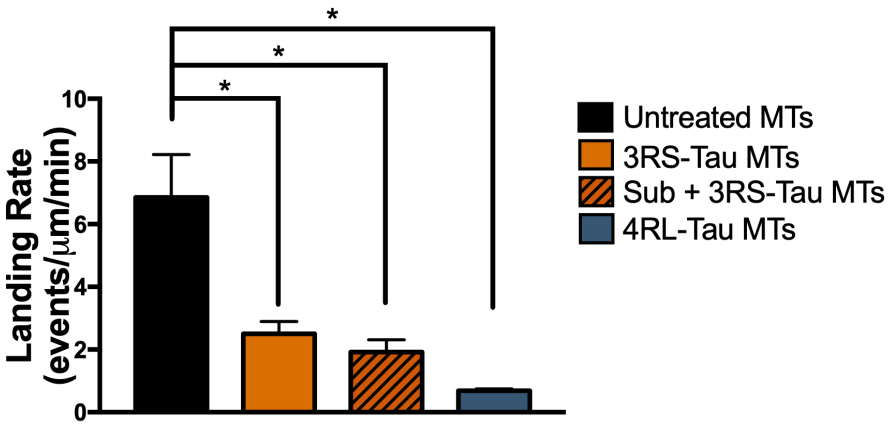

Figure 3-6. Quantification of KIF1A landing rate in the ADP state on indicated microtubule subsets. On undecorated, untreated microtubules, KIF1A had a landing rate of 6.85 ± 1.37 events/μm/min (N=971). Landing rate was significantly reduced with the addition of 3RS-Tau (2.50 ± 0.40 events/μm/min, N=846, 200 nM Tau), subtilisin treatment with the addition of 3RS-Tau (1.92 ± 0.40 events/μm/min, N=742, 200 nM Tau), or with the addition of 4RL-Tau (0.68 ± 0.06 events/μm/min, N=575, 200 nM Tau). * = $p<0.001$ relative to KIF1A on undecorated, untreated microtubules.

Table 3-1. Summary of KIF1A motility and behavior on microtubules (1 μM) across all conditions. Metrics are reported as Mean ± SD. * = $p<0.05$ relative to KIF1A on "No Tau" MTs. ł = $p<0.05$ relative to 3RS- vs. 4RL-Tau at each respective concentration.

Condition	Tau (nM)	Overall Run Length (µm)	Overall Speed (µm/s)	Continuous Run Length (µm)	Continuous Speed (µm/s)	Pause Frequency (# pauses/overall run)	Pause Duration (sec)	Landing Rate (events/µm/sec)
No Tau	-	6.84 ± 2.07	1.37 ± 0.42	2.82 ± 0.67	1.98 ± 0.53	0.97	2.27 ± 3.04	6.85 ± 1.37
3RS Tau	50	4.65 ± 1.83^{*,ł}	1.38 ± 0.34	2.84 ± 0.76	2.09 ± 0.59	0.59^{*,ł}	1.98 ± 1.70	-
3RS Tau	100	3.84 ± 1.50^{*,ł}	1.40 ± 0.37	2.70 ± 0.57	1.95 ± 0.52	0.35^{*,ł}	2.03 ± 1.96^{*,ł}	-
3RS Tau	200	3.31 ± 1.06^{*,ł}	1.59 ± 0.39	2.82 ± 0.73^{*,ł}	2.10 ± 0.58	0.15^{*,ł}	1.89 ± 1.80	2.50 ± 0.40*
4RL Tau	50	3.89 ± 1.36^{*,ł}	1.48 ± 0.45	2.69 ± 0.78*	1.96 ± 0.52	0.47^{*,ł}	1.64 ± 1.41	-
4RL Tau	100	3.09 ± 1.09^{*,ł}	1.54 ± 0.48	2.62 ± 0.83*	1.80 ± 0.56	0.19^{*,ł}	1.92 ± 2.51^{*,ł}	-
4RL Tau	200	2.54 ± 0.94^{*,ł}	1.61 ± 0.35	2.52 ± 0.81^{*,ł}	1.73 ± 0.40	0.08^{*,ł}	1.43 ± 1.47	0.68 ± 0.06*
Sub + 3RS-Tau	200	3.26 ± 1.22 *	1.22 ± 0.23	3.12 ± 1.12	2.10 ± 0.47	0.17*	1.34 ± 0.91	1.92 ± 0.40 *

DISCUSSION

The significance of KIF1A's role in long-range anterograde axonal transport (Hung and Coleman 2016; Carabalona, Hu, and Vallee 2016; Kondo, Takei, and Hirokawa 2012; Lo et al. 2011) is highlighted by the impact of altered KIF1A motility in the disease state (Tanaka et al. 2016; Yonekawa et al. 1998; Lee et al. 2015). Nevertheless, how this long-range transport is regulated for precise spatiotemporal delivery of cargo is poorly understood. The MAP Tau is an attractive possibility due to its disease state relevance and regulation of kinesin-1 motility (Vershinin et al. 2007; Dixit et al. 2008; Stern et al. 2017; Hoeprich et al. 2014), yet the effects of Tau on KIF1A motility and behavior are relatively unexplored. Given our lab's recent study detailing the necessity of tubulin's CTTs for KIF1A pausing behavior (Figure 3-7A) (Lessard et al. 2019), we considered that Tau could regulate KIF1A motility in two mutually non-exclusive ways: 1) as an obstacle that truncates processive motility, and/or 2) by rendering the CTT inaccessible, prohibiting KIF1A from pausing. Here we present a new mechanism of Tau-mediated regulation unique to KIF1A's superprocessive motility and behavior. First, we reported the regulatory capabilities of two Tau isoforms, 3RS- and 4RL-Tau, on KIF1A overall run length. In exploring this finding further, we then demonstrated Tau's regulatory effect occurs during characteristic KIF1A pausing behavior (Lessard et al. 2019). Finally, we were able to indirectly ascribe this regulation specifically to the diffusive binding state of Tau (Figure 3-7B).

When developing our model of Tau-mediated KIF1A regulation (Figure 3-7), it was important to consider how Tau is known to regulate other kinesin motor families. Foundational publications investigating Tau's regulatory role on microtubule based motors

revealed that Tau regulates the processive motility of kinesin-1 motors by acting as an unnavigable obstacle, and that potency of regulation varies by Tau isoform (Vershinin et al. 2007; Dixit et al. 2008). Building upon these findings, our lab was able to ascribe Tau's regulation of kinesin-1 to Tau's static binding state, not the diffusive binding state (Hoeprich et al. 2014; Stern et al. 2017). In contrast, kinesin-2 motors are known to be insensitive to Tau, as their long neck linker allows them to switch microtubule protofilaments and side-step around obstacles (Hoeprich et al. 2017; Shastry and Hancock 2010; Hoeprich et al. 2014).

If Tau regulates KIF1A as a static obstacle while the motor is processing (like kinesin-1 motors), we would expect to have seen a reduction in continuous run length upon addition of Tau, as this parameter is defined as segments where, within a single motility event, KIF1A is moving at a constant velocity (Lessard et al. 2019). However, our study revealed that, while the overall run length of KIF1A is reduced upon addition of either 3RS- or 4RL- Tau, the continuous run length does not change between experimental Tau concentrations (Figure 3-2). Furthermore, when the CTTs of tubulin were removed, biasing 3RS-Tau's binding state to be exclusively static, there was no significant change in KIF1A motility or pausing behavior when compared to 3RS-Tau coated microtubules with CTTs still present (Figure 3-5, 3-7D). Thus, while this study revealed Tau's ability to regulate KIF1A, it does not do so by acting as a static roadblock. Alternatively, these findings lead us to postulate that, like the kinesin-2 family, KIF1A is able to navigate around static Tau obstacles, likely resulting from differences in its neck linker structure (Hoeprich et al. 2017; Phillips et al. 2016). The concept of KIF1A using protofilament side-stepping to navigate around Tau is further supported by recent cryo-electron microscopy reconstructions of Tau

on the microtubule surface, revealing that Tau binds along the crest of a single protofilament (Kellogg et al. 2018). The assessment of KIF1A's ability to side-step, and particularly how this behavior correlates with KIF1A's neck linker length/sequence, is an enticing project for future studies in our lab.

Our current results support a model where Tau regulates KIF1A by rendering the C-terminal tail inaccessible, prohibiting KIF1A from pausing and connecting multiple continuous runs to generate a superprocessive overall run length. Past work in our lab has characterized KIF1A's reliance on tubulin's CTTs to engage in characteristic pausing behavior on the microtubule surface (Figure 3-7A, 3-7C) (Lessard et al. 2019). Furthermore, Tau relies on tubulin's CTTs to engage in its diffusively bound behavioral state (Figure 3-4A-B) (Hinrichs et al. 2012). In further support of our model, both 3RS- and 4RL-Tau isoforms exhibited dosage dependent inhibition on KIF1A pause frequency (Figure 3-3), further confirming that KIF1A is not being regulated in the moments in which it is engaged in processive motility. Specifically, as the more diffusive isoform, 4RL-Tau, has a greater regulatory potency on KIF1A pausing (Figure 3-3C-D) and overall run length when compared to the more static isoform, 3RS-Tau, at each experimental concentration (Figure 3-3C), we propose that the diffusive binding state of Tau is inhibiting KIF1A pausing behavior and subsequent motility.

Differences in affinity between Tau isoforms, or of Tau on different microtubule lattices, are imperative to consider when making dosage-dependent claims of Tau's ability to regulate KIF1A motility. Consequently, a quantitative assessment of statically bound 3RS-Tau on subtilisin-treated microtubules (Figure 3-4B) was conducted over a range of concentrations (Figure 3-4C). These results demonstrated an increased Hill coefficient of

3RS-Tau on subtilisin-treated microtubules (Figure 3-4C) when compared to 3RS-Tau bound to untreated microtubules. While this increased cooperative behavior insinuates Tau's ability to form patches, it is important to note that the lowest concentration our motility assays were conducted at is 50 nM, a concentration that is much higher than past literature where Tau patches were observed (Tan et al. 2019; Dixit et al. 2008). Additionally, these experiments yielded an accurate K_D for 3RS-Tau on subtilisin treated microtubules (Figure 3-4C). Measuring Tau's affinity in each of our experimental scenarios allowed us to calculate the fraction of Tau bound at given experimental concentrations, and adjust accordingly to ensure our KIF1A motors are encountering identical amounts of Tau bound to the microtubule surface.

With Tau now mechanistically characterized as a regulator of KIF1A motility, we can use our findings to further understand disease-state pathology. The regulatory capabilities of Tau's static and diffusive binding behavior on axonal cargo transport are critical to understanding Tau's role in neurodegeneration. In diseases known for impaired axonal transport, such as AD and FTD, changes in Tau isoform expression have been correlated to disease progression (Iqbal et al. 2010). For example, pathological overexpression (Kopeikina, Hyman, and Spires-Jones 2012; Schoch et al. 2016; Goedert and Spillantini 2000) of the more diffusive four-repeat Tau isoforms (McVicker et al. 2014) and reduced transport of KIF1A cargo are observed in FTD (Goetzl et al. 2016; Siddiqui and Straube 2017; Rodriguez-Martin et al. 2016). Our results support a FTD disease state model in which a shift towards the diffusive state of Tau pathologically over-regulates KIF1A cargo transport in two ways. First, 4RL-Tau is significantly more inhibitory to KIF1A's on-rate than 3RS-Tau (Figure 3-6), presenting an increased KIF1A "parking

problem" (Monroy et al. 2018). Second, the KIF1A motors that are able to engage with the microtubule will have impaired motility due to the increase in diffusive Tau isoform expression, resulting in decreased pause frequency and overall run length. Additionally, the irregular localization and aggregation of KIF1A cargo seen in the neuronal pre-synaptic terminals in AD (Hung and Coleman 2016) can now be attributed to a loss of Tau-mediated KIF1A regulation, yielding "overactive" anterograde transport. This loss of regulation further explains an aggregation of KIF1A cargo at the distal neurite tips, as a reduction in microtubule bound Tau is observed in tauopathies resulting from hyperphosphorylation (Avila et al. 2004; Boutajangout and Wisniewski 2014; Medeiros, Baglietto-Vargas, and LaFerla 2011). This logic is supported by recent work in *C. elegans* neurons, revealing that in PTL-1 (*C. elegans* Tau analog) knockdown worms, Unc-104 (KIF1A analog)-mediated synaptic vesicles travelled farther distances down the axon (Tien et al. 2011). Additionally, a disease state loss of Tau on the microtubules can initiate signaling cascades known to alter the motility of *Drosophila* Unc-104 (Voelzmann et al. 2016). In summary, these findings bring clarity to the different pathological phenotypes of KIF1A dysfunction in AD and FTD, highlighting the physiological relevance of Tau's ability to regulate cargo transport through isoform-specific behavioral equilibria and connecting Tau to KIF1A in neurodegenerative disease.

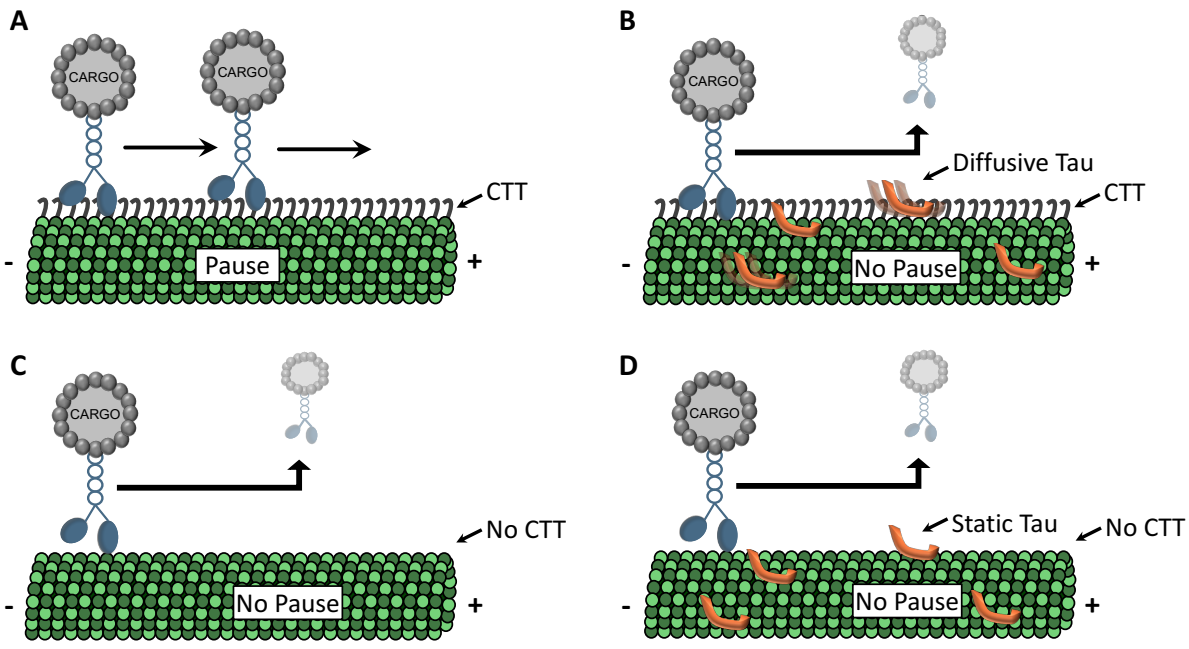

Figure 3-7. Model of Tau-mediated KIF1A regulation. A) In the absence of Tau, KIF1A exhibits an overall run length composed of continuous runs connected by pauses. These pauses are reliant upon accessible C-terminal tails (CTTs) to tether the KIF1A K-loop to the microtubule, before initiating another continuous run. **B)** When Tau is bound to the microtubule surface, the diffusive state of Tau interacts with and occupies the C-terminal tail. KIF1A can still achieve an initial continuous run, and navigate around static Tau obstacles, but cannot interact with the C-terminal tails due to diffusive Tau occupancy. This reduction in pausing decreases KIF1A's ability to string together multiple continuous runs within an overall run length event. **C)** Tau's regulatory behavior on KIF1A is mimicked when C-terminal tails are proteolytically removed from the microtubule surface. A continuous run length can be initiated however, in the absence of C-terminal tails, the motor cannot tether to the microtubule to pause and is unable to string together multiple continuous runs within an overall run length event (as shown in (Lessard et al. 2019). **D)** Addition of Tau to subtilisin-treated microtubules results in a predominantly static population of Tau on the microtubule surface. Similar to panel B, KIF1A maintains the ability to navigate around static Tau obstacles, however, the absence of C-terminal tails limits the motors ability to pause. This reduction in pause frequency results in the inability to string multiple continuous runs together in an overall run length event.

SUPPORTING INFORMATION

Title: The Microtubule Associated Protein Tau Regulates KIF1A Pausing Behavior and Motility

Authors: Dominique V. Lessard[1] and Christopher L. Berger[1]

[1] Department of Molecular Physiology & Biophysics, University of Vermont, Burlington, VT 05405

Materials Included:
Supplemental Figures and Legends 3-1 through 3-5

SI FIGURES

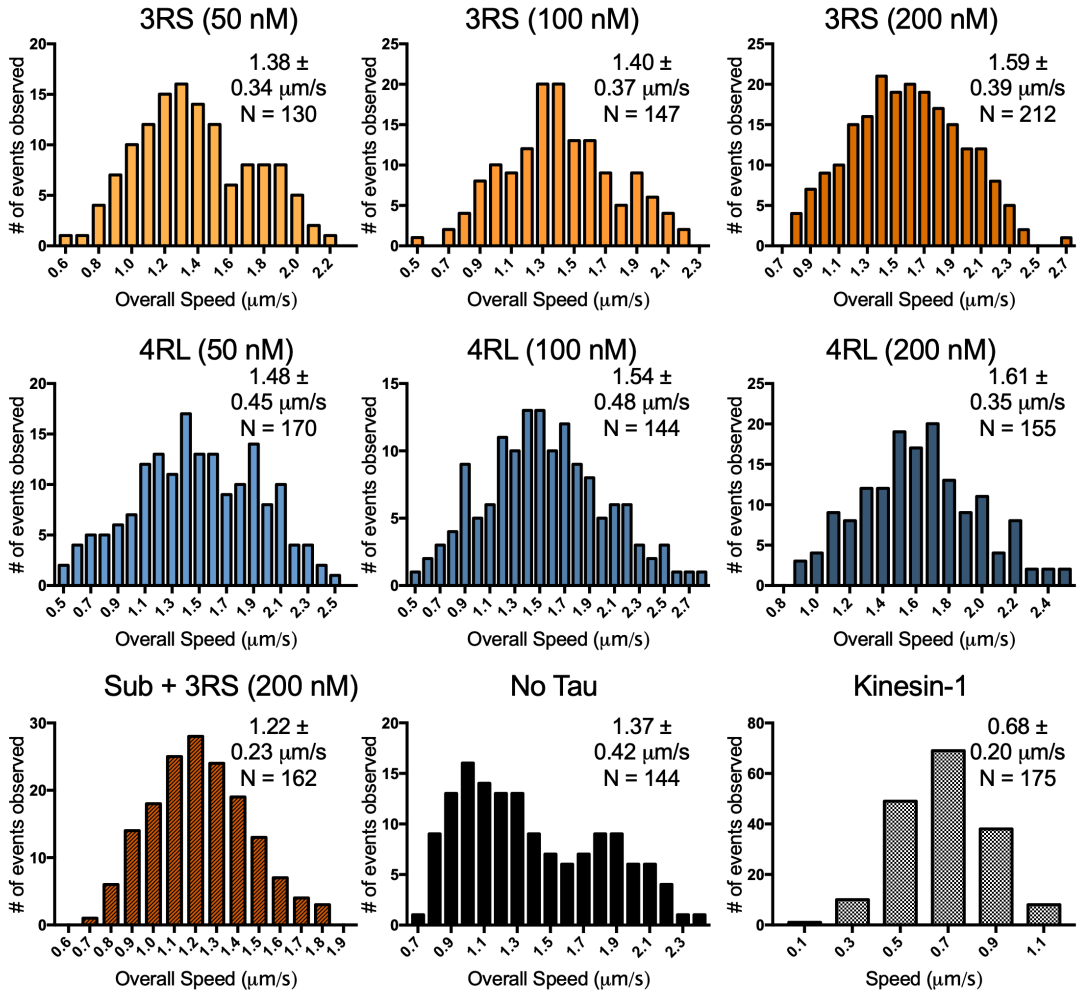

Figure S3-1. Histograms of overall speed across all conditions (Mean ± SD).

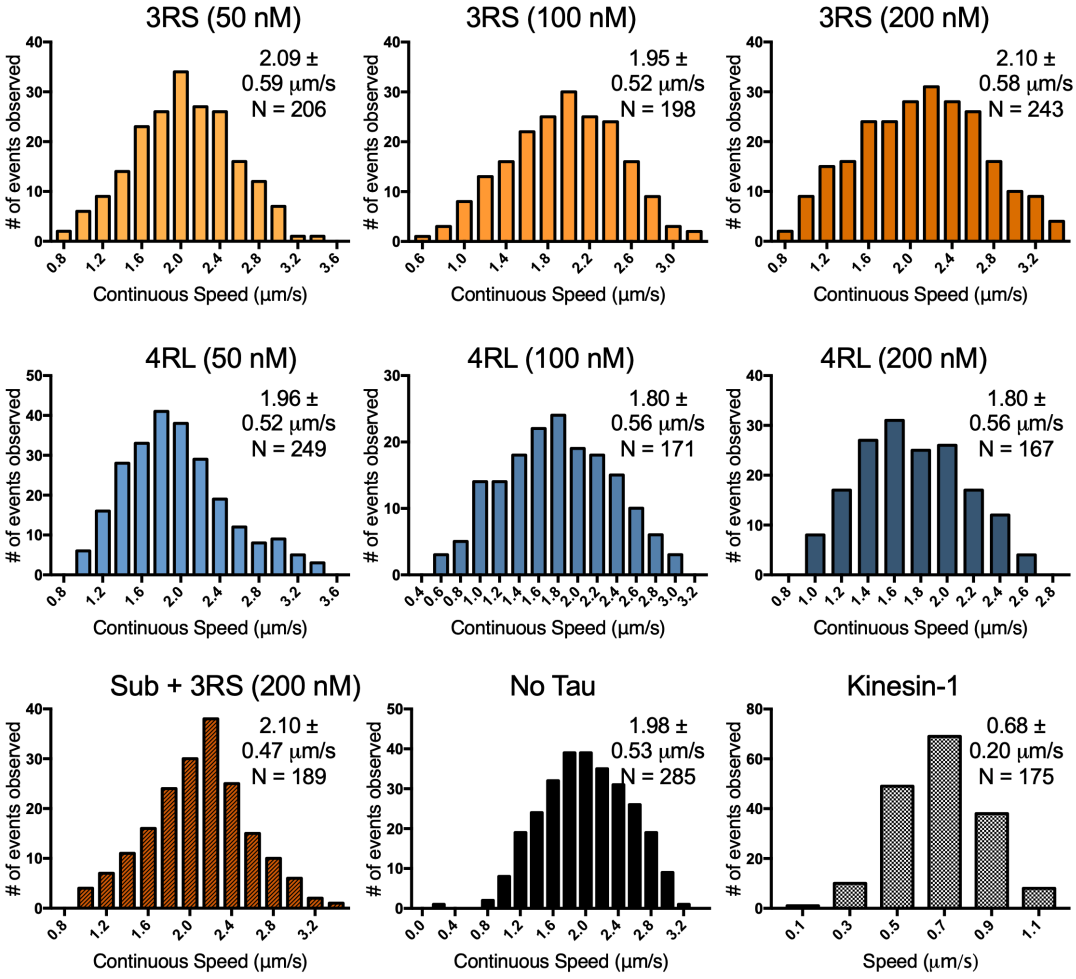

Figure S3-2. Histograms of continuous speed across all conditions (Mean ± SD).

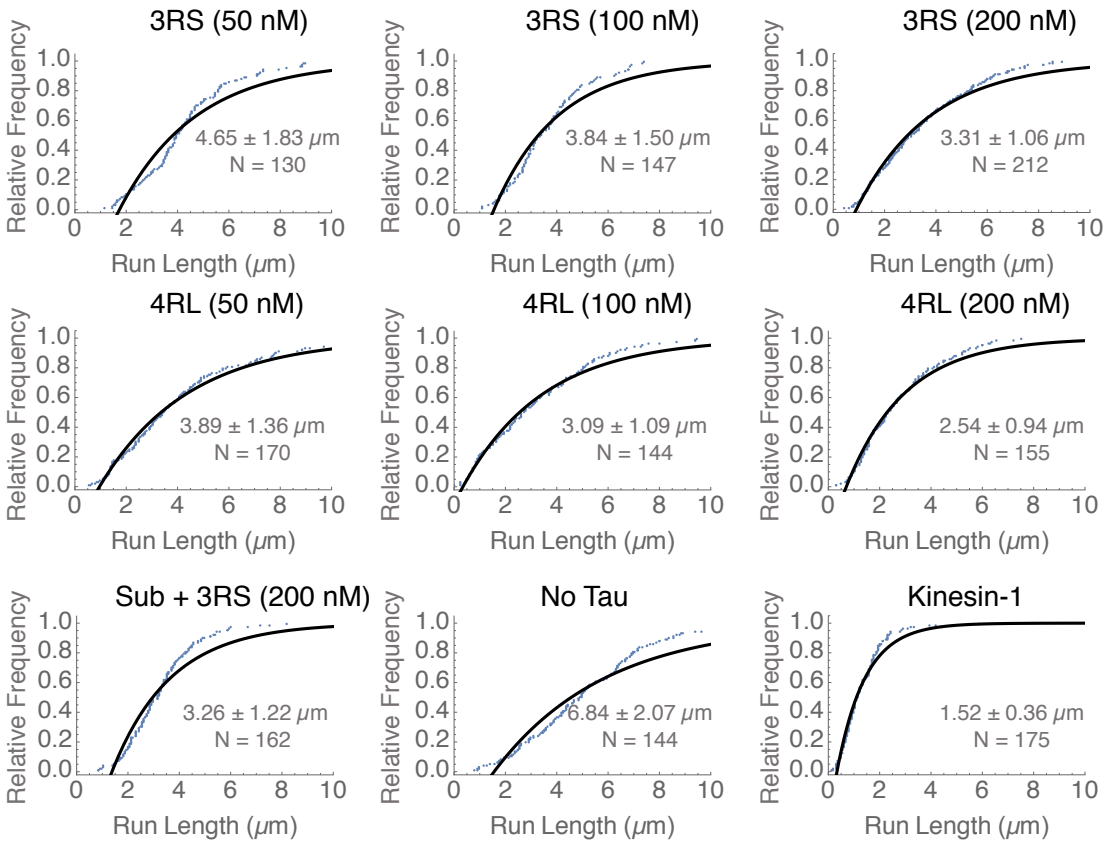

Figure S3-3. Cumulative frequency plots representing the overall run length across all experimental conditions. The raw run length is represented by black dots the observed cumulative frequency is represented by grey dots. Shown within each graph is the overall run length, calculated as previously reported (Thompson, Hoeprich, and Berger 2013) (Mean ± SD).

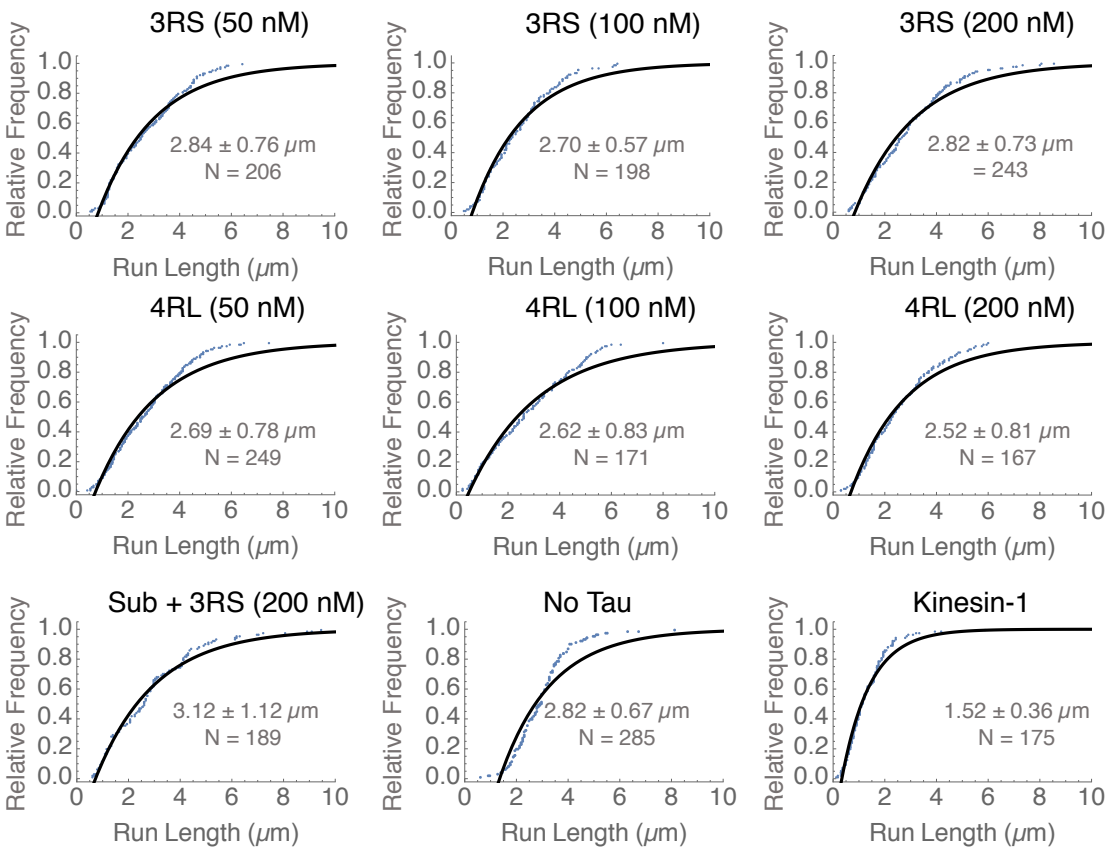

Figure S3-4. Cumulative frequency plots representing the continuous run length across all experimental conditions. The raw run length is represented by black dots the observed cumulative frequency is represented by grey dots. Shown within each graph is the overall run length, calculated as previously reported (Thompson, Hoeprich, and Berger 2013) (Mean ± SD).

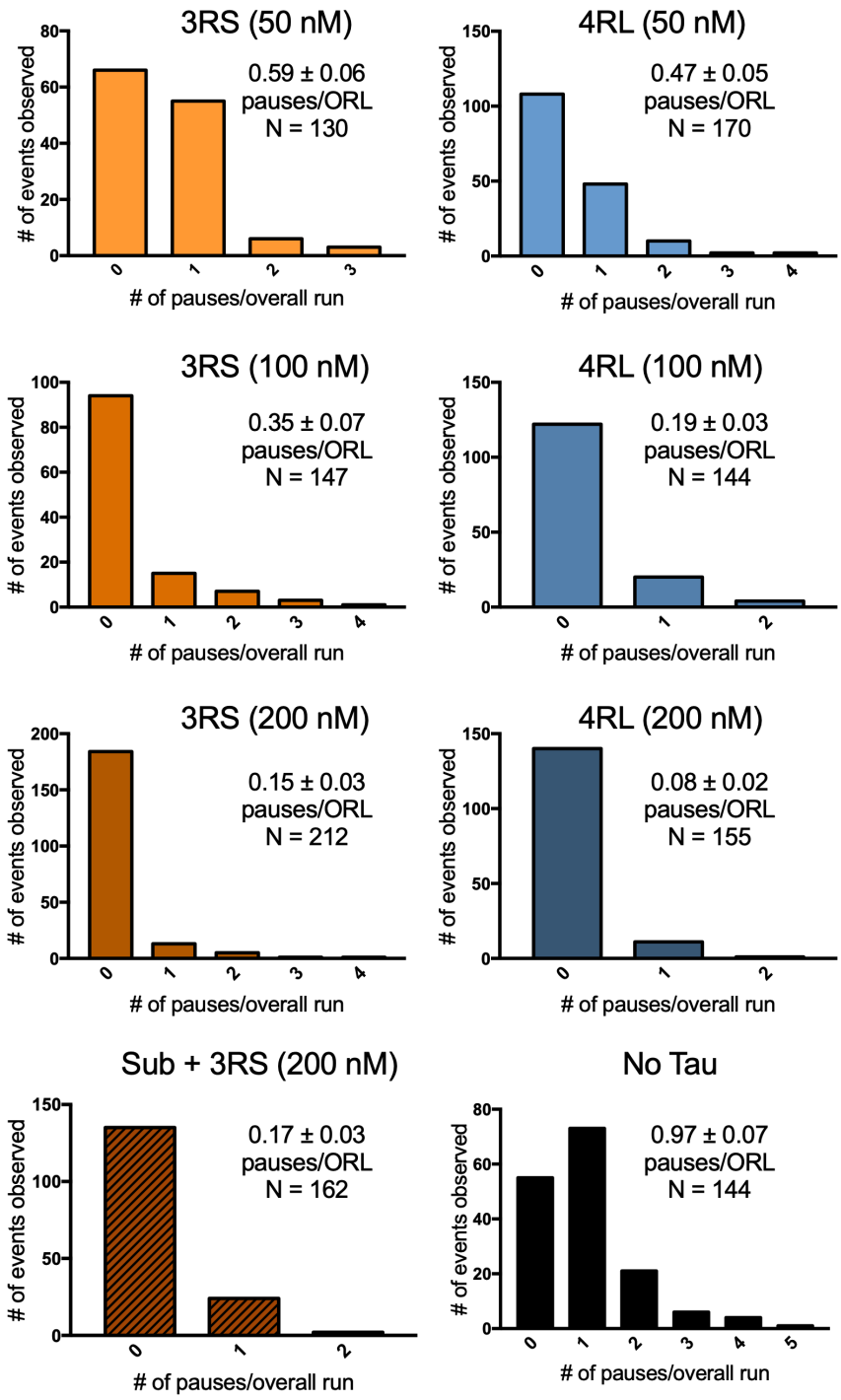

Figure S3-5. Histograms of pause frequency (pauses/overall run [ORL]) across all conditions (Mean ± SEM).

REFERENCES CITED

Avila, J., J. J. Lucas, M. Perez, and F. Hernandez. 2004. 'Role of tau protein in both physiological and pathological conditions', *Physiol Rev*, 84: 361-84.

Ballatore, C., V. M. Lee, and J. Q. Trojanowski. 2007. 'Tau-mediated neurodegeneration in Alzheimer's disease and related disorders', *Nat Rev Neurosci*, 8: 663-72.

Bodea, L. G., A. Eckert, L. M. Ittner, O. Piguet, and J. Gotz. 2016. 'Tau physiology and pathomechanisms in frontotemporal lobar degeneration', *J Neurochem*, 138 Suppl 1: 71-94.

Boutajangout, A., and T. Wisniewski. 2014. 'Tau-based therapeutic approaches for Alzheimer's disease - a mini-review', *Gerontology*, 60: 381-5.

Carabalona, A., D. J. Hu, and R. B. Vallee. 2016. 'KIF1A inhibition immortalizes brain stem cells but blocks BDNF-mediated neuronal migration', *Nat Neurosci*, 19: 253-62.

Chiba, K., H. Takahashi, M. Chen, H. Obinata, S. Arai, K. Hashimoto, T. Oda, R. J. McKenney, and S. Niwa. 2019. 'Disease-associated mutations hyperactivate KIF1A motility and anterograde axonal transport of synaptic vesicle precursors', *Proc Natl Acad Sci U S A*, 116: 18429-34.

Dixit, R., J. L. Ross, Y. E. Goldman, and E. L. Holzbaur. 2008. 'Differential regulation of dynein and kinesin motor proteins by tau', *Science*, 319: 1086-9.

Goedert, M., and M. G. Spillantini. 2000. 'Tau mutations in frontotemporal dementia FTDP-17 and their relevance for Alzheimer's disease', *Biochim Biophys Acta*, 1502: 110-21.

Goetzl, E. J., D. Kapogiannis, J. B. Schwartz, I. V. Lobach, L. Goetzl, E. L. Abner, G. A. Jicha, A. M. Karydas, A. Boxer, and B. L. Miller. 2016. 'Decreased synaptic proteins in neuronal exosomes of frontotemporal dementia and Alzheimer's disease', *FASEB J*, 30: 4141-48.

Hinrichs, M. H., A. Jalal, B. Brenner, E. Mandelkow, S. Kumar, and T. Scholz. 2012. 'Tau protein diffuses along the microtubule lattice', *J Biol Chem*, 287: 38559-68.

Hirokawa, N., R. Nitta, and Y. Okada. 2009. 'The mechanisms of kinesin motor motility: lessons from the monomeric motor KIF1A', *Nat Rev Mol Cell Biol*, 10: 877-84.

Hoeprich, G. J., K. J. Mickolajczyk, S. R. Nelson, W. O. Hancock, and C. L. Berger. 2017. 'The axonal transport motor kinesin-2 navigates microtubule obstacles via protofilament switching', *Traffic*, 18: 304-14.

Hoeprich, G. J., A. R. Thompson, D. P. McVicker, W. O. Hancock, and C. L. Berger. 2014. 'Kinesin's neck-linker determines its ability to navigate obstacles on the microtubule surface', *Biophys J*, 106: 1691-700.

Hung, C. O., and M. P. Coleman. 2016. 'KIF1A mediates axonal transport of BACE1 and identification of independently moving cargoes in living SCG neurons', *Traffic*, 17: 1155-67.

Iqbal, K., F. Liu, C. X. Gong, and I. Grundke-Iqbal. 2010. 'Tau in Alzheimer disease and related tauopathies', *Curr Alzheimer Res*, 7: 656-64.

Kellogg, E. H., N. M. A. Hejab, S. Poepsel, K. H. Downing, F. DiMaio, and E. Nogales. 2018. 'Near-atomic model of microtubule-tau interactions', *Science*, 360: 1242-46.

Kneynsberg, A., B. Combs, K. Christensen, G. Morfini, and N. M. Kanaan. 2017. 'Axonal Degeneration in Tauopathies: Disease Relevance and Underlying Mechanisms', *Front Neurosci*, 11: 572.

Kondo, M., Y. Takei, and N. Hirokawa. 2012. 'Motor protein KIF1A is essential for hippocampal synaptogenesis and learning enhancement in an enriched environment', *Neuron*, 73: 743-57.

Kopeikina, K. J., B. T. Hyman, and T. L. Spires-Jones. 2012. 'Soluble forms of tau are toxic in Alzheimer's disease', *Transl Neurosci*, 3: 223-33.

Lee, J. R., M. Srour, D. Kim, F. F. Hamdan, S. H. Lim, C. Brunel-Guitton, J. C. Decarie, E. Rossignol, G. A. Mitchell, A. Schreiber, R. Moran, K. Van Haren, R. Richardson, J. Nicolai, K. M. Oberndorff, J. D. Wagner, K. M. Boycott, E. Rahikkala, N. Junna, H. Tyynismaa, I. Cuppen, N. E. Verbeek, C. T. Stumpel, M. A. Willemsen, S. A. de Munnik, G. A. Rouleau, E. Kim, E. J. Kamsteeg, T. Kleefstra, and J. L. Michaud. 2015. 'De novo mutations in the motor domain of KIF1A cause cognitive impairment, spastic paraparesis, axonal neuropathy, and cerebellar atrophy', *Hum Mutat*, 36: 69-78.

Lessard, D. V., O. J. Zinder, T. Hotta, K. J. Verhey, R. Ohi, and C. L. Berger. 2019. 'Polyglutamylation of tubulin's C-terminal tail controls pausing and motility of kinesin-3 family member KIF1A', *J Biol Chem*, 294: 6353-63.

Lo, K. Y., A. Kuzmin, S. M. Unger, J. D. Petersen, and M. A. Silverman. 2011. 'KIF1A is the primary anterograde motor protein required for the axonal transport of dense-core vesicles in cultured hippocampal neurons', *Neurosci Lett*, 491: 168-73.

McVicker, D. P., L. R. Chrin, and C. L. Berger. 2011. 'The nucleotide-binding state of microtubules modulates kinesin processivity and the ability of Tau to inhibit kinesin-mediated transport', *J Biol Chem*, 286: 42873-80.

McVicker, D. P., G. J. Hoeprich, A. R. Thompson, and C. L. Berger. 2014. 'Tau interconverts between diffusive and stable populations on the microtubule surface in an isoform and lattice specific manner', *Cytoskeleton (Hoboken)*, 71: 184-94.

Medeiros, R., D. Baglietto-Vargas, and F. M. LaFerla. 2011. 'The role of tau in Alzheimer's disease and related disorders', *CNS Neurosci Ther*, 17: 514-24.

Monroy, B. Y., D. L. Sawyer, B. E. Ackermann, M. M. Borden, T. C. Tan, and K. M. Ori-McKenney. 2018. 'Competition between microtubule-associated proteins directs motor transport', *Nat Commun*, 9: 1487.

Okada, Y., H. Yamazaki, Y. Sekine-Aizawa, and N. Hirokawa. 1995. 'The neuron-specific kinesin superfamily protein KIF1A is a unique monomeric motor for anterograde axonal transport of synaptic vesicle precursors', *Cell*, 81: 769-80.

Phillips, R. K., L. G. Peter, S. P. Gilbert, and I. Rayment. 2016. 'Family-specific Kinesin Structures Reveal Neck-linker Length Based on Initiation of the Coiled-coil', *J Biol Chem*, 291: 20372-86.

Rodriguez-Martin, T., A. M. Pooler, D. H. Lau, G. M. Morotz, K. J. De Vos, J. Gilley, M. P. Coleman, and D. P. Hanger. 2016. 'Reduced number of axonal mitochondria and tau hypophosphorylation in mouse P301L tau knockin neurons', *Neurobiol Dis*, 85: 1-10.

Schoch, K. M., S. L. DeVos, R. L. Miller, S. J. Chun, M. Norrbom, D. F. Wozniak, H. N. Dawson, C. F. Bennett, F. Rigo, and T. M. Miller. 2016. 'Increased 4R-Tau Induces Pathological Changes in a Human-Tau Mouse Model', *Neuron*, 90: 941-7.
Shastry, S., and W. O. Hancock. 2010. 'Neck linker length determines the degree of processivity in kinesin-1 and kinesin-2 motors', *Curr Biol*, 20: 939-43.
Siddiqui, N., and A. Straube. 2017. 'Intracellular Cargo Transport by Kinesin-3 Motors', *Biochemistry (Mosc)*, 82: 803-15.
Soppina, V., S. R. Norris, A. S. Dizaji, M. Kortus, S. Veatch, M. Peckham, and K. J. Verhey. 2014. 'Dimerization of mammalian kinesin-3 motors results in superprocessive motion', *Proc Natl Acad Sci U S A*, 111: 5562-7.
Soppina, V., and K. J. Verhey. 2014. 'The family-specific K-loop influences the microtubule on-rate but not the superprocessivity of kinesin-3 motors', *Mol Biol Cell*, 25: 2161-70.
Stern, J. L., D. V. Lessard, G. J. Hoeprich, G. A. Morfini, and C. L. Berger. 2017. 'Phosphoregulation of Tau modulates inhibition of kinesin-1 motility', *Mol Biol Cell*, 28: 1079-87.
Tan, R., A. J. Lam, T. Tan, J. Han, D. W. Nowakowski, M. Vershinin, S. Simo, K. M. Ori-McKenney, and R. J. McKenney. 2019. 'Microtubules gate tau condensation to spatially regulate microtubule functions', *Nat Cell Biol*, 21: 1078-85.
Tanaka, Y., S. Niwa, M. Dong, A. Farkhondeh, L. Wang, R. Zhou, and N. Hirokawa. 2016. 'The Molecular Motor KIF1A Transports the TrkA Neurotrophin Receptor and Is Essential for Sensory Neuron Survival and Function', *Neuron*, 90: 1215-29.
Thompson, A. R., G. J. Hoeprich, and C. L. Berger. 2013. 'Single-molecule motility: statistical analysis and the effects of track length on quantification of processive motion', *Biophys J*, 104: 2651-61.
Tien, N. W., G. H. Wu, C. C. Hsu, C. Y. Chang, and O. I. Wagner. 2011. 'Tau/PTL-1 associates with kinesin-3 KIF1A/UNC-104 and affects the motor's motility characteristics in C. elegans neurons', *Neurobiol Dis*, 43: 495-506.
Vershinin, M., B. C. Carter, D. S. Razafsky, S. J. King, and S. P. Gross. 2007. 'Multiple-motor based transport and its regulation by Tau', *Proc Natl Acad Sci U S A*, 104: 87-92.
Voelzmann, A., P. Okenve-Ramos, Y. Qu, M. Chojnowska-Monga, M. Del Cano-Espinel, A. Prokop, and N. Sanchez-Soriano. 2016. 'Tau and spectraplakins promote synapse formation and maintenance through Jun kinase and neuronal trafficking', *Elife*, 5.
Yonekawa, Y., A. Harada, Y. Okada, T. Funakoshi, Y. Kanai, Y. Takei, S. Terada, T. Noda, and N. Hirokawa. 1998. 'Defect in synaptic vesicle precursor transport and neuronal cell death in KIF1A motor protein-deficient mice', *J Cell Biol*, 141: 431-41.
Zempel, H., and E. Mandelkow. 2014. 'Lost after translation: missorting of Tau protein and consequences for Alzheimer disease', *Trends Neurosci*, 37: 721-32.

CHAPTER 4: DISCUSSION

Axonal transport is an essential process for neuronal function, and is mediated in part by kinesin-driven anterograde cargo transport down the length of the axon. In the past 10 years, the kinesin-3 family member KIF1A has emerged as an essential long-distance cargo transporter, most notably carrying cargo needed for synaptic health and plasticity. While many initial studies were focused on mechanisms of KIF1A activation, recent efforts have been aimed at understanding how this highly efficient kinesin motor is regulated. One potential regulatory mechanism is the MAP Tau, as it is known to differentially regulate the kinesin-1 and kinesin-2 family of motors involved in axonal transport. Furthermore, both KIF1A and Tau dysfunction are observed in Tauopathies such as AD and FTD, suggesting a relationship between these two proteins. In considering these previous findings, the driving hypothesis of this dissertation was that Tau regulated KIF1A behavior and motility.

Regarding this hypothesis, the most influential experimental pursuit throughout this work was to mechanistically characterize KIF1A's pausing behavior. This work was initially met with criticism and contention from members of the single-molecule kinesin motility field. However, based on the dosage-dependent relationship between Tau concentration and KIF1A pausing, not investigating this behavior would have led to an incomplete and misrepresentative story about Tau-mediated KIF1A regulation. Ultimately, it became clear as to why KIF1A's pausing behavior was unreported and uncharacterized, eventually coming down to differences in experimental set up between investigating teams of scientists. The multiple in-depth discussions between these teams were essential for the findings in both chapter 2 and 3, driving the framework of this dissertation.

Suspecting that a K-loop and CTT interaction mediates KIF1A pausing was a logical starting point, as there had been a prior study highlighting the importance of this interaction on KIF1A landing rate (Soppina and Verhey 2014). Building off of this, investigating how levels of CTT polyglutamylation contribute to KIF1A pausing and motility allowed us to characterize the KIF1A/CTT interaction with an additional level of structural complexity. Not only did tying KIF1A pausing to a main neuronal tubulin PTM significantly clarify the mechanism, but brought the relevance of pausing into axon specific context. Furthermore, attributing levels of polyglutamylation to KIF1A behavior helps explain KIF1A dysfunction on an organismal level, such as altered KIF1A cargo trafficking in the ROSA22 mouse model characterized by low levels of CTT polyglutamylation (Ikegami et al. 2007).

While new information was acquired in the characterization of a KIF1A pausing mechanism, this discovery raises many more experimental questions than it resolves. Perhaps the most obvious follow-up study should be aimed at understanding how a KIF1A motor functions on a catalytic level in comparison to conventional kinesin motors. The catalysis of ATP by dimeric kinesin motors is a fine-tuned mechanochemical cycle that requires an extensive amount of coordination to keep motor domains in opposite phases of ATP binding/hydrolysis (Cochran 2015). In considering this fact, one may wonder- where does pausing fit into this cycle and how is a KIF1A motor able to reinitiate this cycle after being paused? While much work is needed to answer this question, the clue may be in KIF1A's unique pairing of loop 11 and loop 12 used to bind the microtubule surface (Nitta et al. 2004), as discussed in chapter 2. Additionally, the relevance of pausing in a cellular system is an enticing follow-up study. This question is complicated by both the increased

physiological complexity of the axon, as well as the accepted concept that molecular motors work in teams, attached to a single cargo, while processing along the axon.

As mentioned throughout this dissertation, Tau relies on CTTs to engage in diffusive binding behavior. As chapter 2 revealed that KIF1A also relies on CTTs for pausing, the idea that diffusive Tau regulates KIF1A while attempting to engage in a CTT-mediated pause is a considerable leap in logic. While this did end up being our central hypothesis for chapter 3, it was explored gingerly as it contradicted the reigning paradigm of Tau-mediated kinesin regulation in two main ways. First, when connecting how Tau's behavioral binding equilibrium regulates kinesin motors (kinesin-1), past literature credits static Tau as the regulatory binding state (Hoeprich et al. 2014; Vershinin et al. 2007; Dixit et al. 2008; Stern et al. 2017). This "obstacle hypothesis" paints static Tau as being a blockade-style obstacle that is unnavigable to kinesin-1 motors, causing them to prematurely dissociate from the microtubule surface. The obstacle hypothesis also brings to light the second way in which Tau-mediated regulation of KIF1A differs from the past literature. While the obstacle hypothesis shows that Tau inhibits kinesin motors while they are processing on the microtubule, our work presents the concept that Tau can also inhibits motors while they are stalled (paused).

While motility experiments initially revealed that 4RL-Tau was a more potent inhibitor of KIF1A pausing, this was not enough evidence to present a comprehensive picture of this new type of Tau-mediated regulation. Ultimately, in order to accept or reject our hypothesis in chapter 3, we needed to rule out the regulatory capabilities of Tau's static binding state. By creating an experimental set up (Figure 3-5) that builds off of findings from chapter 2 (Figure 2-3) (Lessard et al. 2019), we were able to confirm that static Tau

obstacles are not inhibiting KIF1A, negating the obstacle hypothesis as a plausible explanation and ascribing Tau-mediated KIF1A regulation to the diffusive binding state.

Many questions still remain about Tau-mediated regulation of KIF1A pausing and motility. This dissertation assessed the regulatory capabilities of two Tau isoforms, leaving four isoforms uncharacterized. While it is expected that 3R-/4R-Tau isoform groupings would have a similar regulatory effect due to their similarities in binding equilibrium, there are subtler structural differences between isoforms, like N-terminal acidic inserts, that could modulate Tau's regulatory behavior (Figure 1-5). Additionally, the work in this dissertation revealed that KIF1A walks ~3 μm (~375 steps) before engaging in a pause on both uncoated and Tau-coated microtubules. Even at our lowest Tau concentration, KIF1A is facing a high number of Tau molecules while walking on the microtubule. As we have shown that Tau is not regulating KIF1A during processive movement, it begs the question of how KIF1A is able to navigate through such a crowded microtubule environment while moving. Previous work from our lab may explain how this is happening. As highlighted in chapter 3, kinesin-2 motors are insensitive to the presence of Tau on the microtubule surface, unlike kinesin-1 motors that prematurely dissociate from the microtubule after encountering a Tau obstacle. This insensitivity results from an increased "nimbleness", meaning that kinesin-2 motors can switch microtubule protofilaments (Figure 1-4) and side-step around obstacles. Kinesin-2's nimbleness results from its 17 amino acid neck linker (Figure 1-6). While only being three amino acids longer than kinesin-1's 14 amino acid neck linker, these additional residues allow kinesin-2 to have a longer reach between steps and an increased probability of stepping laterally to an adjacent protofilament (Hoeprich et al. 2014; Hoeprich et al. 2017). Like kinesin-2, the KIF1A neck linker

sequence is 17 amino acids long, suggesting that KIF1A also can side step around obstacles. This concept is a potential explanation for how KIF1A is able to navigate through such a crowded microtubule environment while moving and is an enticing point for future studies.

The findings of this dissertation allow us to paint a more comprehensive picture of how Tau regulates the main kinesin motor families involved in axonal transport. While it was known that Tau regulates kinesin-1 motors, but not kinesin-2 motors, the relationship between KIF1A and Tau was unclear before this work. Based on our findings, it is postulated that Tau-mediated regulation of KIF1A shares similar characteristics with both kinesin-1 (regulated by Tau, but by a different mechanism) and kinesin-2 (likely side-steps around obstacles) motors. By defining the relationship between KIF1A and Tau we have presented a new mechanism of Tau-mediated regulation, and expanded our understanding of how kinesin motor families involved in axonal transport are regulated by Tau (Figure 4-1).

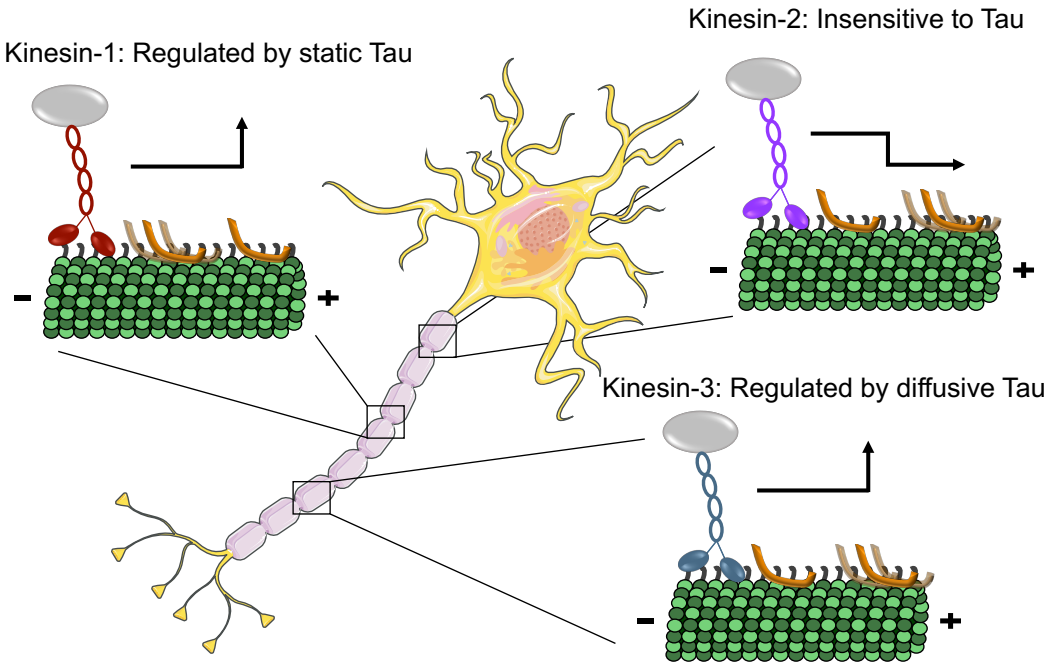

Figure 4-1. Tau differentially regulates the kinesin motor families involved in axonal transport. Kinesin-1 motors are known to be regulated by static Tau obstacles while processing along the microtubule surface. In contrast, kinesin-2 motors are insensitive to Tau obstacles resulting from their ability to side-step around obstacles. Kinesin-3 (KIF1A) is regulated by Tau, but not by static Tau while processing, like kinesin-1. Instead, KIF1A is regulated by diffusive Tau while pausing on the microtubule surface. Is it also postulated that KIF1A can side-step around obstacles while processing on the microtubule surface. The neuron in this image was acquired from Servier Medical Art (SMART) under a Creative Commons Attribution 3.0 Unported license.

Work presented in this dissertation has focused on a significant gap in knowledge regarding the basic molecular mechanisms regulating KIF1A cargo transport and contributes to our understanding of how KIF1A and Tau are related in certain Tauopathies. These findings would not have been uncovered without the use of an *in vitro* reconstituted system, visualized by single-molecule microscopy techniques. To many, the reconstituted system is not an obvious choice when tackling a problem as mysterious as neurodegenerative disease. At times, this bottom-up approach has even been referred to as a "reductionist" system (although many in the field would argue to call it a "constructionist" system). However, by peeling away layers of physiological complexity, an enormous amount of quantitative power is gained, allowing researchers to confirm or refine suspected molecular models that would otherwise be convoluted in cellular, animal, and clinical systems. Using this system, we were able to define Tau's regulation of KIF1A down to a structural level of intricacy that would not be achievable using other experimental models. Thus, while small in scale, it is important to not lose sight of the potential magnitude of these observations.

How does one extrapolate single-molecule data to provide meaning in a clinical disease-setting, particularly when the gap in knowledge between these two scales of research is so expansive? Perhaps, the best approach is not to try and build a direct ladder between molecular biophysics and clinical disease, but instead to identify how our findings contribute to rungs along the way.

Our work now provides mechanistic context for emerging cellular and organismal models of KIF1A regulation. The most direct comparison is to recent work in a *C. elegans* model, in which Unc-104 (KIF1A homolog) cargo transport was quantified in PTL-1 (Tau

homolog) wild-type and knockout worms. When PTL-1 was knocked out, an over accumulation of Unc-104 cargo was observed at the distal ends of neurons, likely due to the loss of PTL-1 mediated regulation (Tien et al. 2011). Additionally, it has been proposed that Unc-104 regulation is mediated by a Tau-spectraplakin complex in primary *Drosophila* neurons (Voelzmann et al. 2016). Taken together, these findings support the idea of a universal relationship between KIF1A and Tau (extended to their homologs) likely due to a regulatory mechanism similar to the one identified in this work.

While assessing the behavioral state of Tau is technically difficult in cellular systems/disease models, our broader characterization of Tau-mediated KIF1A regulation allows us to view disease-state perturbations of KIF1A function through a new lens. A defining characteristic of FTD is the disease state alteration in Tau isoform expression, due to a splicing defect that results in an increase of 4R-Tau isoforms (Chen et al. 2010; D'Souza and Schellenberg 2005). As we know 4R-isoforms of Tau favor the diffusive binding state, and we have shown that the diffusive binding state of Tau regulates KIF1A, we can provide a possible explanation as to why a severe reduction and irregular localization of KIF1A cargo is observed in FTD (Goetzl et al. 2016; Siddiqui and Straube 2017; Rodriguez-Martin et al. 2016), due to heightened systemic regulation of KIF1A function. In this scenario, a shift to favor 4R-isoforms would reduce KIF1A's on rate (Figure 3-6), making it difficult for KIF1A motors to engage with the microtubule and become processive. For the population of KIF1A motors that are able to engage with the microtubule surface, their pausing and subsequent motility would be significantly impaired due to the increased presence of diffusive Tau on the microtubule surface. Conversely, advanced AD pathology is characterized by a *loss* of Tau on axonal microtubules, resulting

from disease-state hyperphosphorylation of Tau (Avila et al. 2004; Boutajangout and Wisniewski 2014; Medeiros, Baglietto-Vargas, and LaFerla 2011). In this same scenario, a pathological hyperaccumulation of both KIF1A and its cargo is observed at the pre-synaptic terminals of AD neurons, suggesting that loss of our proposed regulatory mechanism leads to deleteriously excessive KIF1A function. Taken together, our findings correlate with and provide support for many emerging studies regarding KIF1A and Tau's relationship on multiple levels of physiological intricacy.

Future Directions

Our next goal is to add complexity to our model of Tau-mediated KIF1A regulation presented in this dissertation, by extending our studies into relevant cellular systems. As mentioned in the section above, there is a lack of definition of Tau and KIF1A's relationship in the experimental systems that are between single-molecule biophysics and clinical disease models, highlighting the necessity to investigate how Tau regulates KIF1A in cellular systems.

We have begun this investigation by using a SH-SY5Y neuroblastoma cellular model. SH-SY5Y cells are a valuable model system to gain understanding of Tau-mediated regulation of KIF1A motility in axonal transport. Most notably SH-SY5Y cells generate long neurites, structurally similar to axonal projections, when exposed to differentiating agents like retinoic acid (Shipley, Mangold, and Szpara 2016). Additionally, SH-SY5Y cells endogenously express KIF1A and Tau, the level of which is directly tied to the number of days differentiated (Figure 4-2). Preliminary investigation has revealed that KIF1A localizes in two distinct areas in this cell type (after 7 days of differentiation). First, KIF1A

localizes in distinct puncta along the neurites (Figure 4-2A, white arrows). Second, KIF1A also appears to localize perinuclearly, which intensifies between two nuclei in close contact (Figure 4-2B, red arrow). Additionally, we have shown that Tau expression increases over a 10-day time course of differentiation, with a complete isoform band patterning observed by day 10 (Figure 4-2A). This preliminary data presents us with a compelling cellular system to investigate the relationship between Tau expression and KIF1A localization. Our goal with this system would to be to perturb levels of Tau expression (via knockdown or specific isoform overexpression), and assess changes in KIF1A localization. Generally, we would hypothesize that the number and distribution of KIF1A puncta on SH-SY5Y neurites is directly related to levels of Tau expression. However, there are many parameters of this system that need to be addressed before fine-tuning that hypothesis, most importantly the levels of KIF1A expression over a 10-day time course of differentiation.

Our ultimate future goal would be to directly link Tau-mediated KIF1A regulation to human neurodegenerative disease progression, in a human cellular system that recapitulates the disease-state shifts in 4R:3R Tau isoform expression. Building upon our preliminary results in both *in vitro* reconstituted systems and SH-SY5Y cells, induced pluripotent stem cell (iPSC)-derived dopaminergic (DA) neurons (SCDNs) are one potential system to investigate the effects of 4R:3R isoform expression on KIF1A localization and motility. Structural alterations and neurotransmission deficits in the DA midbrain are known to contribute to both FTD and AD pathology (Nobili et al. 2017; Huey, Putnam, and Grafman 2006; D'Amelio, Puglisi-Allegra, and Mercuri 2018). Additionally, SCDNs are a valuable *in vitro* model of Tau-mediated regulation, as this differentiated cell type is known to express all six mature isoforms of Tau as well as KIF1A (Iovino et al.

2010). Furthermore, the temporal expression of SCDNs Tau isoforms has been previously established. While the relative expression of total *MAPT* transcription peaks at 48 DIV, mature 4R Tau expression increases over time, generating expression patterns comparable to levels from human midbrain tissue (post-mortum) by DIV 190 (Beevers et al. 2017). A number of AD and FTD patient derived iPSCs are commercially available for purchase. This would present us with a cellular model to investigate the effects of cell line endogenous disease-state alterations of 4R:3R expression on KIF1A motility (between AD/FTD patient cell lines and control cell lines) without having to perturb levels of Tau expression ourselves. The potential for experimental design in system this goes far beyond fixing and staining cells to quantify KIF1A localization; many other markers of KIF1A related neuronal health could be assessed, such as synapse formation/function and live cell imaging of KIF1A cargo trafficking.

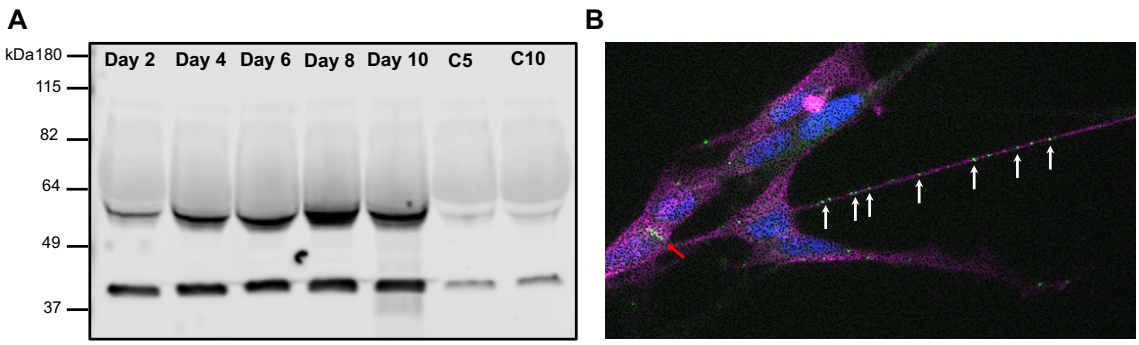

Figure 4-2. Preliminary observations of KIF1A and Tau expression in SH-SY5Y cells. **A)** Western blot of Tau expression from harvested cell lysates on days 2, 4, 6, 8, and 10 of retinoic acid (10 μM) differentiation. A pan-Tau antibody (Tau-5, mouse monoclonal) was used to blot for phosphorylated and non-phosphorylated Tau protein. A predicted high molecular weight (MW) Tau band is observed at ~ 55 kDa MW. Banded patterning of Tau isoforms (37-49 kDa MW) is observed by day 10. GAPDH was used as a loading control (~39 kDa MW) C5: undifferentiated control cells in 5% serum media. C10: undifferentiated control cells in 10% serum media. **B)** Immunofluorescent staining of KIF1A and Tau (7 days post retinoic acid differentiation). White arrows: KIF1A puncta on neurites. Red arrow: perinuclear localization of KIF1A between two contacting cells. Green: KIF1A, magenta: Tau (pan; Tau-5), blue: DAPI. 40x.

LITERATURE CITED

Andres-Barquin, P. J. 2001. 'Ramon y Cajal: a century after the publication of his masterpiece', *Endeavour*, 25: 13-7.

Araque, A., V. Parpura, R. P. Sanzgiri, and P. G. Haydon. 1999. 'Tripartite synapses: glia, the unacknowledged partner', *Trends Neurosci*, 22: 208-15.

Audebert, S., E. Desbruyeres, C. Gruszczynski, A. Koulakoff, F. Gros, P. Denoulet, and B. Edde. 1993. 'Reversible polyglutamylation of alpha- and beta-tubulin and microtubule dynamics in mouse brain neurons', *Mol Biol Cell*, 4: 615-26.

Audebert, S., A. Koulakoff, Y. Berwald-Netter, F. Gros, P. Denoulet, and B. Edde. 1994. 'Developmental regulation of polyglutamylated alpha- and beta-tubulin in mouse brain neurons', *J Cell Sci*, 107 (Pt 8): 2313-22.

Avila, J., J. J. Lucas, M. Perez, and F. Hernandez. 2004. 'Role of tau protein in both physiological and pathological conditions', *Physiol Rev*, 84: 361-84.

Ballatore, C., V. M. Lee, and J. Q. Trojanowski. 2007. 'Tau-mediated neurodegeneration in Alzheimer's disease and related disorders', *Nat Rev Neurosci*, 8: 663-72.

Banks, P., D. Mayor, and D. R. Tomlinson. 1971. 'Further evidence for the involvement of microtubules in the intra-axonal movement of noradrenaline storage granules', *J Physiol*, 219: 755-61.

Bearce, E. A., B. Erdogan, and L. A. Lowery. 2015. 'TIPsy tour guides: how microtubule plus-end tracking proteins (+TIPs) facilitate axon guidance', *Front Cell Neurosci*, 9: 241.

Beevers, J. E., M. C. Lai, E. Collins, H. D. E. Booth, F. Zambon, L. Parkkinen, J. Vowles, S. A. Cowley, R. Wade-Martins, and T. M. Caffrey. 2017. 'MAPT Genetic Variation and Neuronal Maturity Alter Isoform Expression Affecting Axonal Transport in iPSC-Derived Dopamine Neurons', *Stem Cell Reports*, 9: 587-99.

Belyy, V., M. A. Schlager, H. Foster, A. E. Reimer, A. P. Carter, and A. Yildiz. 2016. 'The mammalian dynein-dynactin complex is a strong opponent to kinesin in a tug-of-war competition', *Nat Cell Biol*, 18: 1018-24.

Berezuk, M. A., and T. A. Schroer. 2004. 'Fractionation and characterization of kinesin II species in vertebrate brain', *Traffic*, 5: 503-13.

Black, M. M., and R. J. Lasek. 1980. 'Slow components of axonal transport: two cytoskeletal networks', *J Cell Biol*, 86: 616-23.

Bock, O. 2013. 'Cajal, Golgi, Nansen, Schafer and the neuron doctrine', *Endeavour*, 37: 228-34.

Bodakuntla, S., A. S. Jijumon, C. Villablanca, C. Gonzalez-Billault, and C. Janke. 2019. 'Microtubule-Associated Proteins: Structuring the Cytoskeleton', *Trends Cell Biol*, 29: 804-19.

Bodea, L. G., A. Eckert, L. M. Ittner, O. Piguet, and J. Gotz. 2016. 'Tau physiology and pathomechanisms in frontotemporal lobar degeneration', *J Neurochem*, 138 Suppl 1: 71-94.

Bonnet, C., D. Boucher, S. Lazereg, B. Pedrotti, K. Islam, P. Denoulet, and J. C. Larcher. 2001. 'Differential binding regulation of microtubule-associated proteins MAP1A, MAP1B, and MAP2 by tubulin polyglutamylation', *J Biol Chem*, 276: 12839-48.

Boutajangout, A., A. Boom, K. Leroy, and J. P. Brion. 2004. 'Expression of tau mRNA and soluble tau isoforms in affected and non-affected brain areas in Alzheimer's disease', *FEBS Lett*, 576: 183-9.
Boutajangout, A., and T. Wisniewski. 2014. 'Tau-based therapeutic approaches for Alzheimer's disease - a mini-review', *Gerontology*, 60: 381-5.
Brady, S. T. 1985. 'A novel brain ATPase with properties expected for the fast axonal transport motor', *Nature*, 317: 73-5.
Brown, A., L. Wang, and P. Jung. 2005. 'Stochastic simulation of neurofilament transport in axons: the "stop-and-go" hypothesis', *Mol Biol Cell*, 16: 4243-55.
Bullock, T. H. 1959. 'Neuron doctrine and electrophysiology', *Science*, 129: 997-1002.
Cai, Q., M. L. Davis, and Z. H. Sheng. 2011. 'Regulation of axonal mitochondrial transport and its impact on synaptic transmission', *Neurosci Res*, 70: 9-15.
Cancalon, P., and L. M. Beidler. 1975. 'Distribution along the axon and into various subcellular fractions of molecules labeled with (3H)leucine and rapidly transported in the garfish olfactory nerve', *Brain Res*, 89: 225-44.
Carabalona, A., D. J. Hu, and R. B. Vallee. 2016. 'KIF1A inhibition immortalizes brain stem cells but blocks BDNF-mediated neuronal migration', *Nat Neurosci*, 19: 253-62.
Carter, A. P., A. G. Diamant, and L. Urnavicius. 2016. 'How dynein and dynactin transport cargos: a structural perspective', *Curr Opin Struct Biol*, 37: 62-70.
Cassimeris, L., N. K. Pryer, and E. D. Salmon. 1988. 'Real-time observations of microtubule dynamic instability in living cells', *J Cell Biol*, 107: 2223-31.
Castle, M. J., E. Perlson, E. L. Holzbaur, and J. H. Wolfe. 2014. 'Long-distance axonal transport of AAV9 is driven by dynein and kinesin-2 and is trafficked in a highly motile Rab7-positive compartment', *Mol Ther*, 22: 554-66.
Castoldi, M., and A. V. Popov. 2003. 'Purification of brain tubulin through two cycles of polymerization-depolymerization in a high-molarity buffer', *Protein Expr Purif*, 32: 83-8.
Chaaban, S., and G. J. Brouhard. 2017. 'A microtubule bestiary: structural diversity in tubulin polymers', *Mol Biol Cell*, 28: 2924-31.
Chen, S., K. Townsend, T. E. Goldberg, P. Davies, and C. Conejero-Goldberg. 2010. 'MAPT isoforms: differential transcriptional profiles related to 3R and 4R splice variants', *J Alzheimers Dis*, 22: 1313-29.
Chen, Y., M. M. Rolls, and W. O. Hancock. 2014. 'An EB1-kinesin complex is sufficient to steer microtubule growth in vitro', *Curr Biol*, 24: 316-21.
Chiba, K., H. Takahashi, M. Chen, H. Obinata, S. Arai, K. Hashimoto, T. Oda, R. J. McKenney, and S. Niwa. 2019. 'Disease-associated mutations hyperactivate KIF1A motility and anterograde axonal transport of synaptic vesicle precursors', *Proc Natl Acad Sci U S A*, 116: 18429-34.
Cochran, J. C. 2015. 'Kinesin Motor Enzymology: Chemistry, Structure, and Physics of Nanoscale Molecular Machines', *Biophys Rev*, 7: 269-99.
D'Amelio, M., S. Puglisi-Allegra, and N. Mercuri. 2018. 'The role of dopaminergic midbrain in Alzheimer's disease: Translating basic science into clinical practice', *Pharmacol Res*.

D'Souza, I., and G. D. Schellenberg. 2005. 'Regulation of tau isoform expression and dementia', *Biochim Biophys Acta*, 1739: 104-15.
Dahlstrom, A. B., K. K. Pfister, and S. T. Brady. 1991. 'The axonal transport motor 'kinesin' is bound to anterogradely transported organelles: quantitative cytofluorimetric studies of fast axonal transport in the rat', *Acta Physiol Scand*, 141: 469-76.
Dantas, T. J., A. Carabalona, D. J. Hu, and R. B. Vallee. 2016. 'Emerging roles for motor proteins in progenitor cell behavior and neuronal migration during brain development', *Cytoskeleton (Hoboken)*, 73: 566-76.
Dehmelt, L., and S. Halpain. 2005. 'The MAP2/Tau family of microtubule-associated proteins', *Genome Biol*, 6: 204.
Desai, A., and T. J. Mitchison. 1997. 'Microtubule polymerization dynamics', *Annu Rev Cell Dev Biol*, 13: 83-117.
Dietrich, K. A., C. V. Sindelar, P. D. Brewer, K. H. Downing, C. R. Cremo, and S. E. Rice. 2008. 'The kinesin-1 motor protein is regulated by a direct interaction of its head and tail', *Proc Natl Acad Sci U S A*, 105: 8938-43.
Dillman, J. F., 3rd, L. P. Dabney, and K. K. Pfister. 1996. 'Cytoplasmic dynein is associated with slow axonal transport', *Proc Natl Acad Sci U S A*, 93: 141-4.
Dixit, R., J. L. Ross, Y. E. Goldman, and E. L. Holzbaur. 2008. 'Differential regulation of dynein and kinesin motor proteins by tau', *Science*, 319: 1086-9.
Donato, A., K. Kagias, Y. Zhang, and M. A. Hilliard. 2019. 'Neuronal sub-compartmentalization: a strategy to optimize neuronal function', *Biol Rev Camb Philos Soc*, 94: 1023-37.
Eccles, J. C. 1966. 'The ionic mechanisms of excitatory and inhibitory synaptic action', *Ann N Y Acad Sci*, 137: 473-94.
Eva P. Karasmanis, Cat-Thi Phan, Dimitrios Angelis, Ilona A. Kesisova, Casper C. Hoogenraad, Richard J. McKenney, Elias T. Spiliotis. 2018. 'Polarity of Neuronal Membrane Traffic Requires Sorting of Kinesin Motor Cargo during Entry into Dendrites by a Microtubule-Associated Septin', *Developmental Cell*, 46: 204-18.
Fourniol, F. J., C. V. Sindelar, B. Amigues, D. K. Clare, G. Thomas, M. Perderiset, F. Francis, A. Houdusse, and C. A. Moores. 2010. 'Template-free 13-protofilament microtubule-MAP assembly visualized at 8 A resolution', *J Cell Biol*, 191: 463-70.
Gale, S. A., D. Acar, and K. R. Daffner. 2018. 'Dementia', *Am J Med*.
Ghosh, A., D. L. Sherman, and P. J. Brophy. 2018. 'The Axonal Cytoskeleton and the Assembly of Nodes of Ranvier', *Neuroscientist*, 24: 104-10.
Ghosh-Roy, A., A. Goncharov, Y. Jin, and A. D. Chisholm. 2012. 'Kinesin-13 and tubulin posttranslational modifications regulate microtubule growth in axon regeneration', *Dev Cell*, 23: 716-28.
Ginsburg, A., A. Shemesh, A. Millgram, R. Dharan, Y. Levi-Kalisman, I. Ringel, and U. Raviv. 2017. 'Structure of Dynamic, Taxol-Stabilized, and GMPPCP-Stabilized Microtubule', *J Phys Chem B*, 121: 8427-36.
Goedert, M., B. Ghetti, and M. G. Spillantini. 2000. 'Tau gene mutations in frontotemporal dementia and parkinsonism linked to chromosome 17 (FTDP-17).

Their relevance for understanding the neurogenerative process', *Ann N Y Acad Sci*, 920: 74-83.
Goedert, M., and R. Jakes. 1990. 'Expression of separate isoforms of human tau protein: correlation with the tau pattern in brain and effects on tubulin polymerization', *EMBO J*, 9: 4225-30.
Goedert, M., and M. G. Spillantini. 2000. 'Tau mutations in frontotemporal dementia FTDP-17 and their relevance for Alzheimer's disease', *Biochim Biophys Acta*, 1502: 110-21.
Goetzl, E. J., D. Kapogiannis, J. B. Schwartz, I. V. Lobach, L. Goetzl, E. L. Abner, G. A. Jicha, A. M. Karydas, A. Boxer, and B. L. Miller. 2016. 'Decreased synaptic proteins in neuronal exosomes of frontotemporal dementia and Alzheimer's disease', *FASEB J*, 30: 4141-48.
Gramlich, M. W., L. Conway, W. H. Liang, J. A. Labastide, S. J. King, J. Xu, and J. L. Ross. 2017. 'Single Molecule Investigation of Kinesin-1 Motility Using Engineered Microtubule Defects', *Sci Rep*, 7: 44290.
Gross, G. W., and L. M. Beidler. 1975. 'A quantitative analysis of isotope concentration profiles and rapid transport velocities in the C-fibers of the garfish olfactory nerve', *J Neurobiol*, 6: 213-32.
Gumy, L. F., D. J. Chew, E. Tortosa, E. A. Katrukha, L. C. Kapitein, A. M. Tolkovsky, C. C. Hoogenraad, and J. W. Fawcett. 2013. 'The kinesin-2 family member KIF3C regulates microtubule dynamics and is required for axon growth and regeneration', *J Neurosci*, 33: 11329-45.
Gumy, L. F., E. A. Katrukha, I. Grigoriev, D. Jaarsma, L. C. Kapitein, A. Akhmanova, and C. C. Hoogenraad. 2017. 'MAP2 Defines a Pre-axonal Filtering Zone to Regulate KIF1- versus KIF5-Dependent Cargo Transport in Sensory Neurons', *Neuron*, 94: 347-62 e7.
Hall, D. H., and E. M. Hedgecock. 1991. 'Kinesin-related gene unc-104 is required for axonal transport of synaptic vesicles in C. elegans', *Cell*, 65: 837-47.
Hammond, J. W., T. L. Blasius, V. Soppina, D. Cai, and K. J. Verhey. 2010. 'Autoinhibition of the kinesin-2 motor KIF17 via dual intramolecular mechanisms', *J Cell Biol*, 189: 1013-25.
Hammond, J. W., D. Cai, T. L. Blasius, Z. Li, Y. Jiang, G. T. Jih, E. Meyhofer, and K. J. Verhey. 2009. 'Mammalian Kinesin-3 motors are dimeric in vivo and move by processive motility upon release of autoinhibition', *PLoS Biol*, 7: e72.
Hammond, J. W., C. F. Huang, S. Kaech, C. Jacobson, G. Banker, and K. J. Verhey. 2010. 'Posttranslational modifications of tubulin and the polarized transport of kinesin-1 in neurons', *Mol Biol Cell*, 21: 572-83.
Harada, A., K. Oguchi, S. Okabe, J. Kuno, S. Terada, T. Ohshima, R. Sato-Yoshitake, Y. Takei, T. Noda, and N. Hirokawa. 1994. 'Altered microtubule organization in small-calibre axons of mice lacking tau protein', *Nature*, 369: 488-91.
Harada, A., J. Teng, Y. Takei, K. Oguchi, and N. Hirokawa. 2002. 'MAP2 is required for dendrite elongation, PKA anchoring in dendrites, and proper PKA signal transduction', *J Cell Biol*, 158: 541-9.

Hendricks, A. G., E. Perlson, J. L. Ross, H. W. Schroeder, 3rd, M. Tokito, and E. L. Holzbaur. 2010. 'Motor coordination via a tug-of-war mechanism drives bidirectional vesicle transport', *Curr Biol*, 20: 697-702.

Hinrichs, M. H., A. Jalal, B. Brenner, E. Mandelkow, S. Kumar, and T. Scholz. 2012. 'Tau protein diffuses along the microtubule lattice', *J Biol Chem*, 287: 38559-68.

Hirokawa, N., R. Nitta, and Y. Okada. 2009. 'The mechanisms of kinesin motor motility: lessons from the monomeric motor KIF1A', *Nat Rev Mol Cell Biol*, 10: 877-84.

Hirokawa, N., S. Niwa, and Y. Tanaka. 2010. 'Molecular motors in neurons: transport mechanisms and roles in brain function, development, and disease', *Neuron*, 68: 610-38.

Hirokawa, N., R. Sato-Yoshitake, N. Kobayashi, K. K. Pfister, G. S. Bloom, and S. T. Brady. 1991. 'Kinesin associates with anterogradely transported membranous organelles in vivo', *J Cell Biol*, 114: 295-302.

Hirokawa, N., R. Sato-Yoshitake, T. Yoshida, and T. Kawashima. 1990. 'Brain dynein (MAP1C) localizes on both anterogradely and retrogradely transported membranous organelles in vivo', *J Cell Biol*, 111: 1027-37.

Hirokawa, N., and Y. Tanaka. 2015. 'Kinesin superfamily proteins (KIFs): Various functions and their relevance for important phenomena in life and diseases', *Exp Cell Res*, 334: 16-25.

Hoeprich, G. J., K. J. Mickolajczyk, S. R. Nelson, W. O. Hancock, and C. L. Berger. 2017. 'The axonal transport motor kinesin-2 navigates microtubule obstacles via protofilament switching', *Traffic*, 18: 304-14.

Hoeprich, G. J., A. R. Thompson, D. P. McVicker, W. O. Hancock, and C. L. Berger. 2014. 'Kinesin's neck-linker determines its ability to navigate obstacles on the microtubule surface', *Biophys J*, 106: 1691-700.

Hollenbeck, P. J., and W. M. Saxton. 2005. 'The axonal transport of mitochondria', *J Cell Sci*, 118: 5411-9.

Hong, M., V. Zhukareva, V. Vogelsberg-Ragaglia, Z. Wszolek, L. Reed, B. I. Miller, D. H. Geschwind, T. D. Bird, D. McKeel, A. Goate, J. C. Morris, K. C. Wilhelmsen, G. D. Schellenberg, J. Q. Trojanowski, and V. M. Lee. 1998. 'Mutation-specific functional impairments in distinct tau isoforms of hereditary FTDP-17', *Science*, 282: 1914-7.

Horton, A. C., B. Racz, E. E. Monson, A. L. Lin, R. J. Weinberg, and M. D. Ehlers. 2005. 'Polarized secretory trafficking directs cargo for asymmetric dendrite growth and morphogenesis', *Neuron*, 48: 757-71.

Hotta, T., S. Fujita, S. Uchimura, M. Noguchi, T. Demura, E. Muto, and T. Hashimoto. 2016. 'Affinity Purification and Characterization of Functional Tubulin from Cell Suspension Cultures of Arabidopsis and Tobacco', *Plant Physiol*, 170: 1189-205.

Huey, E. D., K. T. Putnam, and J. Grafman. 2006. 'A systematic review of neurotransmitter deficits and treatments in frontotemporal dementia', *Neurology*, 66: 17-22.

Hung, C. O., and M. P. Coleman. 2016. 'KIF1A mediates axonal transport of BACE1 and identification of independently moving cargoes in living SCG neurons', *Traffic*, 17: 1155-67.

Hutton, M., C. L. Lendon, P. Rizzu, M. Baker, S. Froelich, H. Houlden, S. Pickering-Brown, S. Chakraverty, A. Isaacs, A. Grover, J. Hackett, J. Adamson, S. Lincoln, D. Dickson, P. Davies, R. C. Petersen, M. Stevens, E. de Graaff, E. Wauters, J. van Baren, M. Hillebrand, M. Joosse, J. M. Kwon, P. Nowotny, L. K. Che, J. Norton, J. C. Morris, L. A. Reed, J. Trojanowski, H. Basun, L. Lannfelt, M. Neystat, S. Fahn, F. Dark, T. Tannenberg, P. R. Dodd, N. Hayward, J. B. Kwok, P. R. Schofield, A. Andreadis, J. Snowden, D. Craufurd, D. Neary, F. Owen, B. A. Oostra, J. Hardy, A. Goate, J. van Swieten, D. Mann, T. Lynch, and P. Heutink. 1998. 'Association of missense and 5'-splice-site mutations in tau with the inherited dementia FTDP-17', *Nature*, 393: 702-5.

Huxley, A. F., and R. Stampfli. 1949. 'Evidence for saltatory conduction in peripheral myelinated nerve fibres', *J Physiol*, 108: 315-39.

Hyman, A. A., D. Chretien, I. Arnal, and R. H. Wade. 1995. 'Structural changes accompanying GTP hydrolysis in microtubules: information from a slowly hydrolyzable analogue guanylyl-(alpha,beta)-methylene-diphosphonate', *J Cell Biol*, 128: 117-25.

Ikegami, K., R. L. Heier, M. Taruishi, H. Takagi, M. Mukai, S. Shimma, S. Taira, K. Hatanaka, N. Morone, I. Yao, P. K. Campbell, S. Yuasa, C. Janke, G. R. Macgregor, and M. Setou. 2007. 'Loss of alpha-tubulin polyglutamylation in ROSA22 mice is associated with abnormal targeting of KIF1A and modulated synaptic function', *Proc Natl Acad Sci U S A*, 104: 3213-8.

Ikegami, K., M. Mukai, J. Tsuchida, R. L. Heier, G. R. Macgregor, and M. Setou. 2006. 'TTLL7 is a mammalian beta-tubulin polyglutamylase required for growth of MAP2-positive neurites', *J Biol Chem*, 281: 30707-16.

Iovino, M., R. Patani, C. Watts, S. Chandran, and M. G. Spillantini. 2010. 'Human stem cell-derived neurons: a system to study human tau function and dysfunction', *PLoS One*, 5: e13947.

Iqbal, K., F. Liu, C. X. Gong, and I. Grundke-Iqbal. 2010. 'Tau in Alzheimer disease and related tauopathies', *Curr Alzheimer Res*, 7: 656-64.

Ittner, L. M., T. Fath, Y. D. Ke, M. Bi, J. van Eersel, K. M. Li, P. Gunning, and J. Gotz. 2008. 'Parkinsonism and impaired axonal transport in a mouse model of frontotemporal dementia', *Proc Natl Acad Sci U S A*, 105: 15997-6002.

Janke, C. 2014. 'The tubulin code: molecular components, readout mechanisms, and functions', *J Cell Biol*, 206: 461-72.

Janke, C., and M. Kneussel. 2010. 'Tubulin post-translational modifications: encoding functions on the neuronal microtubule cytoskeleton', *Trends Neurosci*, 33: 362-72.

Janke, C., and G. Montagnac. 2017. 'Causes and Consequences of Microtubule Acetylation', *Curr Biol*, 27: R1287-R92.

Janke, C., K. Rogowski, and J. van Dijk. 2008. 'Polyglutamylation: a fine-regulator of protein function? 'Protein Modifications: beyond the usual suspects' review series', *EMBO Rep*, 9: 636-41.

Janke, C., K. Rogowski, D. Wloga, C. Regnard, A. V. Kajava, J. M. Strub, N. Temurak, J. van Dijk, D. Boucher, A. van Dorsselaer, S. Suryavanshi, J. Gaertig, and B.

Edde. 2005. 'Tubulin polyglutamylase enzymes are members of the TTL domain protein family', *Science*, 308: 1758-62.
Kaeser, P. S., and W. G. Regehr. 2017. 'The readily releasable pool of synaptic vesicles', *Curr Opin Neurobiol*, 43: 63-70.
Kalil, K., and E. W. Dent. 2014. 'Branch management: mechanisms of axon branching in the developing vertebrate CNS', *Nat Rev Neurosci*, 15: 7-18.
Kamal, A., G. B. Stokin, Z. Yang, C. H. Xia, and L. S. Goldstein. 2000. 'Axonal transport of amyloid precursor protein is mediated by direct binding to the kinesin light chain subunit of kinesin-I', *Neuron*, 28: 449-59.
Kanaan, N. M., G. A. Morfini, N. E. LaPointe, G. F. Pigino, K. R. Patterson, Y. Song, A. Andreadis, Y. Fu, S. T. Brady, and L. I. Binder. 2011. 'Pathogenic forms of tau inhibit kinesin-dependent axonal transport through a mechanism involving activation of axonal phosphotransferases', *J Neurosci*, 31: 9858-68.
Kanai, Y., Y. Okada, Y. Tanaka, A. Harada, S. Terada, and N. Hirokawa. 2000. 'KIF5C, a novel neuronal kinesin enriched in motor neurons', *J Neurosci*, 20: 6374-84.
Kandalepas, P. C., K. R. Sadleir, W. A. Eimer, J. Zhao, D. A. Nicholson, and R. Vassar. 2013. 'The Alzheimer's beta-secretase BACE1 localizes to normal presynaptic terminals and to dystrophic presynaptic terminals surrounding amyloid plaques', *Acta Neuropathol*, 126: 329-52.
Kar, A., D. Kuo, R. He, J. Zhou, and J. Y. Wu. 2005. 'Tau alternative splicing and frontotemporal dementia', *Alzheimer Dis Assoc Disord*, 19 Suppl 1: S29-36.
Karasmanis, E. P., C. T. Phan, D. Angelis, I. A. Kesisova, C. C. Hoogenraad, R. J. McKenney, and E. T. Spiliotis. 2018. 'Polarity of Neuronal Membrane Traffic Requires Sorting of Kinesin Motor Cargo during Entry into Dendrites by a Microtubule-Associated Septin', *Dev Cell*, 46: 518-24.
Kellogg, E. H., N. M. A. Hejab, S. Poepsel, K. H. Downing, F. DiMaio, and E. Nogales. 2018. 'Near-atomic model of microtubule-tau interactions', *Science*, 360: 1242-46.
Kern, J. V., Y. V. Zhang, S. Kramer, J. E. Brenman, and T. M. Rasse. 2013. 'The kinesin-3, unc-104 regulates dendrite morphogenesis and synaptic development in Drosophila', *Genetics*, 195: 59-72.
Kikkawa, M., Y. Okada, and N. Hirokawa. 2000. '15 A resolution model of the monomeric kinesin motor, KIF1A', *Cell*, 100: 241-52.
Kim, E., and H. Jung. 2015. 'Local protein synthesis in neuronal axons: why and how we study', *BMB Rep*, 48: 139-46.
Kirkpatrick, J. B., L. Hyams, V. L. Thomas, and P. M. Howley. 1970. 'Purification of intact microtubules from brain', *J Cell Biol*, 47: 384-94.
Klebe, S., A. Lossos, H. Azzedine, E. Mundwiller, R. Sheffer, M. Gaussen, C. Marelli, M. Nawara, W. Carpentier, V. Meyer, A. Rastetter, E. Martin, D. Bouteiller, L. Orlando, G. Gyapay, K. H. El-Hachimi, B. Zimmerman, M. Gamliel, A. Misk, I. Lerer, A. Brice, A. Durr, and G. Stevanin. 2012. 'KIF1A missense mutations in SPG30, an autosomal recessive spastic paraplegia: distinct phenotypes according to the nature of the mutations', *Eur J Hum Genet*, 20: 645-9.
Kneynsberg, A., B. Combs, K. Christensen, G. Morfini, and N. M. Kanaan. 2017. 'Axonal Degeneration in Tauopathies: Disease Relevance and Underlying Mechanisms', *Front Neurosci*, 11: 572.

Knipling, L., J. Hwang, and J. Wolff. 1999. 'Preparation and properties of pure tubulin S', *Cell Motil Cytoskeleton*, 43: 63-71.
Kojima, H., E. Muto, H. Higuchi, and T. Yanagida. 1997. 'Mechanics of single kinesin molecules measured by optical trapping nanometry', *Biophys J*, 73: 2012-22.
Kondo, M., Y. Takei, and N. Hirokawa. 2012. 'Motor protein KIF1A is essential for hippocampal synaptogenesis and learning enhancement in an enriched environment', *Neuron*, 73: 743-57.
Kopeikina, K. J., G. A. Carlson, R. Pitstick, A. E. Ludvigson, A. Peters, J. I. Luebke, R. M. Koffie, M. P. Frosch, B. T. Hyman, and T. L. Spires-Jones. 2011. 'Tau accumulation causes mitochondrial distribution deficits in neurons in a mouse model of tauopathy and in human Alzheimer's disease brain', *Am J Pathol*, 179: 2071-82.
Kopeikina, K. J., B. T. Hyman, and T. L. Spires-Jones. 2012. 'Soluble forms of tau are toxic in Alzheimer's disease', *Transl Neurosci*, 3: 223-33.
L'Hernault, S. W., and J. L. Rosenbaum. 1985. 'Chlamydomonas alpha-tubulin is posttranslationally modified by acetylation on the epsilon-amino group of a lysine', *Biochemistry*, 24: 473-8.
Lacovich, V., S. L. Espindola, M. Alloatti, V. Pozo Devoto, L. E. Cromberg, M. E. Carna, G. Forte, J. M. Gallo, L. Bruno, G. B. Stokin, M. E. Avale, and T. L. Falzone. 2017. 'Tau Isoforms Imbalance Impairs the Axonal Transport of the Amyloid Precursor Protein in Human Neurons', *J Neurosci*, 37: 58-69.
Lacroix, B., and C. Janke. 2011. 'Generation of differentially polyglutamylated microtubules', *Methods Mol Biol*, 777: 57-69.
Lacroix, B., J. van Dijk, N. D. Gold, J. Guizetti, G. Aldrian-Herrada, K. Rogowski, D. W. Gerlich, and C. Janke. 2010. 'Tubulin polyglutamylation stimulates spastin-mediated microtubule severing', *J Cell Biol*, 189: 945-54.
Larcher, J. C., D. Boucher, S. Lazereg, F. Gros, and P. Denoulet. 1996. 'Interaction of kinesin motor domains with alpha- and beta-tubulin subunits at a tau-independent binding site. Regulation by polyglutamylation', *J Biol Chem*, 271: 22117-24.
Lasser, M., J. Tiber, and L. A. Lowery. 2018. 'The Role of the Microtubule Cytoskeleton in Neurodevelopmental Disorders', *Front Cell Neurosci*, 12: 165.
Lassmann, H., R. Weiler, P. Fischer, C. Bancher, K. Jellinger, E. Floor, W. Danielczyk, F. Seitelberger, and H. Winkler. 1992. 'Synaptic pathology in Alzheimer's disease: immunological data for markers of synaptic and large dense-core vesicles', *Neuroscience*, 46: 1-8.
Lee, J. R., H. Shin, J. Ko, J. Choi, H. Lee, and E. Kim. 2003. 'Characterization of the movement of the kinesin motor KIF1A in living cultured neurons', *J Biol Chem*, 278: 2624-9.
Lee, J. R., M. Srour, D. Kim, F. F. Hamdan, S. H. Lim, C. Brunel-Guitton, J. C. Decarie, E. Rossignol, G. A. Mitchell, A. Schreiber, R. Moran, K. Van Haren, R. Richardson, J. Nicolai, K. M. Oberndorff, J. D. Wagner, K. M. Boycott, E. Rahikkala, N. Junna, H. Tyynismaa, I. Cuppen, N. E. Verbeek, C. T. Stumpel, M. A. Willemsen, S. A. de Munnik, G. A. Rouleau, E. Kim, E. J. Kamsteeg, T. Kleefstra, and J. L. Michaud. 2015. 'De novo mutations in the motor domain of

KIF1A cause cognitive impairment, spastic paraparesis, axonal neuropathy, and cerebellar atrophy', *Hum Mutat*, 36: 69-78.
Lessard, D. V., O. J. Zinder, T. Hotta, K. J. Verhey, R. Ohi, and C. L. Berger. 2019. 'Polyglutamylation of tubulin's C-terminal tail controls pausing and motility of kinesin-3 family member KIF1A', *J Biol Chem*, 294: 6353-63.
Lipka, J., L. C. Kapitein, J. Jaworski, and C. C. Hoogenraad. 2016. 'Microtubule-binding protein doublecortin-like kinase 1 (DCLK1) guides kinesin-3-mediated cargo transport to dendrites', *EMBO J*, 35: 302-18.
Lo, K. Y., A. Kuzmin, S. M. Unger, J. D. Petersen, and M. A. Silverman. 2011. 'KIF1A is the primary anterograde motor protein required for the axonal transport of dense-core vesicles in cultured hippocampal neurons', *Neurosci Lett*, 491: 168-73.
Lodish H, Berk A, Zipursky SL, et al. 2000. *Molecular Cell Biology* (W.H. Freeman: New York).
MacNeal, R. K., and D. L. Purich. 1978. 'Stoichiometry and role of GTP hydrolysis in bovine neurotubule assembly', *J Biol Chem*, 253: 4683-7.
Maday, S., A. E. Twelvetrees, A. J. Moughamian, and E. L. Holzbaur. 2014. 'Axonal transport: cargo-specific mechanisms of motility and regulation', *Neuron*, 84: 292-309.
Maday, S., K. E. Wallace, and E. L. Holzbaur. 2012. 'Autophagosomes initiate distally and mature during transport toward the cell soma in primary neurons', *J Cell Biol*, 196: 407-17.
Magiera, M. M., S. Bodakuntla, J. Ziak, S. Lacomme, P. Marques Sousa, S. Leboucher, T. J. Hausrat, C. Bosc, A. Andrieux, M. Kneussel, M. Landry, A. Calas, M. Balastik, and C. Janke. 2018. 'Excessive tubulin polyglutamylation causes neurodegeneration and perturbs neuronal transport', *EMBO J*, 37.
Magiera, M. M., P. Singh, S. Gadadhar, and C. Janke. 2018. 'Tubulin Posttranslational Modifications and Emerging Links to Human Disease', *Cell*, 173: 1323-27.
Majid, T., Y. O. Ali, D. V. Venkitaramani, M. K. Jang, H. C. Lu, and R. G. Pautler. 2014. 'In vivo axonal transport deficits in a mouse model of fronto-temporal dementia', *Neuroimage Clin*, 4: 711-7.
Mandelkow, E. M., K. Stamer, R. Vogel, E. Thies, and E. Mandelkow. 2003. 'Clogging of axons by tau, inhibition of axonal traffic and starvation of synapses', *Neurobiol Aging*, 24: 1079-85.
Marcos, S., J. Moreau, S. Backer, D. Job, A. Andrieux, and E. Bloch-Gallego. 2009. 'Tubulin tyrosination is required for the proper organization and pathfinding of the growth cone', *PLoS One*, 4: e5405.
Mary, J., V. Redeker, J. P. Le Caer, J. Rossier, and J. M. Schmitter. 1996. 'Posttranslational modifications in the C-terminal tail of axonemal tubulin from sea urchin sperm', *J Biol Chem*, 271: 9928-33.
McEwen, B. S., and B. Grafstein. 1968. 'Fast and slow components in axonal transport of protein', *J Cell Biol*, 38: 494-508.
McVicker, D. P., L. R. Chrin, and C. L. Berger. 2011. 'The nucleotide-binding state of microtubules modulates kinesin processivity and the ability of Tau to inhibit kinesin-mediated transport', *J Biol Chem*, 286: 42873-80.

McVicker, D. P., G. J. Hoeprich, A. R. Thompson, and C. L. Berger. 2014. 'Tau interconverts between diffusive and stable populations on the microtubule surface in an isoform and lattice specific manner', *Cytoskeleton (Hoboken)*, 71: 184-94.
Medeiros, R., D. Baglietto-Vargas, and F. M. LaFerla. 2011. 'The role of tau in Alzheimer's disease and related disorders', *CNS Neurosci Ther*, 17: 514-24.
Mennerick, S., and C. F. Zorumski. 1994. 'Glial contributions to excitatory neurotransmission in cultured hippocampal cells', *Nature*, 368: 59-62.
Miki, H., M. Setou, K. Kaneshiro, and N. Hirokawa. 2001. 'All kinesin superfamily protein, KIF, genes in mouse and human', *Proc Natl Acad Sci U S A*, 98: 7004-11.
Minoura, I. 2017. 'Towards an understanding of the isotype-specific functions of tubulin in neurons: Technical advances in tubulin expression and purification', *Neurosci Res*, 122: 1-8.
Mitchison, T., and M. Kirschner. 1984. 'Dynamic instability of microtubule growth', *Nature*, 312: 237-42.
Mohan, R., and A. John. 2015. 'Microtubule-associated proteins as direct crosslinkers of actin filaments and microtubules', *IUBMB Life*, 67: 395-403.
Monroy, B. Y., D. L. Sawyer, B. E. Ackermann, M. M. Borden, T. C. Tan, and K. M. Ori-McKenney. 2018. 'Competition between microtubule-associated proteins directs motor transport', *Nat Commun*, 9: 1487.
Mukai, M., K. Ikegami, Y. Sugiura, K. Takeshita, A. Nakagawa, and M. Setou. 2009. 'Recombinant mammalian tubulin polyglutamylase TTLL7 performs both initiation and elongation of polyglutamylation on beta-tubulin through a random sequential pathway', *Biochemistry*, 48: 1084-93.
Muller, M. J., S. Klumpp, and R. Lipowsky. 2008. 'Tug-of-war as a cooperative mechanism for bidirectional cargo transport by molecular motors', *Proc Natl Acad Sci U S A*, 105: 4609-14.
Nitta, R., M. Kikkawa, Y. Okada, and N. Hirokawa. 2004. 'KIF1A alternately uses two loops to bind microtubules', *Science*, 305: 678-83.
Niwa, S., D. M. Lipton, M. Morikawa, C. Zhao, N. Hirokawa, H. Lu, and K. Shen. 2016. 'Autoinhibition of a Neuronal Kinesin UNC-104/KIF1A Regulates the Size and Density of Synapses', *Cell Rep*, 16: 2129-41.
Niwa, S., Y. Tanaka, and N. Hirokawa. 2008. 'KIF1Bbeta- and KIF1A-mediated axonal transport of presynaptic regulator Rab3 occurs in a GTP-dependent manner through DENN/MADD', *Nat Cell Biol*, 10: 1269-79.
Nobili, A., E. C. Latagliata, M. T. Viscomi, V. Cavallucci, D. Cutuli, G. Giacovazzo, P. Krashia, F. R. Rizzo, R. Marino, M. Federici, P. De Bartolo, D. Aversa, M. C. Dell'Acqua, A. Cordella, M. Sancandi, F. Keller, L. Petrosini, S. Puglisi-Allegra, N. B. Mercuri, R. Coccurello, N. Berretta, and M. D'Amelio. 2017. 'Dopamine neuronal loss contributes to memory and reward dysfunction in a model of Alzheimer's disease', *Nat Commun*, 8: 14727.
Nogales, E., S. G. Wolf, and K. H. Downing. 1998. 'Structure of the alpha beta tubulin dimer by electron crystallography', *Nature*, 391: 199-203.
Ohba, C., K. Haginoya, H. Osaka, K. Kubota, A. Ishiyama, T. Hiraide, H. Komaki, M. Sasaki, S. Miyatake, M. Nakashima, Y. Tsurusaki, N. Miyake, F. Tanaka, H. Saitsu, and N. Matsumoto. 2015. 'De novo KIF1A mutations cause intellectual

deficit, cerebellar atrophy, lower limb spasticity and visual disturbance', *J Hum Genet*, 60: 739-42.
Okada, Y., and N. Hirokawa. 1999. 'A processive single-headed motor: kinesin superfamily protein KIF1A', *Science*, 283: 1152-7.
Okada, Y., and N. Hirokawa. 2000. 'Mechanism of the single-headed processivity: diffusional anchoring between the K-loop of kinesin and the C terminus of tubulin', *Proc Natl Acad Sci U S A*, 97: 640-5.
Okada, Y., H. Yamazaki, Y. Sekine-Aizawa, and N. Hirokawa. 1995. 'The neuron-specific kinesin superfamily protein KIF1A is a unique monomeric motor for anterograde axonal transport of synaptic vesicle precursors', *Cell*, 81: 769-80.
Oriola, D., and J. Casademunt. 2013. 'Cooperative force generation of KIF1A Brownian motors', *Phys Rev Lett*, 111: 048103.
Ovsepian, S. V. 2017. 'The birth of the synapse', *Brain Struct Funct*, 222: 3369-74.
Padzik, A., P. Deshpande, P. Hollos, M. Franker, E. H. Rannikko, D. Cai, P. Prus, M. Magard, N. Westerlund, K. J. Verhey, P. James, C. C. Hoogenraad, and E. T. Coffey. 2016. 'KIF5C S176 Phosphorylation Regulates Microtubule Binding and Transport Efficiency in Mammalian Neurons', *Front Cell Neurosci*, 10: 57.
Paturle-Lafanechere, L., M. Manier, N. Trigault, F. Pirollet, H. Mazarguil, and D. Job. 1994. 'Accumulation of delta 2-tubulin, a major tubulin variant that cannot be tyrosinated, in neuronal tissues and in stable microtubule assemblies', *J Cell Sci*, 107 (Pt 6): 1529-43.
Peichl, L., and H. Wassle. 1983. 'The structural correlate of the receptive field centre of alpha ganglion cells in the cat retina', *J Physiol*, 341: 309-24.
Pfrieger, F. W., and B. A. Barres. 1996. 'New views on synapse-glia interactions', *Curr Opin Neurobiol*, 6: 615-21.
Pfrieger, F. W., and B. A. Barres. 1997. 'Synaptic efficacy enhanced by glial cells in vitro', *Science*, 277: 1684-7.
Phillips, R. K., L. G. Peter, S. P. Gilbert, and I. Rayment. 2016. 'Family-specific Kinesin Structures Reveal Neck-linker Length Based on Initiation of the Coiled-coil', *J Biol Chem*, 291: 20372-86.
Price, R. L., P. Paggi, R. J. Lasek, and M. J. Katz. 1988. 'Neurofilaments are spaced randomly in the radial dimension of axons', *J Neurocytol*, 17: 55-62.
Quarles, Pierre Morell and Richard H. 1999. 'Myelin Formation, Structure and Biochemistry.' in George J Siegel (ed.), *Basic Neurochemistry: Molecular, Cellular and Medical Aspects. 6th edition.* (Lippincott-Raven: Philadelphia).
Ray, K., S. E. Perez, Z. Yang, J. Xu, B. W. Ritchings, H. Steller, and L. S. Goldstein. 1999. 'Kinesin-II is required for axonal transport of choline acetyltransferase in Drosophila', *J Cell Biol*, 147: 507-18.
Reck-Peterson, S. L., W. B. Redwine, R. D. Vale, and A. P. Carter. 2018. 'The cytoplasmic dynein transport machinery and its many cargoes', *Nat Rev Mol Cell Biol*, 19: 382-98.
Regnard, C., E. Desbruyeres, P. Denoulet, and B. Edde. 1999. 'Tubulin polyglutamylase: isozymic variants and regulation during the cell cycle in HeLa cells', *J Cell Sci*, 112 (Pt 23): 4281-9.

Rodriguez-Martin, T., A. M. Pooler, D. H. Lau, G. M. Morotz, K. J. De Vos, J. Gilley, M. P. Coleman, and D. P. Hanger. 2016. 'Reduced number of axonal mitochondria and tau hypophosphorylation in mouse P301L tau knockin neurons', *Neurobiol Dis*, 85: 1-10.
Roy, S. 2014. 'Seeing the unseen: the hidden world of slow axonal transport', *Neuroscientist*, 20: 71-81.
Schnapp, B. J., and T. S. Reese. 1982. 'Cytoplasmic structure in rapid-frozen axons', *J Cell Biol*, 94: 667-9.
Schnapp, B. J., and T. S. Reese. 1989. 'Dynein is the motor for retrograde axonal transport of organelles', *Proc Natl Acad Sci U S A*, 86: 1548-52.
Schnitzer, M. J., and S. M. Block. 1997. 'Kinesin hydrolyses one ATP per 8-nm step', *Nature*, 388: 386-90.
Schoch, K. M., S. L. DeVos, R. L. Miller, S. J. Chun, M. Norrbom, D. F. Wozniak, H. N. Dawson, C. F. Bennett, F. Rigo, and T. M. Miller. 2016. 'Increased 4R-Tau Induces Pathological Changes in a Human-Tau Mouse Model', *Neuron*, 90: 941-7.
Scholey, J. M. 2012. 'Kinesin-2 motors transport IFT-particles, dyneins and tubulin subunits to the tips of Caenorhabditis elegans sensory cilia: relevance to vision research?', *Vision Res*, 75: 44-52.
Shah, J. V., and D. W. Cleveland. 2002. 'Slow axonal transport: fast motors in the slow lane', *Curr Opin Cell Biol*, 14: 58-62.
Shastry, S., and W. O. Hancock. 2010. 'Neck linker length determines the degree of processivity in kinesin-1 and kinesin-2 motors', *Curr Biol*, 20: 939-43.
Shaw, B. H. 1913. 'The Interneuronic Synapse in Disease', *Br Med J*, 1: 989-91.
Shin, H., M. Wyszynski, K. H. Huh, J. G. Valtschanoff, J. R. Lee, J. Ko, M. Streuli, R. J. Weinberg, M. Sheng, and E. Kim. 2003. 'Association of the kinesin motor KIF1A with the multimodular protein liprin-alpha', *J Biol Chem*, 278: 11393-401.
Shipley, M. M., C. A. Mangold, and M. L. Szpara. 2016. 'Differentiation of the SH-SY5Y Human Neuroblastoma Cell Line', *J Vis Exp*: 53193.
Siddiqui, N., and A. Straube. 2017. 'Intracellular Cargo Transport by Kinesin-3 Motors', *Biochemistry (Mosc)*, 82: 803-15.
Simons, M., and K. A. Nave. 2015. 'Oligodendrocytes: Myelination and Axonal Support', *Cold Spring Harb Perspect Biol*, 8: a020479.
Sirajuddin, M., L. M. Rice, and R. D. Vale. 2014. 'Regulation of microtubule motors by tubulin isotypes and post-translational modifications', *Nat Cell Biol*, 16: 335-44.
Soppina, V., S. R. Norris, A. S. Dizaji, M. Kortus, S. Veatch, M. Peckham, and K. J. Verhey. 2014. 'Dimerization of mammalian kinesin-3 motors results in superprocessive motion', *Proc Natl Acad Sci U S A*, 111: 5562-7.
Soppina, V., and K. J. Verhey. 2014. 'The family-specific K-loop influences the microtubule on-rate but not the superprocessivity of kinesin-3 motors', *Mol Biol Cell*, 25: 2161-70.
Spiegelman, B. M., S. M. Penningroth, and M. W. Kirschner. 1977. 'Turnover of tubulin and the N site GTP in Chinese hamster ovary cells', *Cell*, 12: 587-600.
Spillantini, M. G., and M. Goedert. 2001. 'Tau gene mutations and tau pathology in frontotemporal dementia and parkinsonism linked to chromosome 17', *Adv Exp Med Biol*, 487: 21-37.

Stavoe, A. K., S. E. Hill, D. H. Hall, and D. A. Colon-Ramos. 2016. 'KIF1A/UNC-104 Transports ATG-9 to Regulate Neurodevelopment and Autophagy at Synapses', *Dev Cell*, 38: 171-85.

Stern, J. L., D. V. Lessard, G. J. Hoeprich, G. A. Morfini, and C. L. Berger. 2017. 'Phosphoregulation of Tau modulates inhibition of kinesin-1 motility', *Mol Biol Cell*, 28: 1079-87.

Sudhof, T. C. 1995. 'The synaptic vesicle cycle: a cascade of protein-protein interactions', *Nature*, 375: 645-53.

Sullivan, K. F., and D. W. Cleveland. 1986. 'Identification of conserved isotype-defining variable region sequences for four vertebrate beta tubulin polypeptide classes', *Proc Natl Acad Sci U S A*, 83: 4327-31.

Takeda, S., H. Yamazaki, D. H. Seog, Y. Kanai, S. Terada, and N. Hirokawa. 2000. 'Kinesin superfamily protein 3 (KIF3) motor transports fodrin-associating vesicles important for neurite building', *J Cell Biol*, 148: 1255-65.

Tan, R., A. J. Lam, T. Tan, J. Han, D. W. Nowakowski, M. Vershinin, S. Simo, K. M. Ori-McKenney, and R. J. McKenney. 2019. 'Microtubules gate tau condensation to spatially regulate microtubule functions', *Nat Cell Biol*, 21: 1078-85.

Tanaka, Y., Y. Kanai, Y. Okada, S. Nonaka, S. Takeda, A. Harada, and N. Hirokawa. 1998. 'Targeted disruption of mouse conventional kinesin heavy chain, kif5B, results in abnormal perinuclear clustering of mitochondria', *Cell*, 93: 1147-58.

Tanaka, Y., S. Niwa, M. Dong, A. Farkhondeh, L. Wang, R. Zhou, and N. Hirokawa. 2016. 'The Molecular Motor KIF1A Transports the TrkA Neurotrophin Receptor and Is Essential for Sensory Neuron Survival and Function', *Neuron*, 90: 1215-29.

Terenzio, M., G. Schiavo, and M. Fainzilber. 2017. 'Compartmentalized Signaling in Neurons: From Cell Biology to Neuroscience', *Neuron*, 96: 667-79.

Thompson, A. R., G. J. Hoeprich, and C. L. Berger. 2013. 'Single-molecule motility: statistical analysis and the effects of track length on quantification of processive motion', *Biophys J*, 104: 2651-61.

Tien, N. W., G. H. Wu, C. C. Hsu, C. Y. Chang, and O. I. Wagner. 2011. 'Tau/PTL-1 associates with kinesin-3 KIF1A/UNC-104 and affects the motor's motility characteristics in C. elegans neurons', *Neurobiol Dis*, 43: 495-506.

Tint, I., D. Jean, P. W. Baas, and M. M. Black. 2009. 'Doublecortin associates with microtubules preferentially in regions of the axon displaying actin-rich protrusive structures', *J Neurosci*, 29: 10995-1010.

Tomaselli, P. J., A. M. Rossor, A. Horga, M. Laura, J. C. Blake, H. Houlden, and M. M. Reilly. 2017. 'A de novo dominant mutation in KIF1A associated with axonal neuropathy, spasticity and autism spectrum disorder', *J Peripher Nerv Syst*, 22: 460-63.

Trybus, K. M. 2013. 'Intracellular transport: the causes for pauses', *Curr Biol*, 23: R623-5.

Tsacopoulos, M., and P. J. Magistretti. 1996. 'Metabolic coupling between glia and neurons', *J Neurosci*, 16: 877-85.

Tsai, J. W., W. N. Lian, S. Kemal, A. R. Kriegstein, and R. B. Vallee. 2010. 'Kinesin 3 and cytoplasmic dynein mediate interkinetic nuclear migration in neural stem cells', *Nat Neurosci*, 13: 1463-71.

Twelvetrees, A., A. G. Hendricks, and E. L. Holzbaur. 2012. 'SnapShot: axonal transport', *Cell*, 149: 950-50 e1.
Vale, R. D., and R. A. Milligan. 2000. 'The way things move: looking under the hood of molecular motor proteins', *Science*, 288: 88-95.
Vale, R. D., T. S. Reese, and M. P. Sheetz. 1985. 'Identification of a novel force-generating protein, kinesin, involved in microtubule-based motility', *Cell*, 42: 39-50.
Vale, R. D., B. J. Schnapp, T. Mitchison, E. Steuer, T. S. Reese, and M. P. Sheetz. 1985. 'Different axoplasmic proteins generate movement in opposite directions along microtubules in vitro', *Cell*, 43: 623-32.
Vallee, R. B., and G. S. Bloom. 1991. 'Mechanisms of fast and slow axonal transport', *Annu Rev Neurosci*, 14: 59-92.
van de Willige, D., C. C. Hoogenraad, and A. Akhmanova. 2016. 'Microtubule plus-end tracking proteins in neuronal development', *Cell Mol Life Sci*, 73: 2053-77.
van den Pol, A. N. 2012. 'Neuropeptide transmission in brain circuits', *Neuron*, 76: 98-115.
Verhey, K. J., and J. Gaertig. 2007. 'The tubulin code', *Cell Cycle*, 6: 2152-60.
Vershinin, M., B. C. Carter, D. S. Razafsky, S. J. King, and S. P. Gross. 2007. 'Multiple-motor based transport and its regulation by Tau', *Proc Natl Acad Sci U S A*, 104: 87-92.
Voelzmann, A., P. Okenve-Ramos, Y. Qu, M. Chojnowska-Monga, M. Del Cano-Espinel, A. Prokop, and N. Sanchez-Soriano. 2016. 'Tau and spectraplakins promote synapse formation and maintenance through Jun kinase and neuronal trafficking', *Elife*, 5.
Voter, W. A., and H. P. Erickson. 1984. 'The kinetics of microtubule assembly. Evidence for a two-stage nucleation mechanism', *J Biol Chem*, 259: 10430-8.
Walker, R. A., E. T. O'Brien, N. K. Pryer, M. F. Soboeiro, W. A. Voter, H. P. Erickson, and E. D. Salmon. 1988. 'Dynamic instability of individual microtubules analyzed by video light microscopy: rate constants and transition frequencies', *J Cell Biol*, 107: 1437-48.
Widlund, P. O., M. Podolski, S. Reber, J. Alper, M. Storch, A. A. Hyman, J. Howard, and D. N. Drechsel. 2012. 'One-step purification of assembly-competent tubulin from diverse eukaryotic sources', *Mol Biol Cell*, 23: 4393-401.
Wong-Riley, M. T., and J. C. Besharse. 2012. 'The kinesin superfamily protein KIF17: one protein with many functions', *Biomol Concepts*, 3: 267-82.
Xing, B. M., Y. R. Yang, J. X. Du, H. J. Chen, C. Qi, Z. H. Huang, Y. Zhang, and Y. Wang. 2012. 'Cyclin-dependent kinase 5 controls TRPV1 membrane trafficking and the heat sensitivity of nociceptors through KIF13B', *J Neurosci*, 32: 14709-21.
Yogev, S., R. Cooper, R. Fetter, M. Horowitz, and K. Shen. 2016. 'Microtubule Organization Determines Axonal Transport Dynamics', *Neuron*, 92: 449-60.
Yonekawa, Y., A. Harada, Y. Okada, T. Funakoshi, Y. Kanai, Y. Takei, S. Terada, T. Noda, and N. Hirokawa. 1998. 'Defect in synaptic vesicle precursor transport and neuronal cell death in KIF1A motor protein-deficient mice', *J Cell Biol*, 141: 431-41.

Yu, I., C. P. Garnham, and A. Roll-Mecak. 2015. 'Writing and Reading the Tubulin Code', *J Biol Chem*, 290: 17163-72.
Zempel, H., and E. Mandelkow. 2014. 'Lost after translation: missorting of Tau protein and consequences for Alzheimer disease', *Trends Neurosci*, 37: 721-32.
Zhang, R., B. LaFrance, and E. Nogales. 2018. 'Separating the effects of nucleotide and EB binding on microtubule structure', *Proc Natl Acad Sci U S A*, 115: E6191-E200.
Zhang, Y. V., S. B. Hannan, Z. A. Stapper, J. V. Kern, T. R. Jahn, and T. M. Rasse. 2016. 'The Drosophila KIF1A Homolog unc-104 Is Important for Site-Specific Synapse Maturation', *Front Cell Neurosci*, 10: 207.
Zinsmaier, K. E., M. Babic, and G. J. Russo. 2009. 'Mitochondrial transport dynamics in axons and dendrites', *Results Probl Cell Differ*, 48: 107-39.